

UCSF

UC San Francisco Electronic Theses and Dissertations

Title

Hippocampal and hypothalamic CRH neurons in mood related behaviors

Permalink

<https://escholarship.org/uc/item/0dk9d1zb>

Author

Turner, Victoria Sayo

Publication Date

2023

Peer reviewed|Thesis/dissertation

Hippocampal and hypothalamic CRH neurons in mood related behaviors

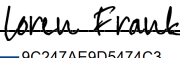
by
Victoria Turner

DISSERTATION
Submitted in partial satisfaction of the requirements for degree of
DOCTOR OF PHILOSOPHY

in
Neuroscience

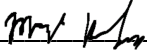
in the
GRADUATE DIVISION
of the
UNIVERSITY OF CALIFORNIA, SAN FRANCISCO

Approved:

DocuSigned by:

9C247AE9D5474C3... Loren Frank
Chair

DocuSigned by:

Zachary Knight

DocuSigned by:

D52190F39543433... Mazen Kheirbek

Committee Members

Copyright 2023
by
Victoria Turner

Acknowledgements

I would like to express my deep gratitude to the people of the Kheirbek Lab. It has been a pleasure to work alongside such a dedicated and talented group of scientists. I thank my graduate school advisor Dr. Mazen Kheirbek for guidance and support. Mark Gergues has been the rising tide that lifts all boats. I am thankful for the privilege of working with Rachel O'Sullivan and Shazreh Hassan. I would also like to recognize and thank the members of my thesis committee: Loren Frank, Zachary Knight, and Lisa Gunaydin.

I want to extend my appreciation to mentors from various stages of my career, including Albert I. Chen, Joshua Johansen, Christopher Zimmerman, Takaaki Ozawa, Josef Trapani, Mary Harrington, and Aimee Kao. Your expertise and wisdom have helped shape me into the researcher I am today.

To my family, Sanae Turner, and Desiree Turner, thank you for your support and encouragement and for withstanding the dense schedules on our vacations.

To my chosen family, Holda Anagho, thank you for being a constant source of inspiration from abroad. Say a country and I will meet you there.

Finally, a special thank you to Lorna Strutt, who kept me from going crazy during the 2020 lockdown.

Thank you all for being a part of this incredible journey.

Contributions

Chapter 1 is written by Victoria Turner.

Chapter 2 is reproduced in an adapted form from the following publication:

Turner VS*, O'Sullivan RO*, Kheirbek MA (2022) Linking external stimuli with internal drives: a role for the ventral hippocampus" Curr Opin Neurobiol *equal contributions.

Chapter 3 is written by Victoria Turner and contains unpublished findings with contributions from Rachel O'Sullivan, Shazreh Hassan, and Mazen Kheirbek.

Chapter 4 is written by Victoria Turner and contains unpublished findings with contributions from Rachel O'Sullivan, Shazreh Hassan, and Mazen Kheirbek.

Chapter 5 is written by Victoria Turner.

“Take this fruit.

It is what I have to offer.

It may not be first, or ever best,

but it is the only way to be sure that I lived at all.”

– Sarah Kay, “A Bird Made of Birds”

Hippocampal and hypothalamic CRH neurons in mood related behaviors

by Victoria Turner

Abstract

Stressful experiences lead to important changes in physiology and behavior, including the release of corticosteroid stress hormones and engagement of behavioral states like vigilance. While normally important for survival, these aspects of the stress response can cause detrimental effects if they are dysregulated and become exaggerated or blunted. It is important to understand how this system is engaged by stressful stimuli and how the magnitude of the stress response is tuned to fit the circumstances that triggered it.

The ventral hippocampus (vHPC) has long been described as an inhibitory regulator of the corticosteroid stress response, part of a system that controls the size of stress responses. Downstream, the hypothalamic CRH-expressing neurons are known to be gatekeepers of the cortisol stress response, but recent studies also implicate a non-hormonal role for these cells in anxiety-related behavior. What is still unknown is how these two regions respond to stressors like approach-avoidance assays used in the study of anxiety-related behavior, and how the ventral hippocampus may be involved in regulating CRH activity in these behaviors.

In Chapter 1, I introduce the hippocampal-hypothalamic circuitry that is implicated in emotion-related behaviors from the stress and anxiety fields. I discuss how this indirect projection has been modelled as a regulator of the neuroendocrine stress response with respect to the corticosteroid response. I then introduce more recent findings that imply this pathway could also be involved in non-neuroendocrine stress responses through neural control of stress-induced behaviors.

In Chapter 2, we review recent work on how vCA1 contributes to a network that associates external stimuli with internal motivational drive states to promote the selection of adaptive behavioral responses. This leads us to propose a model of vHPC function that emphasizes its role in the integration and transformation of internal and external cues to guide behavioral selection when faced with multiple potential outcomes.

In Chapter 3, I present evidence that PVN^{CRH} and vHPC cells respond independently to fear- and anxiety-related stimuli. Immediate, uncontrollable threats and freezing responses to these threats evoke activity in both regions. However, this is not true for exploratory behaviors in an approach-avoidance assay and self-controlled transitions between levels of potential threat; these events reliably evoke activity only in vHPC cells.

In Chapter 4, I investigate the influence of the vHPC on PVN^{CRH} cells and their responses to stressful stimuli. I establish the first in vivo recordings of PVN^{CRH} cells during vHPC chemogenetic perturbation. By inhibiting vHPC activity during the stressful experiences from Chapter 3, I find that vHPC selectively modulates activity of PVN^{CRH}

cells during a subset of behavioral responses to immediate, uncontrollable threat and ambiguous, self-controlled threat.

In Chapter 5, I integrate these experimental findings with knowledge in the field about the roles of vHPC and PVN^{CRH} cells and the regions' contributions to engaging and controlling the stress response as a whole.

Table of Contents

Chapter 1: Introduction	1
References for Chapter 1	8
Chapter 2: The ventral hippocampus's role in linking external stimuli with internal drives	13
References for Chapter 2	30
Chapter 3: Hypothalamic CRH Cells and Ventral Hippocampus Differentially Encode External Threat and Acute Stress	42
Introduction	42
Methods	43
Results	49
Discussion	67
References for Chapter 3	71
Chapter 4: Ventral hippocampal modulation of the hypothalamic CRH stress response	76
Introduction	76
Methods	77
Results	79
Discussion	91
References for Chapter 4	93
Chapter 5: Conclusions.....	114

List of Figures

Figure 1.1. Diagram of the prevailing model of paraventricular nucleus and its modulation by the hippocampus in the stress response.....	3
Figure 1.2. Lesions of the ventral subiculum (vSUB) region in ventral hippocampus cause increases in HPA activation after stress.	4
Figure 2.1. Functional anatomy of the vCA1 circuit.	15
Figure 2.2. Potential anatomical-functional relationships in vCA1.....	18
Figure 2.3. Hypothesized model for vCA1 encoding properties and engagement of downstream targets.	22
Figure 3.1. Recording neural activity in PVN ^{CRH} and vHPC during elevated plus maze and foot shock assay.	50
Figure 3.2. PVN ^{CRH} and vHPC neurons both respond rapidly and robustly to foot shock.....	52
Figure 3.3. Anxiety- and motor-related behaviors in the elevated plus maze.....	53
Figure 3.4. Overall PVN ^{CRH} and vHPC activity and anxiety-related behavior in the elevated plus maze.....	54
Figure 3.5. vHPC activity differentiates between subdivided compartments of the elevated plus maze better than PVN ^{CRH} activity.	55
Figure 3.6. PVN ^{CRH} and vHPC respond differently during trajectories between threat levels in the elevated plus maze.....	57
Figure 3.7. vHPC neurons and PVN ^{CRH} neurons respond similarly during approach and avoidance sequences in the elevated plus maze.	60

Figure 3.8. vHPC neurons and CRH neurons respond differently during risk assessment behavioral motifs in the EPM.	62
Figure 3.9. vHPC neurons and CRH neurons respond differently during stress-related behavioral motifs in the EPM.	63
Figure 4.1. Recording bulk activity in PVN ^{CRH} and DREADDs inhibition of vHPC during elevated plus maze and foot shock assay.	80
Figure 4.2. vHPC inhibition increases PVN ^{CRH} neuron activity during the start of freezing but does not affect PVN ^{CRH} responses to shock.	82
Figure 4.3. Inhibition of vHPC leads to similar motor and anxiety-related behavior in the elevated plus maze.	84
Figure 4.4. Inhibition of vHPC does not significantly affect anxiety-related behavior or overall PVN ^{CRH} signal in the elevated plus maze.	85
Figure 4.5. Inhibition of vHPC does not affect mean PVN ^{CRH} activity in EPM compartments.	86
Figure 4.6. vHPC inhibition slightly increases PVN ^{CRH} activity during trajectories between threat levels in the elevated plus maze.	88
Figure 4.7. Inhibiting vHPC renders CRH neurons responsive to approach-related behavioral motifs.	90

List of Tables

Table 1: Exploratory and anxiety-related behaviors in the elevated plus maze.....	47
Table 2: Observed activity in PVN ^{CRH} and vHPC cells during elevated plus maze exploration.	64
Table 3. Summary of statistical comparisons related to Figures 3.5. – 3.9.	65
Table 4. Summary of statistical comparisons related to Figure 4.7.	91

Chapter 1: Introduction

An essential adaptive function of the nervous system is to organize appropriate physiological and behavioral responses in the face of stressful events. However, this process can become dysregulated in psychiatric disease. Characterizing the neural circuits that gate and modulate the stress response is thus essential to understand how the brain interprets contextual cues about threat and how this process can malfunction.

Overactivation of stress circuits can be maladaptive, leading to hallmark features of anxiety disorders such as excessive avoidance and hyperarousal. Chronic stress exposure can increase the risk of developing mood and anxiety disorders (Pitman et al., 2012). In addition, studies have pointed to hyperactivation of the hypothalamus-pituitary-adrenal (HPA) axis in major depression and underactivation in post-traumatic stress disorder (Sahu et al. 2022; Naughton, Dinan, and Scott 2014; Sbisa et al. 2023).

The HPA stress response

The stress response consists of two canonical physiological responses: the sympathetic-adreno-medullar (SAM) axis, which causes release of epinephrine and norepinephrine from the adrenal medulla, and the HPA axis, which stimulates release of corticosteroids (CORT) (Godoy et al. 2018). The SAM response is triggered by direct sympathetic nerve stimulation of the adrenal medulla to release adrenaline, assisting in the immediate fight-flight-freeze behavioral response, while the HPA axis is activated on a slower timescale of minutes via a cascade of intermediate hormones that must travel through the blood to the adrenal glands to stimulate production and release of corticosteroids. The HPA axis mobilizes energy reserves, pauses digestion and

reproductive functions, and temporarily elevates immune function. A healthy organism can activate these two systems in a stressful scenario and eventually return to a baseline state of low activation when a threat has passed.

The HPA axis can be triggered by physiological stressors like starvation, blood loss, or hypoxia (James P. Herman et al., 2016) but is also important for many psychological stressors such as exploration of an open field, restraint, confinement to an elevated pedestal, shock, or forced swim in water (Spencer and Deak 2017). A population of cells essential to triggering this response is the corticotropin-releasing-hormone cells (CRH) of the hypothalamus.

Only in the past few years has it become apparent that the CRH cells gating the HPA stress response are also important in influencing rapid changes in behaviors that cannot be explained by their role in slow hormonal release (Núria Daviu et al., 2020; Füzesi et al., 2016; J. Kim et al., 2019) (**Figure 1.1**). These behaviors include anxiety-like behaviors like avoidance and displacement or coping behaviors like grooming. An output that may carry information about these behaviors projects from hypothalamic CRH cells to the lateral hypothalamus, a subpopulation of which may collateralize to the bloodstream in the median eminence (Füzesi et al., 2016). Acute stimulation of the hypothalamic CRH projection to the lateral hypothalamus is sufficient to increase grooming and digging, and repeated photostimulation over days reduces motivation to press a lever for sucrose (Mitchell et al., 2023). In addition, activation of the pathway reduces sleep, reminiscent of stress-induced insomnia (Li et al., 2020; Ono et al., 2020).

In addition, CORT hormones appear to be unnecessary for many acute stress-related behaviors. For example, blocking the creation of CORT does not affect post-

stress grooming or rearing behavior (J. S. Kim et al., 2019) and is not required for the return of CRH neuron activity to baseline after an animal receives a shock or for the habituation of CRH responses to stressors (J. S. Kim, Han, and Iremonger 2019). Thus, it seems likely that hypothalamic CRH cells influence behavioral responses to stress independent of their role in triggering hormonal release.

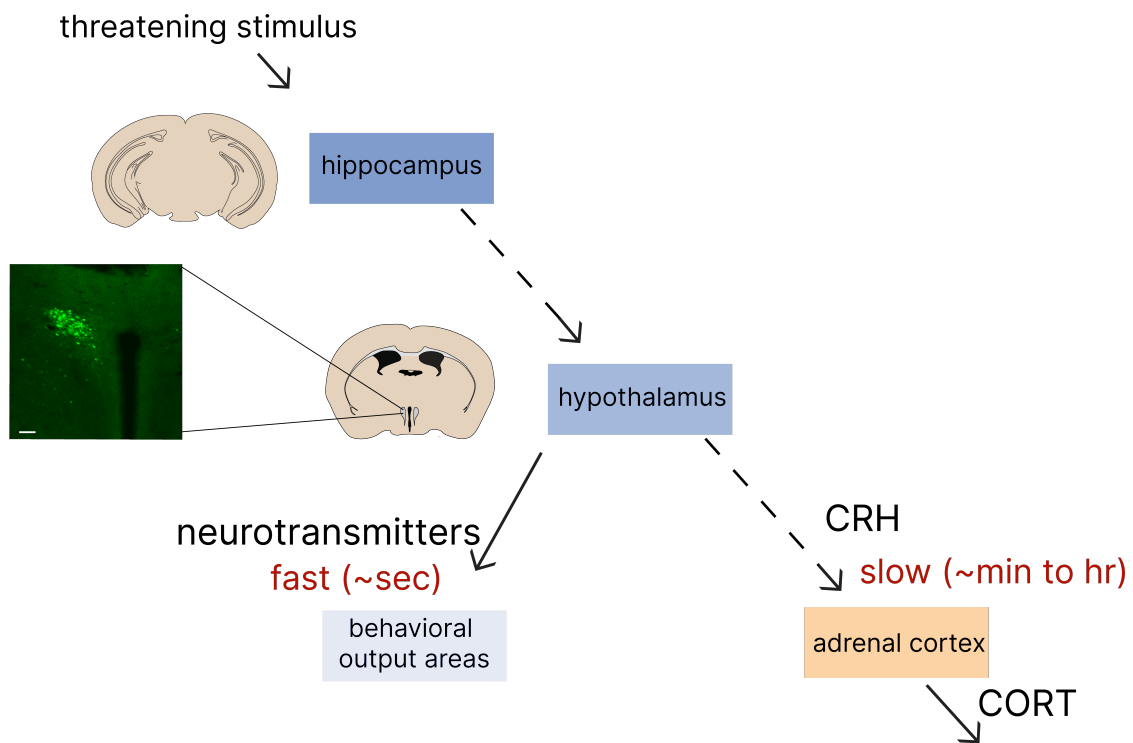
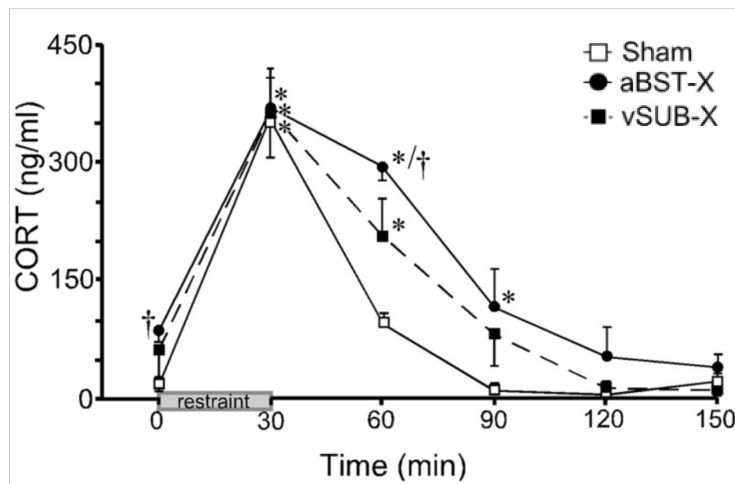


Figure 1.1. Diagram of the prevailing model of paraventricular nucleus and its modulation by the hippocampus in the stress response. The hypothalamic pituitary adrenal axis is a stress response which converts brain activity in response to a threat into body-wide release of corticosteroids via the anterior pituitary and adrenocorticotropic hormone (ACTH). Manipulation of PVN^{CRH} cells causes immediate changes in behavior too fast to be explained by slower action of stress hormones, suggesting a direct input from PVN^{CRH} cells to behavioral output areas. Scale bar, 100 μ m.

Regulation of the stress response

A proposed mechanism for modulating the size or duration of the HPA stress response is an indirect pathway from vHPC to the hypothalamic paraventricular nucleus

A



B

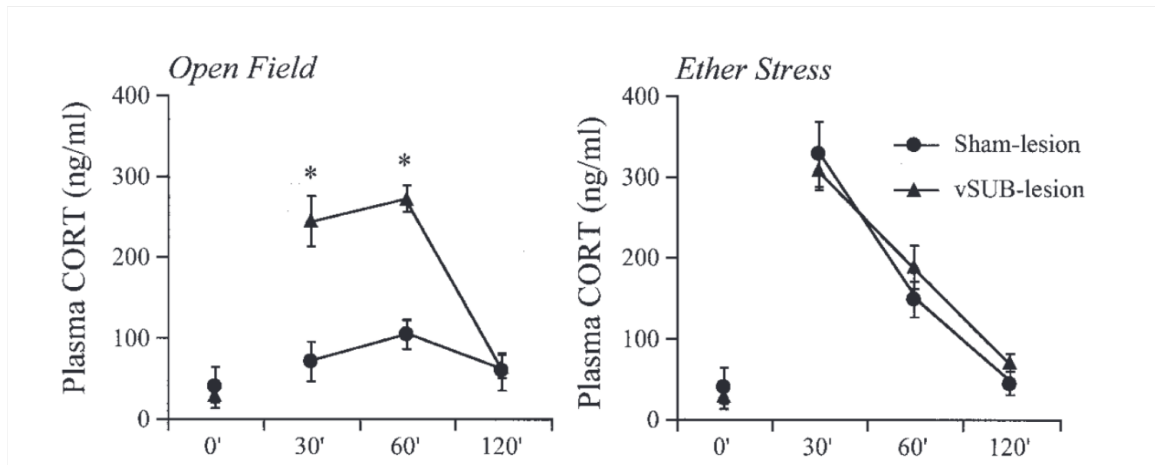


Figure 1.2. Lesions of the ventral subiculum (vSUB) region in ventral hippocampus cause increases in HPA activation after stress. (A) Lesion of the ventral hippocampus subregion causes a prolonged release of corticosteroids (CORT) into the blood after a 30 min restraint stress. Adapted from (Radley and Sawchenko 2011). **(B)** Exploring an open field after vHPC lesion causes a greater release of CORT, but ether inhalation stress after the same vHPC lesion does not suggest an inhibitory role for vHPC in regulating CORT response to this physiological stressor. Adapted from (J. P. Herman, Dolgas, and Carlson 1998).

(PVN) CRH cells. **(Figure 1.1)**. Lesions of vHPC results in greater release of CORT after a 30 min restraint stress or a 5 min exploration of the open field, though not after ether inhalation **(Figure 1.2)** (J. P. Herman et al., 1998; Radley & Sawchenko, 2011). These results suggest vHPC may play an inhibitory role over the HPA axis in response to certain stressors. vHPC lesions also result in greater cellular activation of the PVN cells after restraint stress: a two-fold increase in Fos expression in the PVN and increases in transcription of CRH mRNA in the PVN (Radley & Sawchenko, 2011). This area of research has identified a promising relay to carry information from the vHPC to PVN: the bed nucleus of the stria terminalis (BNST), a region of the basal forebrain, which is a GABAergic relay targeted by vHPC projection neurons that then projects to PVN^{CRH} neurons (Radley et al., 2009; Radley & Sawchenko, 2011).

In concordance with the effects observed after vHPC lesions, stimulation of the vHPC has been demonstrated to increase HPA stress response magnitude. In humans and animal models, stimulation of hippocampus results in decreased circulating CORT levels (Dunn & Orr, 1984; Dupont et al., 1972; Mandell et al., 1963; Rubin et al., 1966). Importantly, these manipulations took place under contexts where CORT was already elevated and a decrease would be easier to measure – anesthesia or cold exposure, both known triggers of the HPA stress response. More recently, optical stimulation of the CA1 pathways to BNST during restraint stress has been shown to increase the release of CORT into the blood (Cole et al., 2022), providing more support for the vHPC-BNST-PVN circuit. These findings are all consistent with an inhibitory role for the intact vHPC over the HPA stress response and PVN^{CRH} activity.

With the recent discovery of additional behavioral roles for the corticotropin-hormone-releasing (CRH) cells of the PVN in directly modifying behavior, an open question is how vHPC modulates the short-term behavioral outputs of PVN^{CRH} cells in the face of stressful experiences. vHPC plays an inhibitory role in the release of stress hormones into the blood over tens of minutes, but does vHPC also exert inhibition over the rapid changes in PVN^{CRH} activity?

Assessing aversive experiences in animal models

Behavioral neuroscientists studying the concept of stress have often employed different assays than scientists studying anxiety or avoidance. The field of stress research, particularly research on acute stress, historically relied on assays like restraint, where the body of a mouse or rat is immobilized with a holding device, or mild electrical shock. Both measures are useful for their scalability—duration of restraint can be shortened or lengthened, and shocks can be adjusted in intensity. Other popular models in the stress field include forced swim, where animals are placed in a bucket of water for a given length of time.

The field of anxiety, on the other hand, typically employs different tasks like the elevated plus maze, open field test, and light dark box. The elevated plus maze is one of the most popular of these assays and is used to assess conflict between a drive to explore and a drive to avoid potential danger, also known as approach-avoidance conflict (La-Vu et al. 2020). The modern version of the maze consists of four elevated arms, two of which are enclosed by tall walls and two of which are exposed to light and the surroundings. Advantages of this assay are the spatially defined zones of conflict,

where animals choose between different areas to explore or avoid, and the ease of analysis, where time spent in exposed zones can be quantified. Measurements like time in open arms reliably increases after administration of many anxiolytic drugs (Rosso et al. 2022) and decreases after stressful experiences (Korte and De Boer 2003).

However, the elevated plus maze is not without its critics. Some disadvantages are that the measurement of anxiety is confounded by other characteristics like exploratory drive (Ennaceur 2014) or impulse control (Bespalov and Steckler 2021).

Despite these potential complicating factors, the elevated plus maze is very useful for geometrically defining approach and avoidance behaviors. In addition, the maze is known to trigger the HPA stress response via release of corticosteroids (File et al., 1994; Rodgers et al., 1999), making it relevant to the field of stress research.

Our approach in the current work was to select a popular stress-related assay (foot shock) and anxiety assay (elevated plus maze) to compare how PVN^{CRH} and the upstream vHPC neurons responded to key behavioral moments in the assays (for example, the initiation of freezing in the foot shock assay or the head dip behavior in the elevated plus maze).

It is unknown how these two regions respond to such contrasting sets of stressful cues, and how the ventral hippocampus may be involved in regulating CRH-related avoidance behaviors. We set out to learn what roles the vHPC and PVN^{CRH} cells serve in response to these two types of stressors.

References for Chapter 1

- Bespalov, Anton, and Thomas Steckler. 2021. "Pharmacology of Anxiety or Pharmacology of Elevated Plus Maze?" *Biological Psychiatry*.
- Cole, Anthony B., Kristen Montgomery, Tracy L. Bale, and Scott M. Thompson. 2022. "What the Hippocampus Tells the HPA Axis: Hippocampal Output Attenuates Acute Stress Responses via Disynaptic Inhibition of CRF+ PVN Neurons." *Neurobiology of Stress* 20 (September): 100473.
- Daviu, Núria, Tamás Füzési, David G. Rosenegger, Neilen P. Rasiah, Toni-Lee Sterley, Govind Peringod, and Jaideep S. Bains. 2020. "Paraventricular Nucleus CRH Neurons Encode Stress Controllability and Regulate Defensive Behavior Selection." *Nature Neuroscience*, February. <https://doi.org/10.1038/s41593-020-0591-0>.
- Dunn, J. D., and S. E. Orr. 1984. "Differential Plasma Corticosterone Responses to Hippocampal Stimulation." *Experimental Brain Research. Experimentelle Hirnforschung. Experimentation Cerebrale* 54 (1): 1–6.
- Dupont, André, Edouard Bastarache, Elemer Endröczy, and Claude Fortier. 1972. "Effect of Hippocampal Stimulation on the Plasma Thyrotropin (THS) and Corticosterone Responses to Acute Cold Exposure in the Rat." *Canadian Journal of Physiology and Pharmacology* 50 (4): 364–67.
- Ennaceur, A. 2014. "Tests of Unconditioned Anxiety - Pitfalls and Disappointments." *Physiology & Behavior* 135 (August): 55–71.

- File, S. E., H. Zangrossi Jr, F. L. Sanders, and P. S. Mabbutt. 1994. "Raised Corticosterone in the Rat after Exposure to the Elevated Plus-Maze." *Psychopharmacology* 113 (3–4): 543–46.
- Füzesi, Tamás, Nuria Daviu, Jaclyn I. Wamstecker Cusulin, Robert P. Bonin, and Jaideep S. Bains. 2016. "Hypothalamic CRH Neurons Orchestrate Complex Behaviours after Stress." *Nature Communications* 7 (June): 11937.
- Godoy, Lívea Dornela, Matheus Teixeira Rossignoli, Polianna Delfino-Pereira, Norberto Garcia-Cairasco, and Eduardo Henrique de Lima Umeoka. 2018. "A Comprehensive Overview on Stress Neurobiology: Basic Concepts and Clinical Implications." *Frontiers in Behavioral Neuroscience* 12 (July): 127.
- Herman, J. P., C. M. Dolgas, and S. L. Carlson. 1998. "Ventral Subiculum Regulates Hypothalamo-Pituitary-Adrenocortical and Behavioural Responses to Cognitive Stressors." *Neuroscience* 86 (2): 449–59.
- Herman, James P., Jessica M. McKlveen, Sriparna Ghosal, Brittany Kopp, Aynara Wulsin, Ryan Makinson, Jessie Scheimann, and Brent Myers. 2016. "Regulation of the Hypothalamic-Pituitary-Adrenocortical Stress Response." *Comprehensive Physiology* 6 (2): 603–21.
- Kim, Jineun, Seongju Lee, Yi-Ya Fang, Anna Shin, Seahyung Park, Koichi Hashikawa, Shreelatha Bhat, et al. 2019. "Rapid, Biphasic CRF Neuronal Responses Encode Positive and Negative Valence." *Nature Neuroscience*, March.
<https://doi.org/10.1038/s41593-019-0342-2>.

- Kim, Joon S., Su Young Han, and Karl J. Iremonger. 2019. "Stress Experience and Hormone Feedback Tune Distinct Components of Hypothalamic CRH Neuron Activity." *Nature Communications* 10 (1): 5696.
- Kinlein, Scott A., Derrick J. Phillips, Chandler R. Keller, and Ilia N. Karatsoreos. 2019. "Role of Corticosterone in Altered Neurobehavioral Responses to Acute Stress in a Model of Compromised Hypothalamic-Pituitary-Adrenal Axis Function." *Psychoneuroendocrinology* 102 (April): 248–55.
- Korte, S. Mechiel, and Sietse F. De Boer. 2003. "A Robust Animal Model of State Anxiety: Fear-Potentiated Behaviour in the Elevated plus-Maze." *European Journal of Pharmacology* 463 (1–3): 163–75.
- La-Vu, Mimi, Brooke C. Tobias, Peter J. Schuette, and Avishek Adhikari. 2020. "To Approach or Avoid: An Introductory Overview of the Study of Anxiety Using Rodent Assays." *Frontiers in Behavioral Neuroscience* 14 (August): 145.
- Li, Shi-Bin, Jeremy C. Borniger, Hiroshi Yamaguchi, Julien Hédou, Brice Gaudilliere, and Luis de Lecea. 2020. "Hypothalamic Circuitry Underlying Stress-Induced Insomnia and Peripheral Immunosuppression." *Science Advances* 6 (37). <https://doi.org/10.1126/sciadv.abc2590>.
- Mandell, A. J., L. F. Chapman, R. W. Rand, and R. D. Walter. 1963. "Plasma Corticosteroids: Changes in Concentration after Stimulation of Hippocampus and Amygdala." *Science* 139 (3560): 1212.
- Mitchell, Caitlin S., Erin J. Campbell, Simon D. Fisher, Laura M. Stanton, Nicholas J. Burton, Amy J. Pearl, Gavan P. McNally, et al. 2023. "Optogenetic Recruitment

- of Hypothalamic Corticotrophin-Releasing-Hormone (CRH) Neurons Reduces Motivational Drive.” *BioRxiv*. <https://doi.org/10.1101/2023.02.03.527084>.
- Naughton, Marie, Timothy G. Dinan, and Lucinda V. Scott. 2014. “Corticotropin-Releasing Hormone and the Hypothalamic-Pituitary-Adrenal Axis in Psychiatric Disease.” *Handbook of Clinical Neurology* 124: 69–91.
- Ono, Daisuke, Yasutaka Mukai, Chi Jung Hung, Srikanta Chowdhury, Takashi Sugiyama, and Akihiro Yamanaka. 2020. “The Mammalian Circadian Pacemaker Regulates Wakefulness via CRF Neurons in the Paraventricular Nucleus of the Hypothalamus.” *Science Advances* 6 (45).
<https://doi.org/10.1126/sciadv.abd0384>.
- Pitman, Roger K., Ann M. Rasmusson, Karestan C. Koenen, Lisa M. Shin, Scott P. Orr, Mark W. Gilbertson, Mohammed R. Milad, and Israel Liberzon. 2012. “Biological Studies of Post-Traumatic Stress Disorder.” *Nature Reviews. Neuroscience* 13 (11): 769–87.
- Radley, Jason J., Kristin L. Gosselink, and Paul E. Sawchenko. 2009. “A Discrete GABAergic Relay Mediates Medial Prefrontal Cortical Inhibition of the Neuroendocrine Stress Response.” *The Journal of Neuroscience: The Official Journal of the Society for Neuroscience* 29 (22): 7330–40.
- Radley, Jason J., and Paul E. Sawchenko. 2011. “A Common Substrate for Prefrontal and Hippocampal Inhibition of the Neuroendocrine Stress Response.” *The Journal of Neuroscience: The Official Journal of the Society for Neuroscience* 31 (26): 9683–95.

- Rodgers, R. J., J. Haller, A. Holmes, J. Halasz, T. J. Walton, and P. F. Brain. 1999. "Corticosterone Response to the Plus-Maze: High Correlation with Risk Assessment in Rats and Mice." *Physiology & Behavior* 68 (1–2): 47–53.
- Rosso, Marianna, Robin Wirz, Ariane Vera Loretan, Nicole Alessandra Sutter, Charlène Tatiana Pereira da Cunha, Ivana Jaric, Hanno Würbel, and Bernhard Voelkl. 2022. "Reliability of Common Mouse Behavioural Tests of Anxiety: A Systematic Review and Meta-Analysis on the Effects of Anxiolytics." *Neuroscience and Biobehavioral Reviews* 143 (December): 104928.
- Rubin, R. T., A. J. Mandell, and P. H. Crandall. 1966. "Corticosteroid Responses to Limbic Stimulation in Man: Localization of Stimulus Sites." *Science* 153 (3737): 767–68.
- Sahu, Manoj K., Rajesh K. Dubey, Alka Chandrakar, Mahesh Kumar, and Mahendra Kumar. 2022. "A Systematic Review and Meta-Analysis of Serum and Plasma Cortisol Levels in Depressed Patients versus Control." *Indian Journal of Psychiatry* 64 (5): 440–48.
- Sbisa, Alyssa M., Kelsey Madden, Catherine Toben, Alexander C. McFarlane, Lisa Dell, and Ellie Lawrence-Wood. 2023. "Potential Peripheral Biomarkers Associated with the Emergence and Presence of Posttraumatic Stress Disorder Symptomatology: A Systematic Review." *Psychoneuroendocrinology* 147 (January): 105954.
- Spencer, Robert L., and Terrence Deak. 2017. "A Users Guide to HPA Axis Research." *Physiology & Behavior* 178 (September): 43–65.

Chapter 2: The ventral hippocampus's role in linking external stimuli with internal drives

The ventral hippocampus (vHPC) is a key node in the extended network that generates emotional and motivated behavior. In recent years, there has been growing interest in vHPC function, the mechanisms by which it contributes to specific behaviors, and how its properties differentiate vHPC networks from the well-studied dorsal hippocampal network. This has led to numerous studies delineating the circuits and cell types in vHPC, specifically within the vCA1 subregion, identifying their unique wiring patterns and their diverse functional properties. The complexity of vCA1 has come to light, with distinct components of its structure (cell types, inputs, and outputs) hypothesized to differentially encode features of an explored environment and ongoing internal drive states to promote adaptive behavioral outputs. The field has progressed considerably since lesion and manipulation studies identified the dorsal HPC (dHPC) as a controller of cognitive functions and vHPC as a regulator of unconditioned fear and anxiety responses (Fanselow and Dong 2010; Kheirbek et al. 2013; Kjelstrup et al. 2002; Strange et al. 2014), and human studies established corresponding roles in the posterior and anterior HPC (Poppenk et al. 2013). Given the new findings, it is time to refine the current abstract model of vCA1 into one that highlights the rich heterogeneity of the region.

In the following sections, we discuss recent progress and put forward a more mechanistic model for vCA1 function. We propose that vCA1 neurons encode stimuli

that have immediate significance for the animal, generating a map that links external stimuli with internal drive states. This is analogous to the well-described properties of assemblies of dCA1 neurons that exhibit location-, stimulus-, and time-specific discharge patterns to generate a map of space (O'Keefe and Nadel 1978; McNaughton et al. 2006), among many others). We suggest that ensembles of vCA1 neurons store experiences imbued with the motivation to avoid danger, eat, find mates, and gain or maintain social status. These ensembles of vCA1 neurons are largely anatomically segregated and, therefore, able to route specific information to distinct downstream targets and drive the selection of appropriate adaptive behavioral responses.

Here, we review recent circuit-based studies in rodents that provide support for this important aspect of HPC function. In addition, we discuss how dysfunction in this process may contribute to mood and anxiety disorders. Owing to the focused nature of this review, we will limit our analysis to the primary output of vHPC, the vCA1/vSub subregions.

Anatomical organization of vCA1

As described in detail, in this review and elsewhere, vCA1 neurons project to several cortical and subcortical areas implicated in mood/anxiety-related behavior, reward seeking, social approach, and neuroendocrine responses to stress (**Figure 2.1, 2.2**). These include (but are not limited to) outputs to the medial prefrontal cortex (mPFC), nucleus accumbens (NAc), lateral hypothalamus (LH), lateral septum (LS), bed nucleus of the stria terminalis (BNST), and basal and central amygdala (BA, CeA). Retrograde tracing studies and single neuron reconstructions have indicated that these

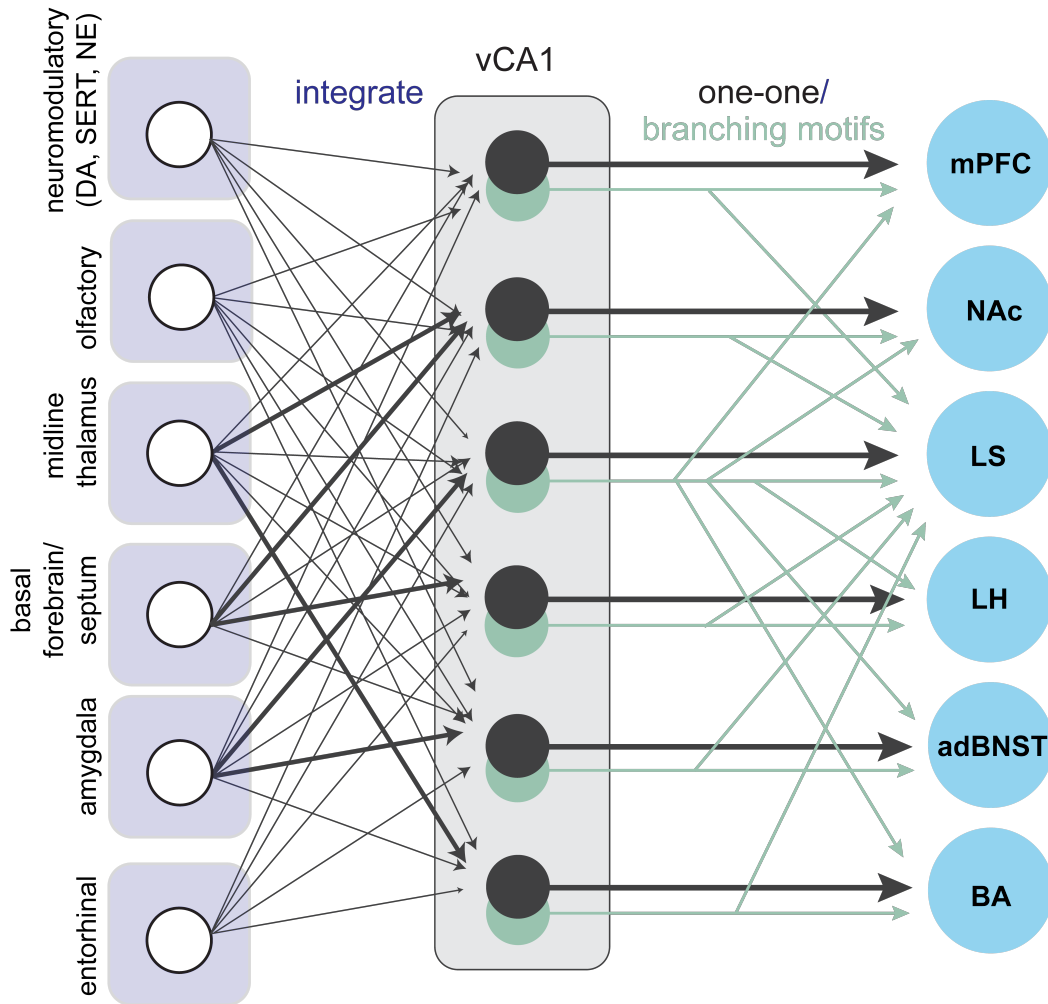


Figure 2.1. Functional anatomy of the vCA1 circuit. Input-output organization of a subset of vCA1 connections. Modified from (Gergues et al. 2020). Based on the analysis of six projection targets of vCA1, it is believed that vCA1 largely integrates input, with some biases in the proportion of upstream input. Output to downstream areas is either via one-to-one connections (black) with a given target or connections that branch to multiple downstream areas (light green). It is important to note that this anatomical map is incomplete, as vCA1 receives input from other areas and sends output to several downstream targets not depicted here, and organizational principles to these areas remain unclear.

outputs are non-overlapping (Arszovszki et al., 2014; Jimenez et al., 2018; W. B. Kim & Cho, 2017; Q. Wang et al., 2016; C. Xu et al., 2016). A recent study using high-throughput sequencing of genetically barcoded neurons (MAPseq) to map the axonal projections of vCA1 neurons found that while many vCA1 neurons show a one-to-one connectivity with downstream areas, as predicted by retrograde tracing, a significant

portion of neurons broadcast to multiple downstream areas in a non-random fashion (Gergues et al. 2020). This indicates that vCA1 contains a mix of single-target neurons and neurons that send highly collateralized outputs (**Figure 2.1**). For example, neurons that project to the LS were found by both MAPseq (Gergues et al. 2020), and single neuron tracing studies (Arszovszki, Borhegyi, and Klausberger 2014) to send collaterals to multiple downstream areas, including the NAc, BNST, LH, and mPFC. The specialized function of these and other collateralized neurons remains to be fully delineated, but their existence suggests that information in a subclass of vCA1 neurons is relayed to many downstream areas. An active area of research is whether these collateralized neurons exhibit information coding properties that are distinct from those of neurons with a single target. One study addressing this question found that vCA1 neurons with trifurcating (or more) projections to the NAc, mPFC, and amygdala were preferentially activated during sharp-wave ripples and during approach/avoidance and reward learning (Ciocchi et al., 2015). Input-output tracing using rabies virus approaches has revealed that vCA1 neurons targeting distinct areas receive similar upstream input, suggesting that vCA1 integrates incoming information and sends it to multiple downstream areas (Gergues et al. 2020). Some subtle biases to input patterns were found that warrant future investigation, such as the preferential targeting of PVT inputs to vCA1-LH neurons versus vCA1-mPFC/vCA1-BA neurons, and the denser innervation of vCA1-BNST neurons by inputs from the amygdala. A recent study also demonstrated that inhibitory and excitatory input from the amygdala to vHPC can differentially modulate projection neurons to the amygdala, mPFC, and BA (AISubaie et al. 2021). Further investigation is needed to elaborate how different inputs to vCA1

shape the region's outputs in a projection-specific way. In addition, it is important to build an understanding of how long-range inputs interface with local vCA1 microcircuits to fine-tune the vCA1 output in the control of behavior. As recently described, PV local interneurons preferentially target vCA1-BA output neurons and receive innervation from vCA1-mPFC neurons (Lee et al. 2014).

vCA1 in motivation to avoid

One of the most well-described properties of vCA1 has been its ability to generate representations of innately anxiogenic or fearful environments and enable an animal to react accordingly. Single-unit electrophysiological recordings and calcium imaging data from rodent models have demonstrated that neurons in vCA1, but not dCA1, have stable responses across anxiety-provoking areas of the elevated plus maze (EPM) and open field test (OFT) (Ciocchi et al., 2015; Jimenez et al., 2018). In the EPM, activity in vCA1 both correlates with baseline anxiety state and scales with the aversive nature of the cues in the task (Jimenez et al., 2018). In addition, optogenetic silencing of vCA1 in mice during exploration of the anxiety-provoking areas of these assays reduces avoidance (Jimenez et al., 2018). Silencing vHPC, but not dHPC, also impedes an animal's ability to associate a specific context with a fearful experience, as measured by the context specificity of tone-signaled active avoidance behavior (Oleksiak et al. 2021). These data demonstrate a role for vCA1 in encoding salient spatial stimuli, scaling these representations based on anxiety state and the aversiveness of the environment, and transforming these representations into an output signal that can be decoded by a downstream area for appropriate action selection (**Figure 2.2**).

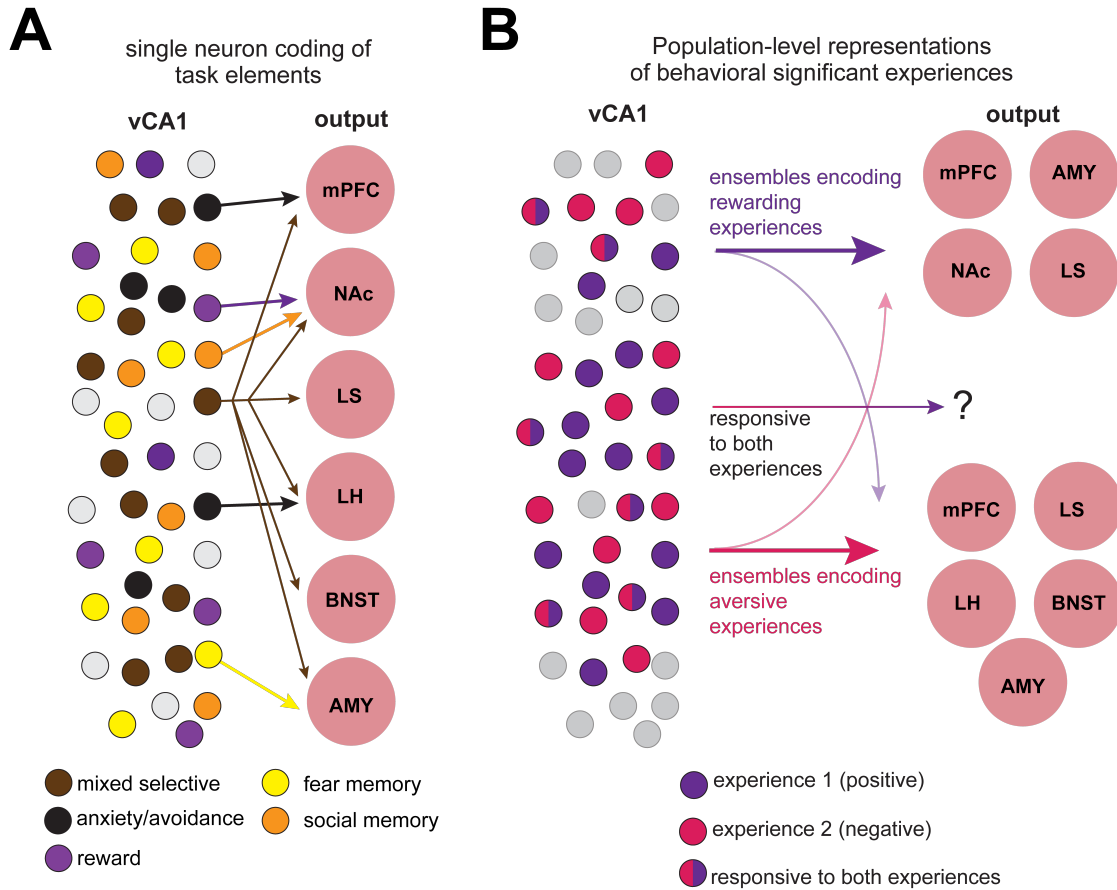


Figure 2.2. Potential anatomical-functional relationships in vCA1. (A) In this well-studied scenario, single neurons encode diverse stimuli and serve different behavioral functions, and this is parcellated into distinct projection streams. Examples of this scenario include the finding that social memory is encoded in vCA1-NAc projections (Okuyama et al. 2016) while vCA1-LH neurons encode anxiety-related stimuli (Jimenez et al. 2018). (B) In an alternate, non-exclusive situation, populations of vCA1 neurons encode behaviorally significant experiences (Biane et al. 2023), and vCA1 ensembles discriminate based on whether the experience is one that promotes approach or avoidance. Then, these ensembles interact with appropriate downstream areas for action selection. Whether different stimuli of the same valence class are encoded by distinct ensembles of neurons, and how different ensembles that encode different salient stimuli route this information to downstream areas remains an open area of investigation.

While vCA1 as a whole is clearly involved in the integration of anxiogenic stimuli and the transformation of this information into appropriate behavior, sub-populations of vCA1 neurons have been implicated in specific aspects of this process (Figure 2.2). vCA1 cells encoding anxiogenic features of mazes are more abundant in populations

projecting to the medial prefrontal cortex (mPFC) or lateral hypothalamus (LH), but not in neurons projecting to the nucleus accumbens (NAc) or the amygdala (Ciocchi et al., 2015; Jimenez et al., 2018). Optogenetic stimulation of vCA1-LH projection neurons decreases the exploration of anxiogenic portions of the EPM and OFT and drives avoidance in a real-time place preference assay, while inhibition reduces open arm avoidance in the EPM (Jimenez et al., 2018). Similarly, when vHPC inputs to mPFC are inhibited either optogenetically or pharmacologically, open arm avoidance decreases (Kjaerby et al. 2016; Padilla-Coreano et al. 2016). Thus, vHPC projections to mPFC and LH play a role in transforming representations of anxiogenic stimuli into actions that promote avoidance. Furthermore, mPFC neurons that encode anxiety-related information in the EPM also synchronize their firing with theta-frequency (4–12 Hz) oscillations in vHPC (Padilla-Coreano et al. 2016; Adhikari, Topiwala, and Gordon 2011, 2010). Interestingly, vCA1 neurons that project to either mPFC or LH do not tend to collateralize (Gergues et al., 2020; Jimenez et al., 2018; Wee & MacAskill, 2020), raising the interesting possibility that these distinct output streams from vCA1 may encode specific features of a fearful environment that drive diverse classes of behavior not captured by the gross assessments used in previous studies. Recent experiments indicate that, even within the projection to mPFC, there exists functional heterogeneity, with deep and superficial layer projection neurons differentially responding to safe versus anxiogenic areas of the EPM (Sánchez-Bellot et al., 2022). Active areas of investigation include how distinct subclasses of projection neurons encode features of an anxiogenic environment and how local circuits contribute to the transformation of this

information into an output signal that is decoded by mPFC and LH to initiate appropriate approach/avoidance decisions.

Unlike the projections to mPFC and LH, vCA1-basal amygdala (BA) projecting neurons do not seem to encode anxiogenic features of anxiety-based assays but do respond to foot shocks in a contextual fear conditioning assay and are necessary for encoding context-fear associations (Graham et al., 2021; Jimenez et al., 2020, 2018; C. Xu et al., 2016). Meanwhile, vCA1 projections to the central nucleus of the amygdala (CeA) have been implicated in context-dependent fear renewal (C. Xu et al., 2016), which has also been shown to recruit vCA1 outputs to prelimbic (PL) and infralimbic cortex (IL) (Q. Wang et al., 2016). This leads to the hypothesis that certain vCA1 projections, like vCA1-LH, may link external stimuli with internal drives to avoid more distal/diffuse threats, while other vCA1 projections, like vCA1-amygdala, vCA1-PL, and vCA1-IL, may create relationships between contextual stimuli and internal drives to avoid more proximal and immediate threats. More recently, a role for vHPC has been identified in observational fear learning. This study found that a subset of vHPC neurons responds to a familiar demonstrator mouse during observational fear by reactivating previously learned context-fear ensembles in the BLA (Terranova et al. 2022).

Another area involved in the processing of diffuse threats, the BNST, receives dense input from vCA1 and has been less well studied. High-frequency electrical stimulation of vHPC can induce anxiolysis in rats, an effect blocked by intra-BNST NMDA antagonists (Glangetas et al. 2017). In addition, vCA1 may exert its inhibitory control of the stress response (Jacobson and Sapolsky 1991) through the BNST; the BNST sends a GABAergic projection to the paraventricular hypothalamic nucleus (PVN)

of the hypothalamic-pituitary-adrenal (HPA) axis (Cullinan et al., 1993; Radley & Sawchenko, 2011, 2015). With respect to other projection outputs, mice susceptible to chronic stress show increased activity in vHPC-NAc projection neurons (Bagot et al. 2015), and individual differences in the activity of this pathway predict vulnerability to stress (Muir et al. 2020). In addition, excess corticosterone in adolescence weakens vHPC inputs to the orbitofrontal cortex (Barfield and Gourley 2019). Finally, chronic stress produces a reduction in synaptic strength at vHPC-NAc synapses, specifically on D1-receptor containing medium spiny neurons, an effect that can be reversed by chronic antidepressant treatment (LeGates et al. 2018). These studies are only a few of the many that have attempted to understand how vHPC activity may be impacted in chronic stress, and future functional mapping studies can uncover how stress modulates vCA1 during related behavioral phenotypes, including avoidance and anhedonia (Xia and Kheirbek 2020). Together, these results demonstrate the dual roles these vHPC projections play in both the integration of information and the translation of this information into a behavioral response (**Figure 2.3**).

vHPC and motivation to seek reward

Recent studies have highlighted the role of reward in modifying representations of diverse stimuli in the hippocampus (Biane et al. 2023; Woods et al. 2020). In addition, place-reward representations have been well studied in HPC, and there are many excellent recent reviews on this topic (e.g., (Nyberg et al. 2022; Sosa and Giocomo

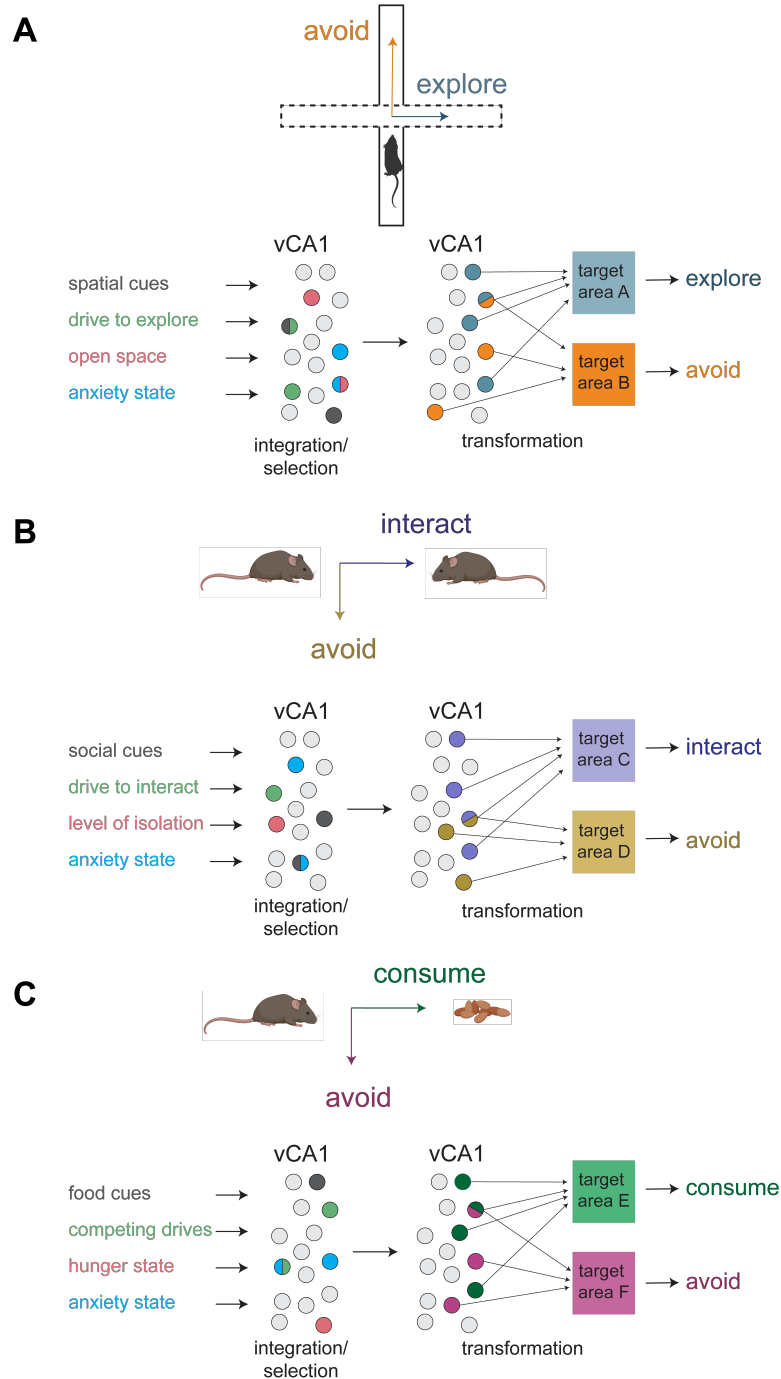


Figure 2.3. Hypothesized model for vCA1 encoding properties and engagement of downstream targets. First, vCA1 integrates diverse external and internal stimuli and then shapes output signals to engage downstream areas for appropriate behavioral selection. This is a shared feature among several approach/avoidance behaviors such as in the elevated plus maze (**A**), social interaction (**B**), and food approach/consumption (**C**). The circuit mechanisms and local computations in vCA1 that integrate inputs to tune output signals remains an area of active investigation.

2021)). Both dHPC and vHPC project to and functionally interact with NAc during navigation for reward (Sosa, Joo, and Frank 2020; Trouche et al. 2019). In the vHPC, antidromically identified vCA1-NAc projection neurons are activated during the approach to a goal location in maze-based tasks (Ciocchi et al., 2015).

Independent of place, recent work has identified a role for this vHPC-NAc circuit in connecting the hedonic value of food with the internal drive to seek food (**Figure 2.3**). Low-frequency photostimulation of this pathway, but not other inputs to the NAc, increased the palatability of a sugar reward (as measured in licks per bout) and drove preference to a flavor paired with the stimulation, while inhibition reduced innate preference for a high-value reward (Yang et al. 2020). In addition to the role vHPC-NAc plays in encoding palatability, vHPC-NAc activity has been implicated in the transition from anticipatory-feeding behavior to consumption. This occurs when the hunger-promoting hormone ghrelin inhibits vHPC-NAc neurons via GHSR1a receptors (Wee et al. 2021). In line with this, optogenetic inhibition of vHPC-NAc stimulated greater eating in animals given free access to food (Reed et al. 2018). Ghrelin may also exert its effects via the vHPC-LH pathway, where it can attenuate satiety signals by generating an interoceptive energy-deficient state (Suarez et al. 2020). Ghrelin infusion into vHPC promotes sated sucrose seeking and increases meal size. These effects are driven by vHPC outputs to LH orexin neurons that in turn project to the lateral dorsal tegmental nucleus (LDTg) (Suarez et al. 2020). These experiments highlight the rich heterogeneity of vHPC, demonstrating that vHPC engages distinct pathways involved in at least two different aspects of feeding: palatability and consumption. Future studies identifying how

distinct targets of vHPC modulate these different components of feeding will shed new light on the role of vCA1 in food approach and consumption.

The vHPC has been implicated in modulating adaptive learning in pursuit of reward. For example, a recent study using odor-guided learning found that vCA1 neurons do not represent odorants at baseline and only gain representations after odor-reward learning. Odor-reward learning rapidly reorganized ensembles of neurons in vCA1 and stored these rewarded odor representations for days after learning (Biane et al. 2023). In addition, recent work has indicated that these outputs from vCA1 can be modified via novelty—mice that explored a novel arena prior to testing in a reward-guided T-maze showed weakened vHPC-mPFC functional connectivity and were better able to learn the task. This indicates that one function of vCA1 (specifically vCA1-mPFC) is to recognize novelty and use it to modify encoded representations so that animals are better able to successfully seek reward (Park et al. 2021).

While these studies indicate that distinct pathways may encode stimuli of specific valences, this specification is most likely plastic. For example, a recent study found that vCA1-BLA and vCA1-NAc projections could drive either preference or avoidance behavior depending on whether the neurons were associated with a positive or negative engram (Shpokayte et al. 2022). Such data suggest that these projections do not have fixed roles, and that context is extremely important when understanding the function of vCA1 projections in motivated behavior.

vCA1 in motivation to seek social interaction

In recent years, vHPC has been linked to social behavior, social interaction, social memory, and the representation of social hierarchy (Meira et al. 2018; Montagnin, Saiote, and Schiller 2018; Okuyama et al. 2016; Watarai et al. 2021) (**Figure 2.2**). An animal may be motivated to approach, avoid, or ignore another animal based on characteristics of both social partners such as sex or relative social standing and by the familiarity or novelty of the other moiety. vCA1 neurons can distinguish between a familiar and novel mouse, and targeted inhibition of either whole vCA1 or CA1-NAc projection neurons (but not vCA1-BLA) reduces discrimination between novel and familiar mice (Okuyama et al. 2016). In addition, vCA1 social memory neurons are reactivated during sharp-wave ripples (SWRs) offline, with a similar temporal pattern to that observed during online social interaction (Tao et al. 2022). Interestingly, in a mouse model for autism (Shank3 KO), the number of vCA1 social memory neurons is reduced, and the sequence of neurons reactivated during offline SWRs was disrupted, suggesting a role for vCA1 in social deficits of autism-related mouse models (Tao et al. 2022). In rats, vCA1 cells that respond when a rat interacts with a conspecific are sensitive to whisker touch interactions and ultrasonic vocalizations but show little response to an inanimate object (Rao et al. 2019). The vCA1-mPFC projection has also been implicated in social behavior—chemogenetic excitation of this pathway or overactivity (in a mouse model of Rett syndrome) produces deficits in discriminating a novel and a familiar mouse (Phillips, Robinson, and Pozzo-Miller 2019). Local silencing of PV-expressing interneurons in vCA1 can impair social discrimination, revealing an important role for local circuit dynamics in vCA1 storage of social memories. CA2 plays

a central role in encoding social information (Hitti and Siegelbaum 2014) and projects to vCA1, creating a local circuit known to be important for social memory (Meira et al. 2018). Other ventral hippocampal subregions, such as CA3, have also been linked to social memory (James P. Herman & Mueller, 2006). In contrast, the inhibition of dCA1 or the pathway from vCA1 to BLA does not affect social discrimination (Okuyama et al. 2016). Thus, specific pathways from vCA1 to NAc and mPFC are important for integrating external social cues with the internal motivation to interact with conspecifics **(Figure 2.3)**.

Human studies have hinted at the importance of the hippocampus in social relationships and interactions. In a game where power and affiliation were modeled as two dimensions of social distance, the left hippocampus represented social distance between the participant and virtual characters in the game (James P. Herman & Mueller, 2006; Myers et al., 2012). This signal was also influenced by the participant's personality traits—participants who reported less social avoidance and neuroticism showed stronger hippocampal tracking of the relative social standing. Future studies are needed to address the contributions of specific hippocampal subregions to social interaction.

Anterior hippocampus in psychiatric illness and mood

The human hippocampus has been studied for decades in relation to psychiatric illness, and the region plays an important role in the motivations to avoid danger, pursue reward, and seek social interaction, and to the formation of internal models of these three drives. Foundational work has shown decreased overall hippocampal volume in

psychiatric mood disorders (O'Doherty et al. 2015). More specifically, mood disorders have been associated with a decrease in the number of neurons of the anterior hippocampus (aHPC) which was reversible with antidepressant treatment (Boldrini et al. 2014).

The primate aHPC, while analogous to vHPC in rodents, is typically larger than the posterior hippocampus, features unique extensions like the uncus, and carries more hippocampal commissural connections (Zeidman and Maguire 2016; Maguire et al. 2000). Bulk sequencing shows transcriptional similarities and functional covariance between aHPC and brain networks active during social and emotional cognition and motivational tasks (Vogel et al. 2020). Single-nucleus sequencing of the human hippocampus has demonstrated that genes identified in gene-wide association studies and linked to major depression and bipolar disorder are significantly upregulated in the aHPC (Ayhan et al. 2021).

Depressed patients show reduced functional connectivity between the anterior/intermediate hippocampus and the insula/NAc, and symptoms of depression are positively correlated with aHPC-NAc connectivity (Nuria Daviu & Bains, 2021). Similarly, patients diagnosed with post-traumatic stress disorder (PTSD) display alterations in hippocampal functional connectivity. Resting-state functional connectivity of the hippocampus as a whole is not detectably different between PTSD patients and trauma-exposed controls without PTSD. However, separating the anterior and posterior hippocampus reveals differences in anterior-posterior connectivity between the hippocampus and the precuneus and posterior cingulate cortex in trauma-exposed controls, whereas PTSD patients lack these differences (Lazarov et al. 2017). In

another study, veterans with PTSD showed an inverse correlation between PTSD symptoms and the anatomical and functional connectivity of the aHPC, with symptoms of hypervigilance being positively associated with reduced anatomical connectivity between the aHPC and the prefrontal cortex (Abdallah et al. 2017). At the functional level, a meta-analysis of fMRI activation in the brains of PTSD patients revealed greater aHPC activity during each of the phases of fear conditioning: conditioning, extinction, and recall (Suarez-Jimenez et al. 2020). Finally, in a human intracranial EEG study, increased variance in HPC-amygdala coherence at the beta frequency range could predict a worsening in the subjective mood of a patient subset (Kirkby et al. 2018).

Together, these studies show predispositions and alterations in aHPC structure and activity that correspond to alterations in human behavior and motivational drives. Future studies linking these changes to actionable biomarkers could be used to pinpoint the early stages of psychiatric disorders when symptoms and changes in hippocampal structure are less pronounced and potentially more treatable.

Conclusion

In recent years, there has been an increasing interest in the vHPC's role in motivated and emotional behaviors. This paper reviews several important studies that have dissected the principles of the inputs and outputs of vCA1 and highlighted how distinct output streams may represent diverse features of an explored space to drive adaptive behaviors. However, a number of questions remain. First, how ensembles of vCA1 neurons interact to encode divergent behavioral states remains unknown. How these dynamics map on to the well-described anatomy of vCA1 also remains

understudied (**Figure 2.3**). Second, it is not well understood how emotional state (such as chronic stress, antidepressant treatment, and exercise) impacts the encoding properties of anatomically and functionally defined ensembles described here. Finally, as anxiety is fundamentally a response to diffuse and unknown threats that may elicit harm in the future, it remains important to understand how prospective coding in the vHPC relates to its role in anxiety-related behavior. Functional MRI studies in humans have suggested that the aHPC can recombine details from past experience to construct an imagined future (Addis and Schacter 2011). In dCA1, there is a rapid alternation between the representation of possible future goal locations (Kay et al. 2020); in vCA1, future research will determine how prospective coding represents safe versus aversive options. Understanding these phenomena may explain why individuals with mood and anxiety disorders generate less positive and less detailed imagined futures (Dere et al. 2018; Miloyan, Pachana, and Suddendorf 2014; Moustafa, Morris, and ElHaj 2018). Together, future studies dissecting the cell types, population activity patterns, and behavioral functions of CA1 circuits will undoubtedly enrich our understanding of emotional and motivated states in health and disease.

References for Chapter 2

- Abdallah, C. G., K. M. Wrocklage, C. L. Averill, T. Akiki, B. Schweinsburg, A. Roy, B. Martini, S. M. Southwick, J. H. Krystal, and J. C. Scott. 2017. "Anterior Hippocampal Dysconnectivity in Posttraumatic Stress Disorder: A Dimensional and Multimodal Approach." *Translational Psychiatry* 7 (2): e1045.
- Addis, Donna Rose, and Daniel L. Schacter. 2011. "The Hippocampus and Imagining the Future: Where Do We Stand?" *Frontiers in Human Neuroscience* 5: 173.
- Adhikari, Avishek, Mihir A. Topiwala, and Joshua A. Gordon. 2010. "Synchronized Activity between the Ventral Hippocampus and the Medial Prefrontal Cortex during Anxiety." *Neuron* 65 (2): 257–69.
- . 2011. "Single Units in the Medial Prefrontal Cortex with Anxiety-Related Firing Patterns Are Preferentially Influenced by Ventral Hippocampal Activity." *Neuron* 71 (5): 898–910.
- AlSubaie, Rawan, Ryan Ws Wee, Anne Ritoux, Karyna Mishchanchuk, Jessica Passlack, Daniel Regester, and Andrew F. MacAskill. 2021. "Control of Parallel Hippocampal Output Pathways by Amygdalar Long-Range Inhibition." *ELife* 10 (November). <https://doi.org/10.7554/eLife.74758>.
- Arszovszki, Antónia, Zsolt Borhegyi, and Thomas Klausberger. 2014. "Three Axonal Projection Routes of Individual Pyramidal Cells in the Ventral CA1 Hippocampus." *Frontiers in Neuroanatomy* 8 (June): 53.
- Ayhan, Fatma, Ashwinikumar Kulkarni, Stefano Berto, Karthigayini Sivaprakasam, Connor Douglas, Bradley C. Lega, and Genevieve Konopka. 2021. "Resolving

Cellular and Molecular Diversity along the Hippocampal Anterior-to-Posterior Axis in Humans.” *Neuron* 109 (13): 2091-2105.e6.

Bagot, Rosemary C., Eric M. Parise, Catherine J. Peña, Hong-Xing Zhang, Ian Maze, Dipesh Chaudhury, Brianna Persaud, et al. 2015. “Ventral Hippocampal Afferents to the Nucleus Accumbens Regulate Susceptibility to Depression.” *Nature Communications* 6 (May): 7062.

Barfield, Elizabeth T., and Shannon L. Gourley. 2019. “Glucocorticoid-Sensitive Ventral Hippocampal-Orbitofrontal Cortical Connections Support Goal-Directed Action - Curt Richter Award Paper 2019.” *Psychoneuroendocrinology* 110 (104436): 104436.

Biane, Jeremy S., Max A. Ladow, Fabio Stefanini, Sayi P. Boddu, Austin Fan, Shazreh Hassan, Naz Dundar, et al. 2023. “Neural Dynamics Underlying Associative Learning in the Dorsal and Ventral Hippocampus.” *Nature Neuroscience* 26 (5): 798–809.

Boldrini, Maura, Tanya H. Butt, Adrienne N. Santiago, Hadassah Tamir, Andrew J. Dwork, Gorazd B. Rosoklija, Victoria Arango, René Hen, and J. John Mann. 2014. “Benzodiazepines and the Potential Trophic Effect of Antidepressants on Dentate Gyrus Cells in Mood Disorders.” *The International Journal of Neuropsychopharmacology* 17 (12): 1923–33.

Chiang, Ming-Ching, Arthur J. Y. Huang, Marie E. Wintzer, Toshio Ohshima, and Thomas J. McHugh. 2018. “A Role for CA3 in Social Recognition Memory.” *Behavioural Brain Research* 354 (November): 22–30.

- Ciocchi, S., J. Passecker, H. Malagon-Vina, N. Mikus, and T. Klausberger. 2015. "Brain Computation. Selective Information Routing by Ventral Hippocampal CA1 Projection Neurons." *Science* 348 (6234): 560–63.
- Cullinan, W. E., J. P. Herman, and S. J. Watson. 1993. "Ventral Subicular Interaction with the Hypothalamic Paraventricular Nucleus: Evidence for a Relay in the Bed Nucleus of the Stria Terminalis." *The Journal of Comparative Neurology* 332 (1): 1–20.
- Dere, Ekrem, Dorothea Dere, Maria Angelica de Souza Silva, Joseph P. Huston, and Armin Zlomuzica. 2018. "Fellow Travellers: Working Memory and Mental Time Travel in Rodents." *Behavioural Brain Research* 352 (October): 2–7.
- Fanselow, Michael S., and Hong-Wei Dong. 2010. "Are the Dorsal and Ventral Hippocampus Functionally Distinct Structures?" *Neuron* 65 (1): 7–19.
- Gergues, Mark M., Kasey J. Han, Hye Sun Choi, Brandon Brown, Kelsey J. Clausing, Victoria S. Turner, Ilia D. Vainchtein, Anna V. Molofsky, and Mazen A. Kheirbek. 2020. "Circuit and Molecular Architecture of a Ventral Hippocampal Network." *Nature Neuroscience* 23 (11): 1444–52.
- Glangetas, Christelle, Léma Massi, Giulia R. Fois, Marion Jalabert, Delphine Girard, Marco Diana, Keisuke Yonehara, et al. 2017. "NMDA-Receptor-Dependent Plasticity in the Bed Nucleus of the Stria Terminalis Triggers Long-Term Anxiolysis." *Nature Communications* 8 (February): 14456.
- Graham, Jalina, Alexa F. D'Ambra, Se Jung Jung, Yusuke Teratani-Ota, Nina Vishwakarma, Rasika Venkatesh, Abhijna Parigi, Evan G. Antzoulatos, Diasynou Fioravante, and Brian J. Wiltgen. 2021. "High-Frequency Stimulation of Ventral

- CA1 Neurons Reduces Amygdala Activity and Inhibits Fear.” *Frontiers in Behavioral Neuroscience* 15 (March): 595049.
- Hitti, Frederick L., and Steven A. Siegelbaum. 2014. “The Hippocampal CA2 Region Is Essential for Social Memory.” *Nature* 508 (7494): 88–92.
- Hu, Jun, Jiahui Liu, Yu Liu, Xianran Wu, Kaixiang Zhuang, Qunlin Chen, Wenjing Yang, Peng Xie, Jiang Qiu, and Dongtao Wei. 2021. “Dysfunction of the Anterior and Intermediate Hippocampal Functional Network in Major Depressive Disorders across the Adult Lifespan.” *Biological Psychology* 165 (108192): 108192.
- Jacobson, L., and R. Sapolsky. 1991. “The Role of the Hippocampus in Feedback Regulation of the Hypothalamic-Pituitary-Adrenocortical Axis.” *Endocrine Reviews* 12 (2): 118–34.
- Jimenez, Jessica C., Jack E. Berry, Sean C. Lim, Samantha K. Ong, Mazen A. Kheirbek, and Rene Hen. 2020. “Contextual Fear Memory Retrieval by Correlated Ensembles of Ventral CA1 Neurons.” *Nature Communications* 11 (1): 3492.
- Jimenez, Jessica C., Katy Su, Alexander R. Goldberg, Victor M. Luna, Jeremy S. Biane, Gokhan Ordek, Pengcheng Zhou, et al. 2018. “Anxiety Cells in a Hippocampal-Hypothalamic Circuit.” *Neuron* 97 (3): 670-683.e6.
- Kay, Kenneth, Jason E. Chung, Marielena Sosa, Jonathan S. Schor, Mattias P. Karlsson, Margaret C. Larkin, Daniel F. Liu, and Loren M. Frank. 2020. “Constant Sub-Second Cycling between Representations of Possible Futures in the Hippocampus.” *Cell* 180 (3): 552-567.e25.

- Kheirbek, Mazen A., Liam J. Drew, Nesha S. Burghardt, Daniel O. Costantini, Lindsay Tannenholz, Susanne E. Ahmari, Hongkui Zeng, André A. Fenton, and René Hen. 2013. “Differential Control of Learning and Anxiety along the Dorsoventral Axis of the Dentate Gyrus.” *Neuron* 77 (5): 955–68.
- Kim, Woong Bin, and Jun-Hyeong Cho. 2017. “Synaptic Targeting of Double-Projecting Ventral CA1 Hippocampal Neurons to the Medial Prefrontal Cortex and Basal Amygdala.” *The Journal of Neuroscience: The Official Journal of the Society for Neuroscience* 37 (19): 4868–82.
- Kirkby, Lowry A., Francisco J. Luongo, Morgan B. Lee, Mor Nahum, Thomas M. Van Vleet, Vikram R. Rao, Heather E. Dawes, Edward F. Chang, and Vikaas S. Sohal. 2018. “An Amygdala-Hippocampus Subnetwork That Encodes Variation in Human Mood.” *Cell* 175 (6): 1688-1700.e14.
- Kjaerby, Celia, Jegath Athilingam, Sarah E. Robinson, Jillian Iafrati, and Vikaas S. Sohal. 2016. “Serotonin 1B Receptors Regulate Prefrontal Function by Gating Callosal and Hippocampal Inputs.” *Cell Reports* 17 (11): 2882–90.
- Kjelstrup, Kirsten G., Frode A. Tuvnes, Hill-Aina Steffenach, Robert Murison, Edvard I. Moser, and May-Britt Moser. 2002. “Reduced Fear Expression after Lesions of the Ventral Hippocampus.” *Proceedings of the National Academy of Sciences of the United States of America* 99 (16): 10825–30.
- Lazarov, Amit, Xi Zhu, Benjamin Suarez-Jimenez, Bret R. Rutherford, and Yuval Neria. 2017. “Resting-State Functional Connectivity of Anterior and Posterior Hippocampus in Posttraumatic Stress Disorder.” *Journal of Psychiatric Research* 94 (November): 15–22.

- Lee, Sang-Hun, Ivan Marchionni, Marianne Bezaire, Csaba Varga, Nathan Danielson, Matthew Lovett-Barron, Attila Losonczy, and Ivan Soltesz. 2014. "Parvalbumin-Positive Basket Cells Differentiate among Hippocampal Pyramidal Cells." *Neuron* 82 (5): 1129–44.
- LeGates, Tara A., Mark D. Kvarta, Jessica R. Tooley, T. Chase Francis, Mary Kay Lobo, Meaghan C. Creed, and Scott M. Thompson. 2018. "Reward Behaviour Is Regulated by the Strength of Hippocampus-Nucleus Accumbens Synapses." *Nature* 564 (7735): 258–62.
- Maguire, E. A., D. G. Gadian, I. S. Johnsrude, C. D. Good, J. Ashburner, R. S. Frackowiak, and C. D. Frith. 2000. "Navigation-Related Structural Change in the Hippocampi of Taxi Drivers." *Proceedings of the National Academy of Sciences of the United States of America* 97 (8): 4398–4403.
- McNaughton, Bruce L., Francesco P. Battaglia, Ole Jensen, Edvard I. Moser, and May-Britt Moser. 2006. "Path Integration and the Neural Basis of the 'Cognitive Map.'" *Nature Reviews. Neuroscience* 7 (8): 663–78.
- Meira, Torcato, Felix Leroy, Eric W. Buss, Azahara Oliva, Jung Park, and Steven A. Siegelbaum. 2018. "A Hippocampal Circuit Linking Dorsal CA2 to Ventral CA1 Critical for Social Memory Dynamics." *Nature Communications* 9 (1): 4163.
- Miloyan, Beyon, Nancy A. Pachana, and Thomas Suddendorf. 2014. "The Future Is Here: A Review of Foresight Systems in Anxiety and Depression." *Cognition & Emotion* 28 (5): 795–810.
- Montagrin, Alison, Catarina Saiote, and Daniela Schiller. 2018. "The Social Hippocampus." *Hippocampus* 28 (9): 672–79.

- Moustafa, Ahmed A., Alejandro N. Morris, and Mohamad ElHaj. 2018. "A Review on Future Episodic Thinking in Mood and Anxiety Disorders." *Reviews in the Neurosciences* 30 (1): 85–94.
- Muir, Jessie, Yiu Chung Tse, Eshaan S. Iyer, Julia Biris, Vedrana Cvetkovska, Joëlle Lopez, and Rosemary C. Bagot. 2020. "Ventral Hippocampal Afferents to Nucleus Accumbens Encode Both Latent Vulnerability and Stress-Induced Susceptibility." *Biological Psychiatry* 88 (11): 843–54.
- Nyberg, Nils, Éléonore Duvelle, Caswell Barry, and Hugo J. Spiers. 2022. "Spatial Goal Coding in the Hippocampal Formation." *Neuron* 110 (3): 394–422.
- O'Doherty, Daniel C. M., Kate M. Chitty, Sonia Saddiqui, Maxwell R. Bennett, and Jim Lagopoulos. 2015. "A Systematic Review and Meta-Analysis of Magnetic Resonance Imaging Measurement of Structural Volumes in Posttraumatic Stress Disorder." *Psychiatry Research* 232 (1): 1–33.
- O'Keefe, John, and Lynn Nadel. 1978. *The Hippocampus as a Cognitive Map*. London, England: Oxford University Press.
- Okuyama, Teruhiro, Takashi Kitamura, Dheeraj S. Roy, Shigeyoshi Itohara, and Susumu Tonegawa. 2016. "Ventral CA1 Neurons Store Social Memory." *Science* 353 (6307): 1536–41.
- Oleksiak, Cecily R., Karthik R. Ramanathan, Olivia W. Miles, Sarah J. Perry, Stephen Maren, and Justin M. Moscarello. 2021. "Ventral Hippocampus Mediates the Context-Dependence of Two-Way Signaled Avoidance in Male Rats." *Neurobiology of Learning and Memory* 183 (September): 107458.

- Padilla-Coreano, Nancy, Scott S. Bolkan, Georgia M. Pierce, Dakota R. Blackman, William D. Hardin, Alvaro L. Garcia-Garcia, Timothy J. Spellman, and Joshua A. Gordon. 2016. "Direct Ventral Hippocampal-Prefrontal Input Is Required for Anxiety-Related Neural Activity and Behavior." *Neuron* 89 (4): 857–66.
- Park, Alan J., Alexander Z. Harris, Kelly M. Martyniuk, Chia-Yuan Chang, Atheir I. Abbas, Daniel C. Lowes, Christoph Kellendonk, Joseph A. Gogos, and Joshua A. Gordon. 2021. "Reset of Hippocampal-Prefrontal Circuitry Facilitates Learning." *Nature* 591 (7851): 615–19.
- Phillips, Mary L., Holly Anne Robinson, and Lucas Pozzo-Miller. 2019. "Ventral Hippocampal Projections to the Medial Prefrontal Cortex Regulate Social Memory." *ELife* 8 (May). <https://doi.org/10.7554/eLife.44182>.
- Poppenk, Jordan, Hallvard R. Evensmoen, Morris Moscovitch, and Lynn Nadel. 2013. "Long-Axis Specialization of the Human Hippocampus." *Trends in Cognitive Sciences* 17 (5): 230–40.
- Radley, Jason J., and Paul E. Sawchenko. 2011. "A Common Substrate for Prefrontal and Hippocampal Inhibition of the Neuroendocrine Stress Response." *The Journal of Neuroscience: The Official Journal of the Society for Neuroscience* 31 (26): 9683–95.
- . 2015. "Evidence for Involvement of a Limbic Paraventricular Hypothalamic Inhibitory Network in Hypothalamic-Pituitary-Adrenal Axis Adaptations to Repeated Stress." *The Journal of Comparative Neurology* 523 (18): 2769–87.

- Rao, Rajnish P., Moritz von Heimendahl, Viktor Bahr, and Michael Brecht. 2019. "Neuronal Responses to Conspecifics in the Ventral CA1." *Cell Reports* 27 (12): 3460-3472.e3.
- Reed, Sean J., Christopher K. Lafferty, Jesse A. Mendoza, Angela K. Yang, Thomas J. Davidson, Logan Grosenick, Karl Deisseroth, and Jonathan P. Britt. 2018. "Coordinated Reductions in Excitatory Input to the Nucleus Accumbens Underlie Food Consumption." *Neuron* 99 (6): 1260-1273.e4.
- Sánchez-Bellot, Candela, Rawan AlSubaie, Karyna Mishchanchuk, Ryan W. S. Wee, and Andrew F. MacAskill. 2022. "Two Opposing Hippocampus to Prefrontal Cortex Pathways for the Control of Approach and Avoidance Behaviour." *Nature Communications* 13 (1): 339.
- Shpokayte, Monika, Olivia McKissick, Xiaonan Guan, Bingbing Yuan, Bahar Rahsepar, Fernando R. Fernandez, Evan Ruesch, et al. 2022. "Hippocampal Cells Segregate Positive and Negative Engrams." *Communications Biology* 5 (1): 1009.
- Sosa, Marielena, and Lisa M. Giocomo. 2021. "Navigating for Reward." *Nature Reviews. Neuroscience* 22 (8): 472–87.
- Sosa, Marielena, Hannah R. Joo, and Loren M. Frank. 2020. "Dorsal and Ventral Hippocampal Sharp-Wave Ripples Activate Distinct Nucleus Accumbens Networks." *Neuron* 105 (4): 725-741.e8.
- Strange, Bryan A., Menno P. Witter, Ed S. Lein, and Edvard I. Moser. 2014. "Functional Organization of the Hippocampal Longitudinal Axis." *Nature Reviews. Neuroscience* 15 (10): 655–69.

- Suarez, Andrea N., Clarissa M. Liu, Alyssa M. Cortella, Emily E. Noble, and Scott E. Kanoski. 2020. "Ghrelin and Orexin Interact to Increase Meal Size through a Descending Hippocampus to Hindbrain Signaling Pathway." *Biological Psychiatry* 87 (11): 1001–11.
- Suarez-Jimenez, Benjamin, Anton Albajes-Eizagirre, Amit Lazarov, Xi Zhu, Ben J. Harrison, Joaquim Radua, Yuval Neria, and Miquel A. Fullana. 2020. "Neural Signatures of Conditioning, Extinction Learning, and Extinction Recall in Posttraumatic Stress Disorder: A Meta-Analysis of Functional Magnetic Resonance Imaging Studies." *Psychological Medicine* 50 (9): 1442–51.
- Tao, Kentaro, Myung Chung, Akiyuki Watarai, Ziyang Huang, Mu-Yun Wang, and Teruhiro Okuyama. 2022. "Disrupted Social Memory Ensembles in the Ventral Hippocampus Underlie Social Amnesia in Autism-Associated Shank3 Mutant Mice." *Molecular Psychiatry* 27 (4): 2095–2105.
- Tavares, Rita Morais, Avi Mendelsohn, Yael Grossman, Christian Hamilton Williams, Matthew Shapiro, Yaacov Trope, and Daniela Schiller. 2015. "A Map for Social Navigation in the Human Brain." *Neuron* 87 (1): 231–43.
- Terranova, Joseph I., Jun Yokose, Hisayuki Osanai, William D. Marks, Jun Yamamoto, Sachie K. Ogawa, and Takashi Kitamura. 2022. "Hippocampal-Amygdala Memory Circuits Govern Experience-Dependent Observational Fear." *Neuron* 110 (8): 1416-1431.e13.
- Trouche, Stéphanie, Vadim Koren, Natalie M. Doig, Tommas J. Ellender, Mohamady El-Gaby, Vítor Lopes-dos-Santos, Hayley M. Reeve, et al. 2019. "A Hippocampus-

- Accumbens Tripartite Neuronal Motif Guides Appetitive Memory in Space.” *Cell* 0 (0). <https://doi.org/10.1016/j.cell.2018.12.037>.
- Vogel, Jacob W., Renaud La Joie, Michel J. Grothe, Alexandr Diaz-Papkovich, Andrew Doyle, Etienne Vachon-Presseau, Claude Lepage, et al. 2020. “A Molecular Gradient along the Longitudinal Axis of the Human Hippocampus Informs Large-Scale Behavioral Systems.” *Nature Communications* 11 (1): 960.
- Wang, Qian, Jingji Jin, and Stephen Maren. 2016. “Renewal of Extinguished Fear Activates Ventral Hippocampal Neurons Projecting to the Prelimbic and Infralimbic Cortices in Rats.” *Neurobiology of Learning and Memory* 134 Pt A (October): 38–43.
- Watarai, Akiyuki, Kentaro Tao, Mu-Yun Wang, and Teruhiro Okuyama. 2021. “Distinct Functions of Ventral CA1 and Dorsal CA2 in Social Memory.” *Current Opinion in Neurobiology* 68 (June): 29–35.
- Wee, Ryan W. S., and Andrew F. MacAskill. 2020. “Biased Connectivity of Brain-Wide Inputs to Ventral Subiculum Output Neurons.” *Cell Reports* 30 (11): 3644-3654.e6.
- Wee, Ryan W. S., Karyna Mishchanchuk, Rawan AlSubaie, and Andrew F. MacAskill. 2021. “Internal State Dependent Control of Feeding Behaviour via Hippocampal Ghrelin Signalling.” *BioRxiv*. <https://doi.org/10.1101/2021.11.05.467326>.
- Woods, Nicholas I., Fabio Stefanini, Daniel L. Apodaca-Montano, Isabelle M. C. Tan, Jeremy S. Biane, and Mazen A. Kheirbek. 2020. “The Dentate Gyrus Classifies Cortical Representations of Learned Stimuli.” *Neuron* 107 (1): 173-184.e6.

Xia, Frances, and Mazen A. Kheirbek. 2020. "Circuit-Based Biomarkers for Mood and Anxiety Disorders." *Trends in Neurosciences* 43 (11): 902–15.

Xu, Chun, Sabine Krabbe, Jan Gründemann, Paolo Botta, Jonathan P. Fadok, Fumitaka Osakada, Dieter Saur, et al. 2016. "Distinct Hippocampal Pathways Mediate Dissociable Roles of Context in Memory Retrieval." *Cell* 167 (4): 961-972.e16.

Yang, Angela K., Jesse A. Mendoza, Christopher K. Lafferty, Franca Lacroix, and Jonathan P. Britt. 2020. "Hippocampal Input to the Nucleus Accumbens Shell Enhances Food Palatability." *Biological Psychiatry* 87 (7): 597–608.

Zeidman, Peter, and Eleanor A. Maguire. 2016. "Anterior Hippocampus: The Anatomy of Perception, Imagination and Episodic Memory." *Nature Reviews Neuroscience* 17 (3): 173–82.

Chapter 3: Hypothalamic CRH Cells and Ventral Hippocampus Differentially

Encode External Threat and Acute Stress

Introduction

The corticotropin-releasing-hormone (CRH) cells of the hypothalamus gate the release of circulating stress hormones that are essential to an organism's stress response (Herman & Mueller, 2006). Recently, the first in vivo recordings of CRH neurons established that they respond in seconds to stressful stimuli and are important mediators of the rapid behavioral responses to stress, in addition to their role in the slow release of stress hormones (J. Kim et al., 2019; Vom Berg-Maurer et al., 2016; Yuan et al., 2019).

However, it is unknown how the CRH cells respond to other self-initiated types of stressors. To explore this question, we recorded CRH activity in the elevated plus maze, a task widely used to study anxiety as well as stress-induced changes in behavior (Walf & Frye, 2007). To the best of our knowledge, there are no recordings of PVN^{CRH} cells while a mouse explores this arena, though it is known that undergoing the assay causes increases in stress hormones downstream of the PVN^{CRH} cells (File et al., 1994; Rodgers et al., 1999) and that stimulation of PVN^{CRH} cells in the similar open field assay can reduce time in the exposed center area (Füzesi et al., 2016). In addition, mice placed in an open arm of the elevated plus maze, without the ability to explore the maze, experience an increase in PVN^{CRH} activity (Li et al., 2020).

We also recorded an upstream area, the ventral hippocampus (vHPC), which is a known modulator of the stress axis (Herman & Mueller, 2006; Myers et al., 2012) and responds strongly to exploration of the elevated plus maze (Ciocchi et al., 2015; Jimenez et al., 2018). Using this approach, we were able to describe PVN^{CRH} cell activity as well as activity of an upstream region, the vHPC cells, during novel and established behavioral assays.

We anticipated that the CRH cells activity would align with exploration of potentially threatening locations, given recent papers demonstrating rapid changes in CRH activity after a mouse encounters positive or negative stimuli (J. Kim et al., 2019; S. Xu et al., 2020; Yuan et al., 2019) and increases in CRH activity observed when an animal is placed within a single open arm (Li et al., 2020). We also predicted that vHPC cells would generally respond inversely to PVN^{CRH} cells, given the modulatory disynaptic input that is thought to inhibit the stress response through PVN^{CRH} cells (Cole et al., 2022; Myers et al., 2012; Radley & Sawchenko, 2011).

Methods

Animals

Male and female Crh-IRES-Cre hemizygous mice were bred from pairs of homozygous Crh-IRES-Cre mice (*B6(Cg)-Crhtm1(cre)Zjh/J*, Jax #012704, *RRID:IMSR_JAX:012704*) and C57BL/6 mice (The Jackson Laboratory). Mice were housed under a 12 h light/dark cycle with ad libitum access to food and water. All experiments were conducted during the light cycle in accordance with the U.S. National Institutes of Health Guide for the Care and Use of Laboratory Animals and the

institutional Animal Care and Use Committees at University of California, San Francisco.

Surgical procedures

At 8-12 weeks old, mice were injected unilaterally with AAV1-syn-jGCaMP7s-WPRE in the ventral hippocampus (vHPC) and Cre-dependent AAV1-syn-FLEX-jGCaMP7s-WPRE (Addgene) in the paraventricular nucleus of the hypothalamus (PVN) at the following stereotaxic coordinates: *PVN* AP -0.6, ML -0.2, DV -4.9 (64 nL), DV -4.8 (32 nL), DV - 4.7(128 nL) from bregma; *vHPC* AP -3.20 ML +3.35, DV -3.85 (32 nL), DV -3.75 (96 nL), -3.65 (32 nL) from cortical surface. During surgery, mice were anesthetized with 1.5% isoflurane and then head-fixed in a stereotaxic frame (David Kopf). Craniotomies were made with a round 0.5-mm drill bit (David Kopf), and a Nanoject II syringe (Drummond Scientific) was used with a pulled glass pipette to inject virus. Following viral injection and a diffusion period of 10 minutes, the viral injection pipette was withdrawn, and a fiber optic photometry cannula (\varnothing 400 μ m, Doric Lenses) was implanted over each of the two brain regions (*PVN* DV -4.60 from bregma, *vHPC* DV -3.75 from cortical surface) and secured with dental cement (C&B Metabond, Parkell).

All mice were administered lidocaine, meloxicam, and buprenorphine during surgery and post-surgical care. Mice recovered for at least 5 weeks and were habituated to handling before experiments began. Experiments began after observing a clear increase in PVN^{CRH} activity when a mouse was picked up by the tail.

Behavioral experiments

On the day of each experiment, mice were habituated outside the colony in a quiet room for 1-2 hours. Fiber photometry optical fibers were bleached for a minimum of 2 hours before each recording. *Foot shock assay*. Animals underwent the shock paradigm in operant chambers (Med Associates) using FreezeFrame software system (Actimetrics) as follows: 3 shocks (2 sec each, 0.75 mA, 100 sec inter-shock interval) delivered through floor bars, with the first at 15 minutes. Each trial was 50 minutes long total, included pre and post shock periods. *Elevated plus maze*. Animals were first recorded in their homecage for 2-5 min. Animals were then transferred to the center of an elevated plus maze arena (150 lux) and remained in the arena while photometry recording took place for the duration of the experiment (10-15 min).

Animals were recorded in the elevated plus maze assay before foot shock to assess innate anxiety responses prior to any experience of shock.

Signal processing

Recordings were performed using Synapse software with an RZ5P processor (Tucker-Davis Technologies) and optical components (LED drivers, LEDs, photoreceivers, Doric Lenses). Two sets of excitation LEDs at 465 nm and 405 nm were sinusoidally modulated and relayed through respective filtered fluorescence minicubes (Doric Lenses). All signals were acquired at 10 kHz and downsampled to 10 Hz during analysis to match the behavioral video recorded at 10 Hz.

Calculation of df/f was performed as described previously by fitting each UV signal to its corresponding GCaMP signal with a linear fit and subtracting the fitted UV from the GCaMP signal. (Lerner et al., 2015)

Photometry recordings were excluded from analysis if df/f range was less than 10% or if recording noise level was larger than signal by visual inspection as in (Murphy et al., 2023). In the case of animals with implants in two brain areas where one area's signal did not meet quality requirements, recordings from the brain region with good quality were excluded from intra-animal analysis but included in pooled analysis of brain area activity where within-animal effects were not considered. The artifacts created at the start and end of each recording (approximately 3 seconds) were replaced with NaNs.

After df/f calculation and z-scoring across the session, session-length analysis was carried out on the signal (such as average signal across all open arm time). For peri-event average analysis, a linear fit was first performed and subtracted from the z-scored df/f across the session to remove bleaching during the experiment using `scipy.signal.detrend`. The signal was then smoothed with a Savitsky-Golay filter using a window length of 11 and polynomial order of 2, and z-scored to the baseline period when analysis normalized for baseline.

Behavioral analysis

Foot shock assay. Mobility and freezing were manually scored using the manual scoring module of Ethovision XT, version 17 (Noldus). Shock times and the start and end of session were manually scored using VLC (VideoLan), where scoring was

performed based on a cue light that went on during each shock and for 2 seconds at the start and end of the session. Behavioral annotation was performed blinded to experimental group.

Elevated plus maze assay. Time spent, zone entries, speed, distance traveled, and latency to first entries into zones were analyzed using Ethovision XT (Noldus).

Annotation of behavioral motifs in the elevated plus maze (**Table 1**) was

Table 1: Exploratory and anxiety-related behaviors in the elevated plus maze

<i>Behavioral Motif</i>	<i>Operational Definition</i>
Avoid	Stretching movement where the mouse extends its body forward and ultimately retracts back into the position of the rear legs. (elongation, followed by retraction)
Approach	Stretching movement where the mouse extends its body forward and ultimately begins walking forward (elongation, followed by locomotion forward).
Head dip	Casting movement when a mouse moves its nose in a curve, especially to see around a corner or to scan its surroundings. In open arms, when the mouse moves its head past the edge of the arena in a similar movement.
Contraction	Contraction of body and/or short twitching movement of the head, ending in the same posture and typically when the animal is stationary.
Rearing	Rearing onto back legs, with one or more paws placed onto the wall of the arena.
Grooming	Stereotypical allogrooming motions, including licking fur or skin and creating symmetric or asymmetric arm sweeps over the face, head, and body.

performed using Observer XT 14 (Noldus) by two experimenters. Each experimenter was assigned to annotate specific behaviors in order to minimize variability, as inter-

rater variability has been shown to be greater than intra-rater variability (Segalin et al., 2021). Behavioral annotation was performed blinded to experimental group.

Quantification and statistical analysis

General data analysis and graphing was performed using custom Python code, and statistical testing was performed using Prism 9 (Graphpad).

For transitions between zones in the elevated plus maze, activity was normalized to the baseline -4 to 0 sec (baseline z-score) or to the entire session in the elevated plus maze (session z-score). Trajectories were defined as when the center of the mouse moved from an arm into the center and then out of the center; the activity was then aligned to the moment the center of the mouse moved from a starting arm to the center. A given trajectory was included for averaging and plotting if a mouse spent the entire baseline from -4 to 0 seconds in a specified arm and spent the entire post period from 0 to 4 sec in the center and destination arm.

For behavioral motifs, calcium activity traces were calculated based on the start or end of a given behavior. Activity was normalized to the baseline -8 to -4 sec in order not to wash out effects in the time window -4 to 0 sec. Grooming and rearing were filtered for behavioral motifs that lasted for a minimum of 2 sec. Significance was defined as p values below 0.05.

Verification of imaging sites and histology

Expression of viruses was confirmed for all animals included in the study. Mice were injected with 2:1 ketamine/xylazine solution intraperitoneally, then perfused

transcardially with saline and then 4% paraformaldehyde solution. Brains were extracted and placed in 4% paraformaldehyde for 2-5 days, then transferred to 30% sucrose until equilibrated to the solution. Coronal slices of 35-50 μm were collected on an SM2000 microtome (Leica) and mounted on glass slides for imaging.

Results

To establish the moment-to-moment relationship between vHPC and PVN^{CRH} activity during different stressful experiences, we expressed the calcium indicator GCaMP7s in both areas and recorded the signal using fiber photometry in mice subjected to the foot shock assay and the elevated plus maze assay (**Figure 3.1**). The foot shock assay imposes an inescapable and uncontrollable stress. By contrast, the elevated plus maze is an approach-avoidance assay used to test elements of innate anxiety; it exposes mice to a self-initiated, mild level of stress with ambiguous threats.

Both the foot shock assay and the elevated plus maze trigger the release of corticosteroids (Dos Santos Corrêa et al., 2019; File et al., 1994; Rodgers et al., 1999), making these assays suitable for our study of circuits underlying the HPA stress response. Our main question was how PVN^{CRH} cells respond to a stressor like the elevated plus maze. We predicted that the activity in both areas would distinguish when a mouse is located in high- and low-threat areas.

Both ventral hippocampus and hypothalamic CRH activity rise when mice experience large uncontrollable stressors

First, we confirmed previous work that shows PVN^{CRH} cells respond to stressful stimuli. Foot shocks produced large and rapid responses in the PVN^{CRH} neurons (**Figure 3.2B**). vHPC cells also responded rapidly to both stimuli (**Figure 3.2B**).

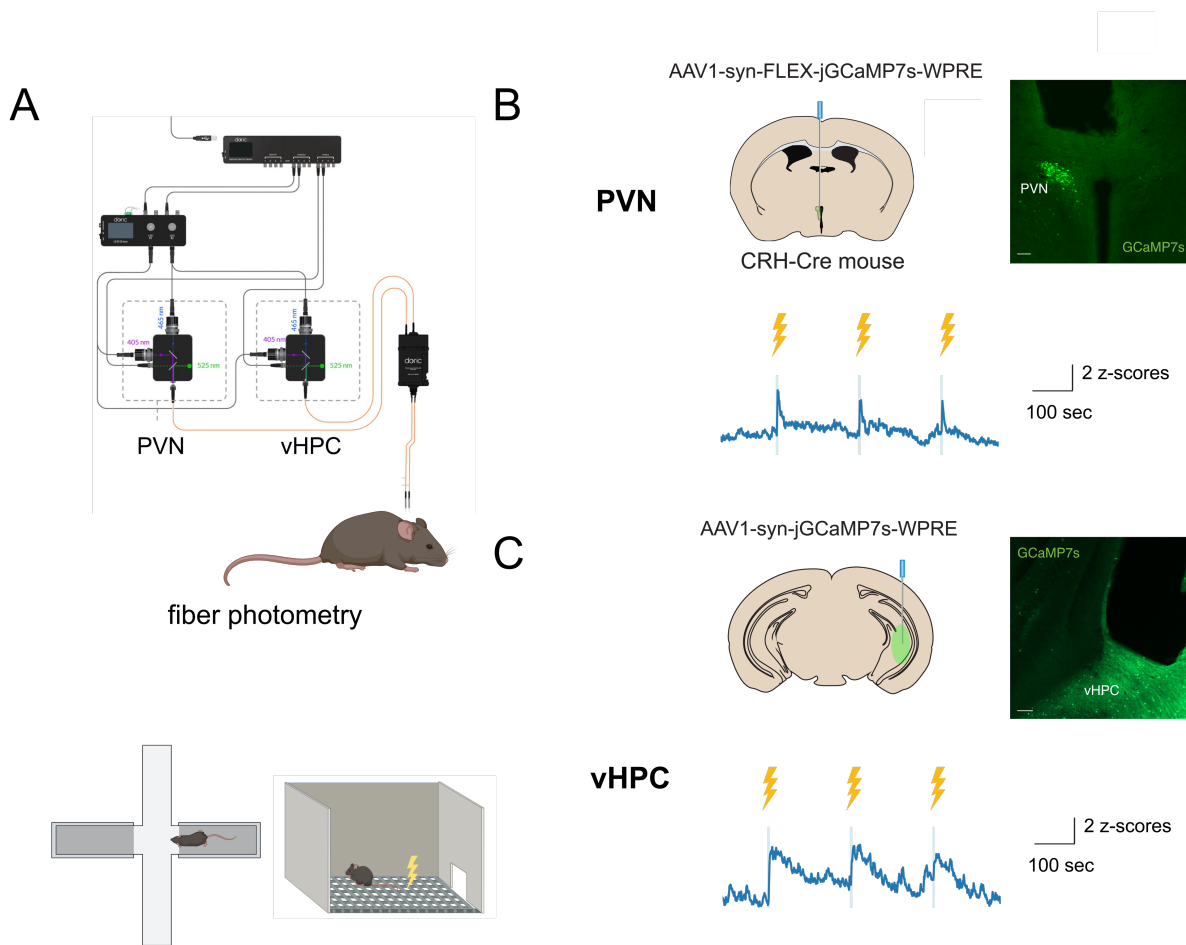


Figure 3.1. Recording neural activity in PVN^{CRH} and vHPC during elevated plus maze and foot shock assay. (A) Diagram of dual photometry recording setup and behavioral assays. (B) Viral strategy to record from populations of CRH cells in PVN. Viral expression of GCaMP indicator and example traces in response to a series of foot shocks. Blue bars indicate shocks. (C) Viral strategy to record from general cell population in vHPC. Viral expression of GCaMP indicator in vHPC and example traces in response to a series of foot shocks. Blue bars indicate timing of shocks. Scale bars, 100 μ m.

Interestingly, the PVN^{CRH} cells return to baseline activity more quickly and overshoot their baseline level, while vHPC cells remain elevated in activity for much longer. Next, we assessed the activity in both areas during an active coping behavior, freezing. PVN^{CRH} cells tended to increase in activity, though not consistently, and vHPC cells ramped up in activity before the start of a freezing bout (**Figure 3.2C**). When stratified by the length, we saw the same overall responses in each freezing bout, though shorter freezing bouts tended to be preceded by larger peaks in activity in PVN^{CRH} cells (**Figure 3.2D**). Overall, we confirmed that uncontrollable, immediately aversive stimuli strongly recruit both the PVN^{CRH} neurons and the upstream vHPC neurons. In addition, we found evidence that vHPC activity predicts the beginning of freezing bouts.

Ventral hippocampus activity, but not hypothalamic CRH activity, rises when mice enter exposed areas of the elevated plus maze

We next investigated the effects of the elevated plus maze on the activity of vHPC and PVN^{CRH} cells. As expected, animals preferred the closed arm of the elevated plus maze and exhibited individual variability in levels of exploration (**Figure 3.3**).

It is known that about half of vHPC cells increase in activity when a mouse enters the anxiety-provoking center and the open arms of the elevated plus maze (Ciocchi et al., 2015; Jimenez et al., 2018). In line with those results, we recorded an increase in bulk vHPC activity in mice occupying the center or open areas compared to mice in the closed arms (**Figure 3.4**). By contrast, PVN^{CRH} activity was not significantly higher in mice located in the center/open area than in mice remaining in the closed arms. When

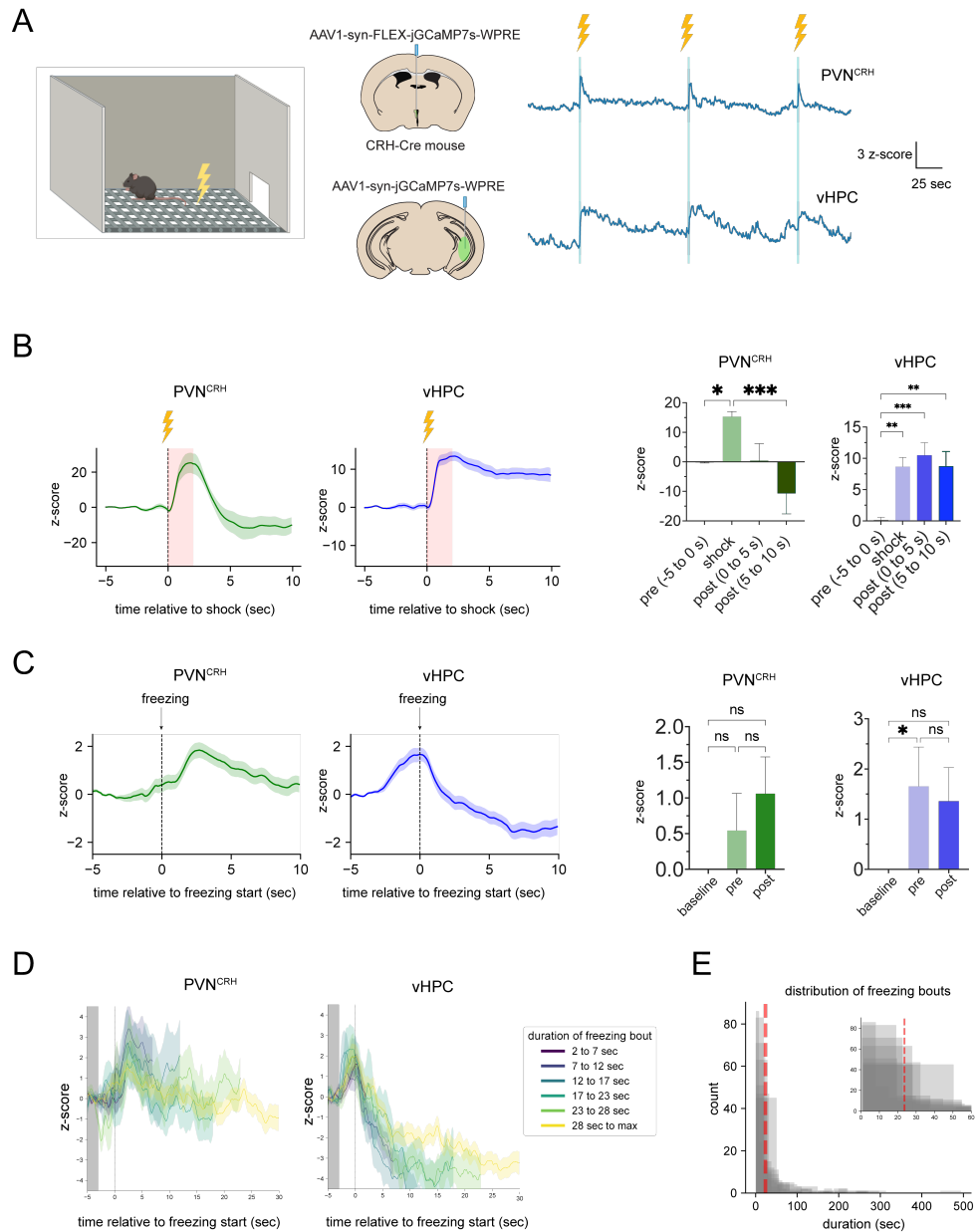


Figure 3.2. PVN^{CRH} and vHPC neurons both respond rapidly and robustly to foot shock. (A) Diagram of viral strategy used to record PVN^{CRH} and vHPC activity during foot shock assay and example traces from PVN^{CRH} and vHPC cells. (B) Calcium activity in PVN^{CRH} and vHPC centered around the start of a 2 sec shock. See Table 3 for statistical comparisons. (C) Same as (B) but aligned to the start of a freezing bout. (D) Calcium activity in PVN^{CRH} and vHPC aligned to start of freezing bouts, stratified into different lengths of freezing bout. Freezing bouts were filtered for minimum duration of 2 sec and occurring at least 10 sec after the last shock. Baseline was defined as -5 to -3 sec, pre as -3 to -1 sec, and post as 0 to 2 sec relative to start of freezing. (E) Distribution of freezing bout durations. Red line represents average duration of freezing bout. All data except the distributions are represented at mean +/- SEM.

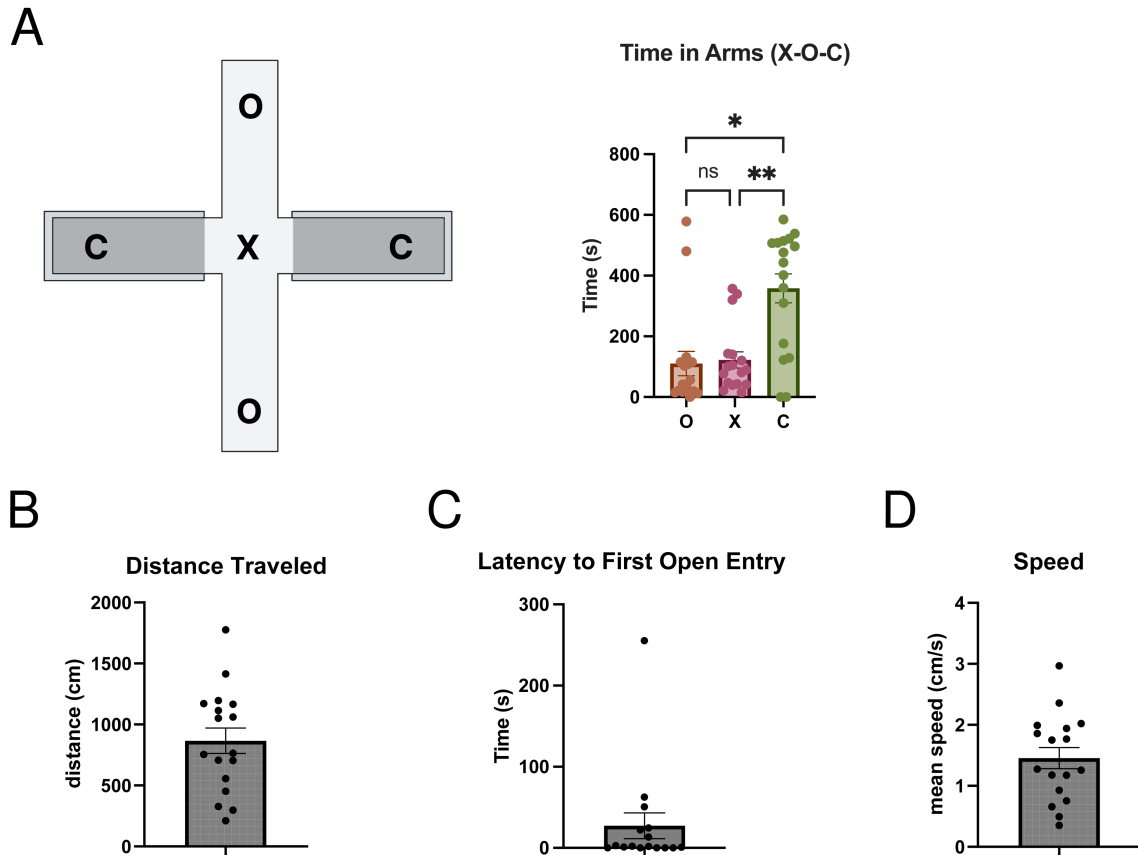
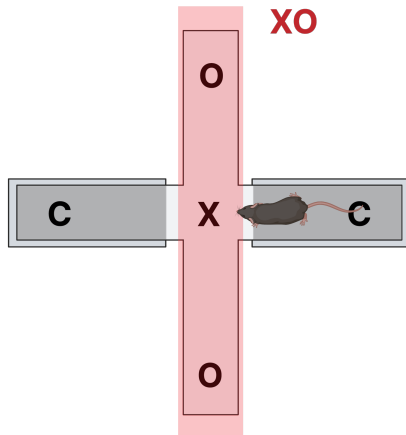
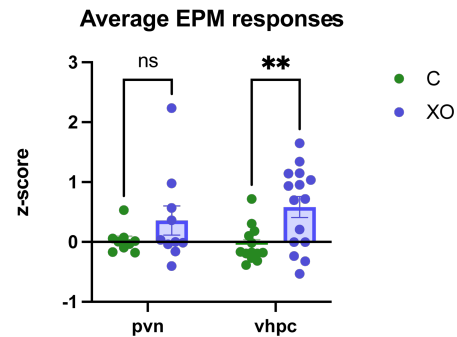


Figure 3.3. Anxiety- and motor-related behaviors in the elevated plus maze. (A) Time in arms during first 10 minutes of the elevated plus maze ($n = 17$ mice). (One-way ANOVA, arena compartment factor $F(1.536, 24.58) = 8.525$, $P = 0.0030$, Sidak's multiple comparison test, O vs X $p = 0.9930$; O vs C, $p = 0.0252$; X vs C, $p = 0.0082$ ($n = 17$ mice). Here, we distinguish the center (C) from the two open arms (O). **(B)** Distance travelled in first 10 minutes of the elevated plus maze ($n = 17$ mice). Mean: 866.1 cm. **(C)** Latency to first open arm entry of mice in first 10 minutes of the elevated plus maze ($n = 16$ mice). Mean: 27.3 sec. **(D)** Average speed of mice in first 10 minutes of the elevated plus maze ($n = 17$ mice). Mean: 1.455 cm/s. Data are displayed as mean \pm SEM. C: closed arm, O: open arm, X: center.

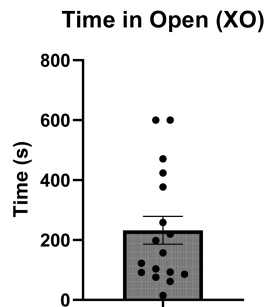
A



B



C



D

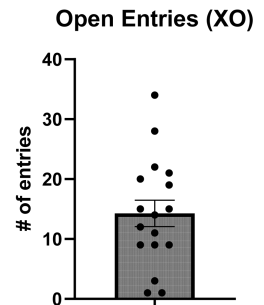


Figure 3.4. Overall PVN^{CRH} and vHPC activity and anxiety-related behavior in the elevated plus maze. (A) Schematic of locations in the elevated plus maze, showing open arms (O), closed arms (C), and the center zone (X). The open zone (XO) spans the center and the two open arms. **(B)** Average z-scored df/f in either the closed (C) or open (XO) compartments of the elevated plus maze (EPM) defined in (A). (Two-way ANOVA, arena compartment factor $F(1, 43) = 8.498$, $P = 0.0056$; Sidak's Multiple Comparisons Test, PVN C vs PVN XO ($n = 9$ C mice, 10 XO mice) $p = 0.3542$; vHPC C vs vHPC XO ($n = 13$ C mice, 15 XO mice) $p = 0.0092$. Data are displayed as mean \pm SEM. **(C)** Time mice spent in the open zone (XO) in the first 10 minutes after being placed in the elevated plus maze ($n = 17$ mice) Mean: 232.6 sec. **(D)** Number of times mice entered the open zone (XO) in the first 10 minutes after being placed in the elevated plus maze ($n = 17$ mice). Mean: 14.29 entries Data are displayed as mean \pm SEM. C: closed arm, XO: open arm, including center.

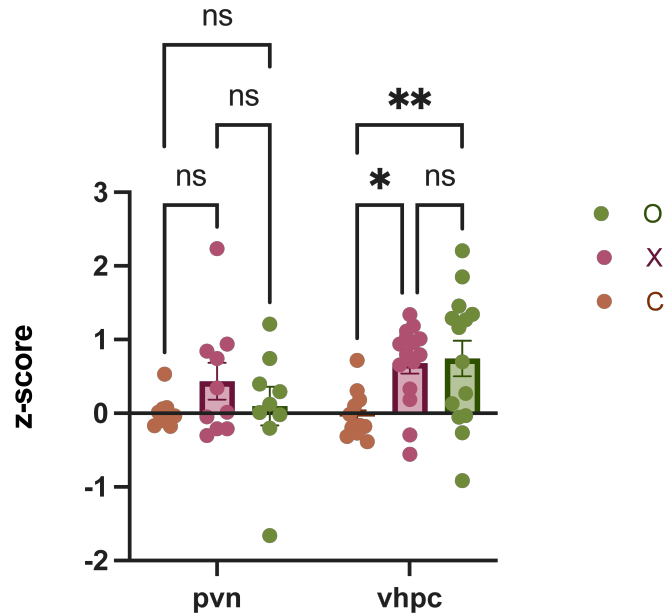


Figure 3.5. vHPC activity differentiates between subdivided compartments of the elevated plus maze better than PVN^{CRH} activity. Average z-scored df/f in closed arm (C), open arm (O), and center zone (X) in the elevated plus maze (EPM). (Two-way ANOVA, arena compartment factor $F(2, 64) = 4.659$, $P = 0.0129$; Sidak's Multiple Comparisons Test, PVN C vs PVN X $p = 0.4284$; PVN C vs PVN O $p = 0.9924$; PVN X vs PVN O $p = 0.5985$; vHPC C vs vHPC X $p = 0.0130$; vHPC C vs vHPC O $p = 0.0070$, vHPC X vs vHPC O $p = 0.9906$. $n = 17$ mice)

broken down into three zones of ascending threat (closed, center, and open), we found that both center and open zone exploration resulted in increases in average vHPC signal but not in PVN^{CRH} signal (**Figure 3.5**). These results imply that vHPC cells play a greater role than do the PVN^{CRH} cells in the response to different threat levels in the elevated plus maze, or that vHPC cells are more sensitive than PVN^{CRH} cells to the stress elicited by the elevated plus maze.

Distinct ventral hippocampal activity and hypothalamic CRH activity during trajectories between zones in the elevated plus maze

To compare the second-to-second dynamics of activity in vHPC cells and PVN^{CRH} cells, we next analyzed how the two cell populations respond when the mouse is moving between zones of the elevated plus maze. Overall, vHPC and PVN^{CRH} cells differed in their encoding of a mouse's trajectories between zones in the elevated plus maze.

vHPC activity robustly tracked the threat level of the environment, increasing substantially when mice move to aversive areas and decreasing to a similar degree when mice exited from an open arm to a closed arm (**Figure 3.6 A, B**). Trajectories from closed arm to closed arm and open arm to open arm corresponded to constant levels of activity (**Figure 3.6 C, D**). These findings agree with previous work demonstrating vHPC cells increase in activity when a mouse moves from a closed to open arm and decrease in activity when the mouse moves from an open to a closed arm (Jimenez et al., 2018). We did not observe any obvious pre-transition activity before mice crossed into the center in any of the transitions studied (**Figure 3.6**), in contrast with a study that observed changes in vHPC cells projecting to the prefrontal cortex as a mouse prepared to move from a closed arm to an open arm or vice versa (Sánchez-Bellot et al., 2022).

Activity in the PVN^{CRH} cells was distinct from vHPC cell activity and appeared more variable during the trajectories. First, we found that PVN^{CRH} cells transiently increased in activity when mice exited the open arms, whether mice next entered the closed or open arms (**Figure 3.6 B, C**). This transient increase may reflect a response

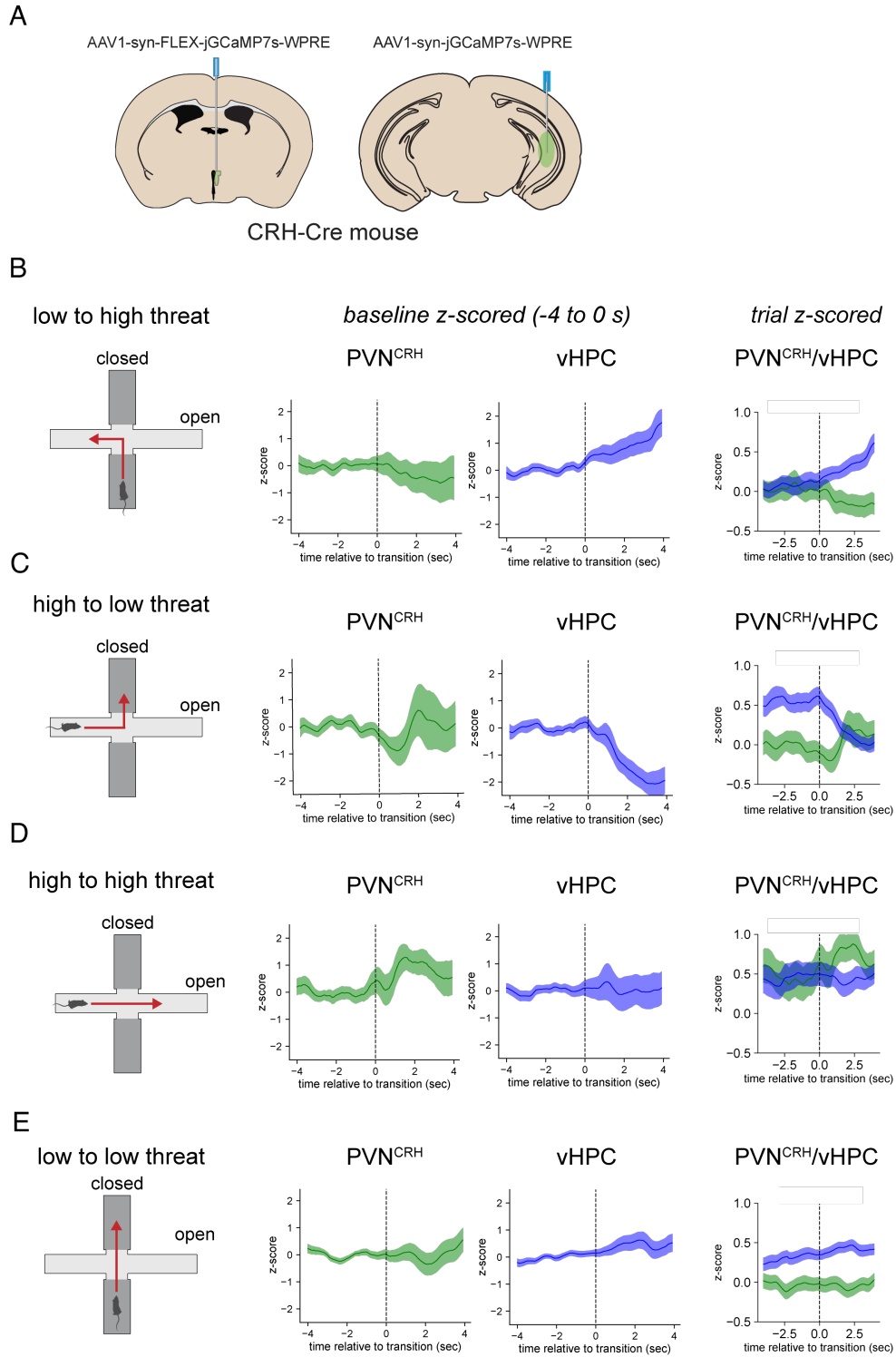


Figure 3.6. PVN^{CRH} and vHPC respond differently during trajectories between threat levels in the elevated plus maze. (A) Diagram of viral strategy used to record PVN^{CRH} and vHPC activity during exploration of the maze. (continued on the next page)

(Figure 3.6., continued from the previous page) **(B)** When mice move from a closed arm to an open arm (increase in threat), vHPC increases in activity while PVN^{CRH} activity declines slightly. n = 44 transitions in 12 vHPC animals, n = 22 transitions in 8 PVN^{CRH} animals. **(C)** When mice move from an open arm to a closed arm, vHPC activity decreases while PVN^{CRH} activity increases transiently. n = 31 transitions in 10 vHPC animals, n = 21 transitions in 6 PVN^{CRH} animals. **(D)** When mice move from an open arm to an open arm, vHPC activity remains constant while PVN^{CRH} activity increases transiently. n = 34 transitions in 9 vHPC animals, n = 16 transitions in 6 PVN^{CRH} animals. **(E)** When mice move from a closed arm to a closed arm, both vHPC and PVN^{CRH} activity remain constant. n = 91 transitions in 13 vHPC animals. n = 73 transitions in 9 PVN^{CRH} animals. Data are represented as mean +/- SEM. Left and middle columns represent activity z-scored to the baseline period t = -4 s to t = 0 s. Right columns represent activity which is normalized to the entire elevated plus maze trial. Number of animals in each graph is determined by how many animals performed each trajectory.

to moving through the center that is only unmasked after exploration of the open arm, perhaps due to heightened arousal and a generalized drive to move and escape.

Surprisingly, activity in PVN^{CRH} cells did not correspond strongly to directions traveled in the elevated plus maze like that seen in vHPC neurons.

In summary, changes in activity were less pronounced in PVN^{CRH} cells than in vHPC cells and appeared to depend on where an animal was starting a trajectory rather than in which arm a trajectory ended or the relative aversiveness of start and end. vHPC cells are more sensitive to a mouse's location in the elevated plus maze than PVN^{CRH} cells, perhaps reflecting external threat cues around the mouse or an internal state influenced by exposure to the environment (Table 2).

Distinct ventral hippocampal activity and hypothalamic CRH activity during behavioral motifs performed by mice in the elevated plus maze

In the experiments described above, we analyzed the activity of vHPC cells and PVN^{CRH} cells based on the movements of mice between more and less aversive locations in the elevated plus maze.

We confirmed that vHPC tracks the aversive nature of different compartments in the maze, but we were surprised that PVN^{CRH} cells did not change activity drastically between open and closed arms.

Stress and anxiety-related states are also known to manifest in more naturalistic behaviors. Head dips are have been classically defined as moments of investigation (Pellow et al., 1985; Walf & Frye, 2007) which also correlate with increases in vHPC activity (Jimenez et al., 2018). Risk assessment behaviors like stretched-attend postures have been correlated with corticosteroid levels in the elevated plus maze (Rodgers et al., 1999), and animals self-groom as a response to stress (Kalueff et al., 2016; Song et al., 2016).

Given the potential importance of naturalistic behaviors in explaining vHPC and PVN^{CRH} activity in the elevated plus maze, we assessed the neural correlates of 8 naturalistic behavioral motifs. These behaviors were selected based on the literature and our observations to index three relevant themes: approach-avoidance, risk assessment, and stress-related behaviors. The behaviors included were a version of stretch-attend (“elongation”), head dips, rearing, grooming, and a potentially stress-related behavior we called contraction (Table 1).

We observed vHPC activity did not rise significantly as the mice elongated from a stationary position towards the open arms whether this was followed by approach or avoidance of the open arms (**Figure 3.7 A, B, C**). Though our plotted traces suggest a slight rise in vHPC activity during and immediately after the mouse elongation, we did

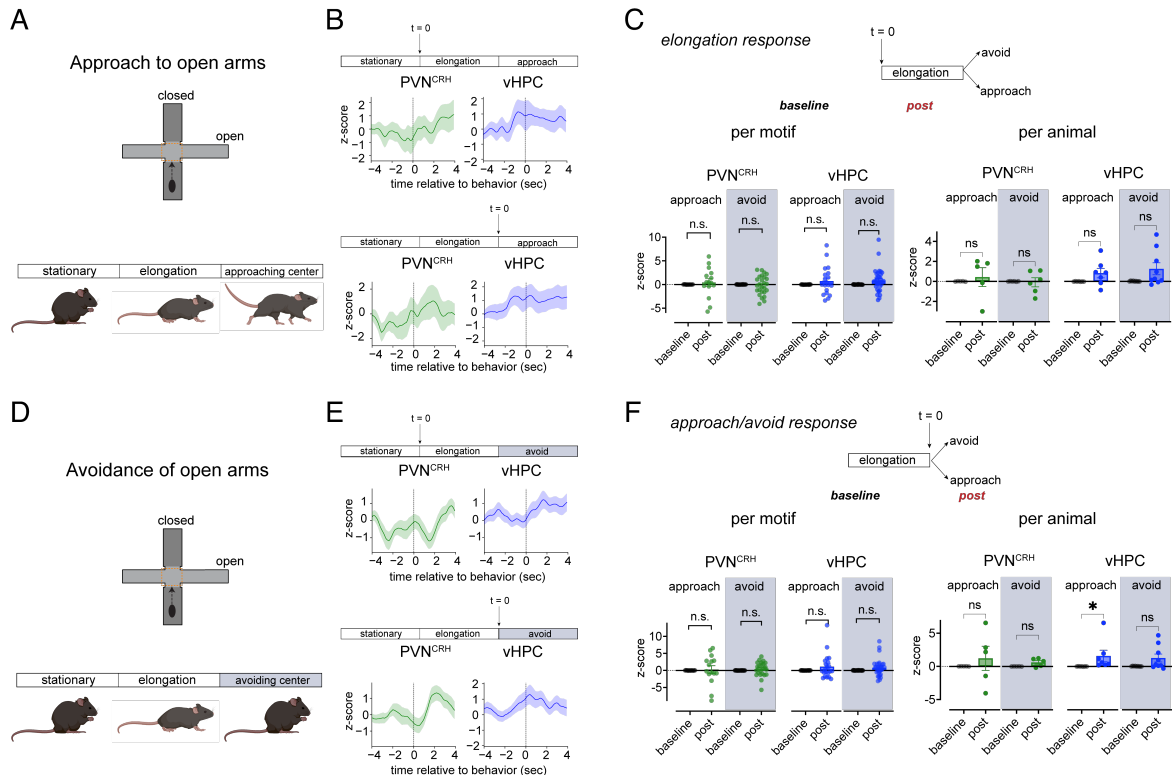


Figure 3.7. vHPC neurons and PVN^{CRH} neurons respond similarly during approach and avoidance sequences in the elevated plus maze. (A) Behavioral sequence used to define approach to open arms from closed arms. **(B)** Calcium activity in PVN^{CRH} and vHPC during approach sequences, centered around the stationary-to-elongation transition (top graphs) or the elongation-to-approach transition (bottom graphs). z-scores are normalized to the baseline value over the -8 to -4 sec preceding t = 0. Data are displayed as mean +/- SEM. **(C)** Calcium activity during the baseline period and the elongation phase preceding approach (white background) or avoidance (grey background) (see Table 3). Each dot represents activity from one behavioral motif (left) or one animal (right). An animal is represented by averaged activity over all behavioral motifs it performed. Data are displayed as mean +/- SEM. **(D, E, F)** Same as (A, B, C) but for avoidance sequences.

not detect a significant difference except at the end of elongation before approach. Together, these results suggest that vHPC activity does not necessarily predict the animal's future risk-taking behavior in this type of risk-assessment behavior.

Head dip behavior elicited strong increases in vHPC activity both when the animals' bodies were in the open or closed arms (**Figure 3.8 A, B, C**), and rearing also elicited a strong increase in vHPC activity (**Figure 3.8 D, E, F**).

In contrast, PVN^{CRH} neurons did not consistently change in activity across most of the behaviors assessed.

Interestingly, both regions responded strongly during a behavior where mice contract their whole bodies while they are sitting coiled into a ball, which we termed "contraction" (**Figure 3.9 A, B, C**). In this behavior, the overall activity was not increased but there was a clear transient response in the seconds after the behavior. We reasoned this response was not a movement artifact as the peak in activity tended to occur 1 - 2 sec after the movement and lasted longer than the movement, which was always less than a second in duration. The contraction behavior may represent a rapid defensive response made in the closed arms of the maze, though future work is needed to characterize the behavior.

In summary, vHPC activity tracked several naturalistic exploratory and stress-related behaviors, including end of elongation of the body before approach of the center, protected and unprotected head dips, rearing, and contraction (Table 2). PVN^{CRH} cells, surprisingly, did not strongly change their activity during any of these behaviors except a fleeting response in contraction. This suggests the increase in circulating corticosteroids seen in animals after undergoing the elevated plus maze may

stem from the transfer to the maze and general exposure to the maze rather than specific behaviors in the maze affecting PVN^{CRH} activity.

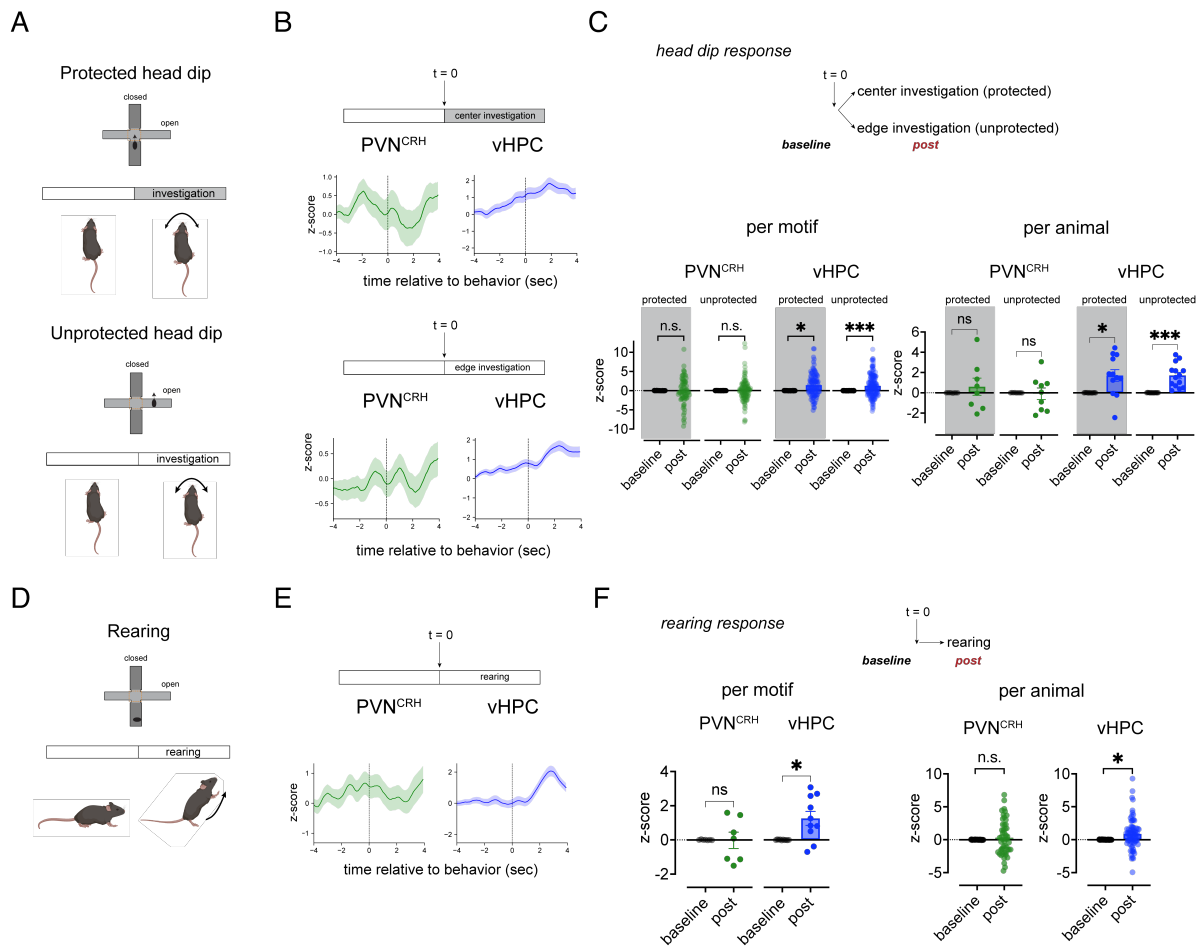


Figure 3.8. vHPC neurons and CRH neurons respond differently during risk assessment behavioral motifs in the EPM. (A) Behavioral sequence and body location used to define protected (top) and unprotected (bottom) head dips. **(B)** Calcium activity in PVN^{CRH} and vHPC during protected head dips, centered around the start of investigating center of the maze (top graphs) or unprotected head dips, centered around the start of investigating edge of the open arms (bottom graphs). z-scores are normalized to the baseline value over the -8 to -4 sec preceding t = 0. Data are displayed as mean +/- SEM. **(C)** Calcium activity during the baseline period and the investigation phase in the protected center (grey background) or unprotected open arms (white background) (see Table 3). Each dot represents activity from one behavioral motif (left) or one animal (right). An animal is represented by averaged activity over all behavioral motifs it performed. Data are displayed as mean +/- SEM. **(D)** Behavioral sequence and body location used to define rearing onto closed arm walls. **(E)** Same as in (B) but for rearing behaviors, aligned to time both paws leave the floor. **(F)** Same as in (C) but for rearing behaviors.

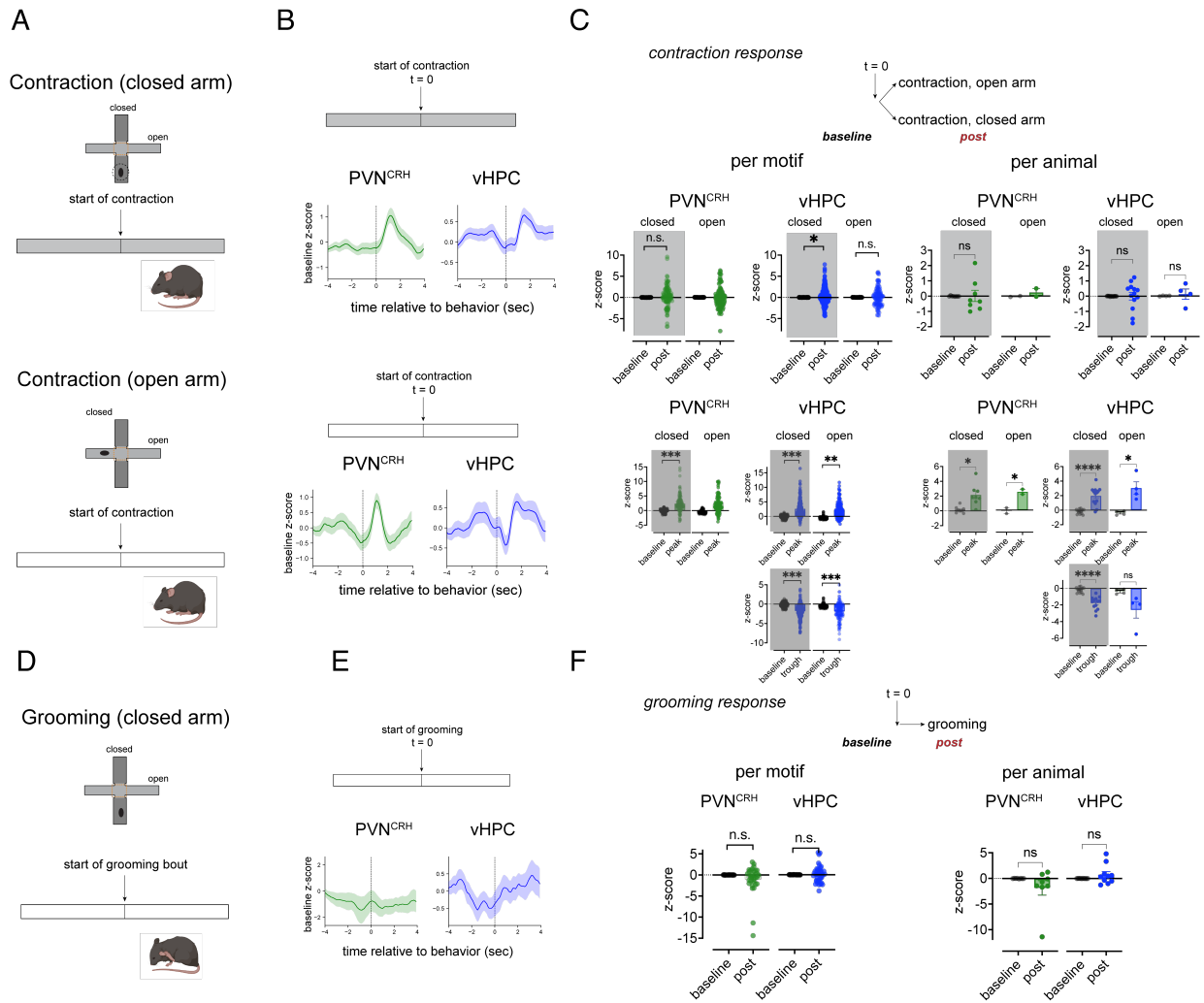


Figure 3.9. vHPC neurons and CRH neurons respond differently during stress-related behavioral motifs in the EPM. (A) Behavioral sequence and body location used to define contraction behavior in closed (top) and open (bottom) arms. **(B)** Calcium activity in PVN^{CRH} and vHPC during contraction in the closed arms (top graphs) or open arms (bottom graphs), centered on the initiation of contraction. z-scores are normalized to the baseline value over the -8 to -4 sec preceding $t = 0$. Data are displayed as mean \pm SEM. **(C)** Calcium activity during the baseline period and the 4 sec during/after contraction in the closed arms (grey background) or open arms (white background) (see Table 3). Each dot represents activity from one behavioral motif (left) or one animal (right). An animal is represented by averaged activity over all behavioral motifs it performed. Bottom rows are same as above but for baseline period average activity and the peak activity in the post period rather than the average. **(D)** Behavioral sequence and body location used to define grooming. Data are displayed as mean \pm SEM. **(E)** Same as in (B) but for grooming behaviors, aligned to time both front limbs leave the floor. **(F)** Same as in (C) but for grooming behaviors.

Table 2: Observed activity in PVN^{CRH} and vHPC cells during elevated plus maze exploration.

	PVN CRH	vHPC	PVN CRH Interpretation	vHPC Interpretation
closed → open (safe to aversive change in context)	- / ↓	↑↑	Activity in PVN changes slightly but overall does not track the aversive nature of the context	Activity in vHPC tracks the aversive nature of the context
open → closed (aversive to safe change in context)	- / ↑	↓↓		
open → open Aversive to aversive	- / ↑	-		
closed → closed	-	-		
risk assessment, leading to approach	- / ↑	- / ↑	No activity related to decision to approach or avoid	Activity in vHPC increases regardless of whether the animal approaches or avoids, suggesting vHPC tracks context but not the decision to approach or avoid
risk assessment leading to avoidance	- / ↑	↑		
head dip in open arm	Variable from motif to motif	↑↑		
head dip in closed arm	Variable from motif to motif	↑↑		
rearing	Variable from motif to motif	↑↑		
contraction (open, closed arms)	↑↑	↑	Strong but transient responses	Strong but transient responses
grooming	-	-		

Table 3. Summary of statistical comparisons related to Figures 3.5. – 3.9.

Figure	Variable	Unit of Comparison	n	Test	Results
Fig. 3.5B	PVN CRH shock	pre vs shock vs post vs second post	24 mean values from 6 animals	RM one-way ANOVA	$F(3,15) = 8.53, P = 0.0015$
Fig. 3.5B	vHPC shock	pre vs shock vs post vs second post	32 mean values from 8 animals	RM one-way ANOVA	$F(3,21) = 11.59, P = 0.001$
Fig. 3.5B	PVN CRH shock	pre (-5 to 0 s) vs shock	12 mean values from 6 animals	Post hoc Tukey's multiple comparisons	$P = 0.0405$
Fig. 3.5B	PVN CRH shock	shock vs post (5 to 10 s)	12 mean values from 6 animals	Post hoc Tukey's multiple comparisons	$P = 0.050$
Fig. 3.5B	vHPC shock	pre (-5 to 0 s) vs shock	16 mean values from 8 animals	Post hoc Tukey's multiple comparisons	$P = 0.0013$
Fig. 3.5B	vHPC shock	vHPC shock	16 mean values from 8 animals	Post hoc Tukey's multiple comparisons	$P < 0.001$
Fig. 3.5B	vHPC shock	pre (-5 to 0 s) vs post (5 to 10 s)	16 mean values from 8 animals	Post hoc Tukey's multiple comparisons	$P = 0.0012$
Fig. 3.5C	PVN CRH freezing	pre vs shock vs post vs second post	18 mean values from 6 animals	RM one-way ANOVA	$F(2,10) = 2.857, P = 0.1044$
Fig. 3.5C	vHPC freezing	pre vs shock vs post vs second post	24 mean values from 8 animals	RM one-way ANOVA	$F(2,14) = 4.053, P = 0.0409$
Fig. 3.5C	PVN CRH freezing	baseline vs pre	12 values from 6 animals	Post hoc Tukey's multiple comparisons	$P = 0.467$
Fig. 3.5C	PVN CRH freezing	baseline vs post	12 values from 6 animals	Post hoc Tukey's multiple comparisons	$P = 0.088$
Fig. 3.5C	PVN CRH freezing	pre vs post	12 values from 6 animals	Post hoc Tukey's multiple comparisons	$P = 0.498$
Fig. 3.5C	vHPC freezing	baseline vs pre	16 values from 8 animals	Post hoc Tukey's multiple comparisons	$P = 0.0454$
Fig. 3.5C	vHPC freezing	baseline vs post	16 values from 8 animals	Post hoc Tukey's multiple comparisons	$P = 0.107$
Fig. 3.5C	vHPC freezing	pre vs post	16 values from 8 animals	Post hoc Tukey's multiple comparisons	$P = 0.883$
Fig. 3.7C	PVN CRH approach: elongation start, by motif	baseline vs post	15 instances from 5 animals	Mixed effects model	$F(1, 18) = 0.08524, p = 0.7737$
Fig. 3.7C	PVN CRH avoid: elongation start, by motif	baseline vs post	26 instances from 6 animals	Mixed effects model	$F(1, 36) = 1.177, p = 0.2852$
Fig. 3.7C	vHPC approach elongation start, by motif	baseline vs post	21 instances from 7 animals	Mixed effects model	$F(1, 30) = 0.8186, p = 0.3728$
Fig. 3.7C	vHPC avoid elongation start, by motif	baseline vs post	33 instances from 9 animals	Mixed effects model	$F(1, 52) = 1.469, p = 0.2310$
Fig. 3.7C	PVN CRH approach: elongation start, by animal	baseline vs post	5 animals	Wilcoxon test	$p = 0.8125$
Fig. 3.7C	PVN CRH avoid: elongation start, by animal	baseline vs post	6 animals	Wilcoxon test	$p > 0.9999$
Fig. 3.7C	vHPC approach elongation start, by animal	baseline vs post	7 animals	Wilcoxon test	$p = 0.1094$
Fig. 3.7C	vHPC avoid elongation start, by animal	baseline vs post	9 animals	Wilcoxon test	$p = 0.0547$
Fig. 3.7F	PVN CRH approach: elongation end, by motif	baseline vs post	15 instances from 5 animals	Mixed effects model	$F(1, 8) = 0.0006651, p = 0.9801$
Fig. 3.7F	PVN CRH avoid: elongation end, by motif	baseline vs post	25 instances from 5 animals	Mixed effects model	$F(1, 34) = 0.08143, p = 0.7771$
Fig. 3.7F	vHPC approach elongation end, by motif	baseline vs post	21 instances from 7 animals	Mixed effects model	$F(1, 30) = 0.8713, p = 0.3580$
Fig. 3.7F	vHPC avoid elongation end, by motif	baseline vs post	31 instances from 8 animals	Mixed effects model	$F(1, 48) = 0.9242, p = 0.3412$
Fig. 3.7F	PVN CRH approach: elongation end, by animal	baseline vs post	5 animals	Wilcoxon test	$p = 0.6250$
Fig. 3.7F	PVN CRH avoid: elongation end, by animal	baseline vs post	5 animals	Wilcoxon test	$p = 0.1875$

Figure	Variable	Unit of Comparison	n	Test	Results
Fig. 3.7F	vHPC approach elongation end, by animal	baseline vs post	7 animals	Wilcoxon test	p = 0.0156
Fig. 3.7F	vHPC avoid elongation end, by animal	baseline vs post	8 animals	Wilcoxon test	p = 0.0547
Fig 3.8C	PVN CRH protected head dip start, by motif	baseline vs post	73 instances from 8 animals	Mixed effects model	F (1, 14) = 0.06332, p = 0.8050
Fig 3.8C	PVN CRH unprotected head dip start, by motif	baseline vs post	115 instances from 9 animals	Mixed effects model	F (1, 16) = 0.2837 p = 0.6016
Fig 3.8C	vHPC protected head dip start, by motif	baseline vs post	104 instances from 12 animals	Mixed effects model	F (1, 22) = 4.772, p = 0.0399
Fig 3.8C	vHPC unprotected head dip start, by motif	baseline vs post	176 instances from 14 animals	Mixed effects model	F (1, 26) = 20.70, p < 0.001
Fig 3.8C	PVN CRH protected head dip start, by animal	baseline vs post	8 animals	Wilcoxon test	p = 0.7422
Fig 3.8C	PVN CRH unprotected head dip start, by animal	baseline vs post	9 animals	Wilcoxon test	p = 0.8203
Fig 3.8C	vHPC protected head dip start, by animal	baseline vs post	12 animals	Wilcoxon test	p = 0.0269
Fig 3.8C	vHPC unprotected head dip start, by animal	baseline vs post	14 animals	Wilcoxon test	p < 0.001
Fig. 3.8F	PVN CRH rearing start, by motif	baseline vs post	50 instances from 7 animals	Mixed effects model	F (1, 12) = 3.010, p = 0.1083
Fig. 3.8F	vHPC rearing start, by motif	baseline vs post	77 instances from 10 animals	Mixed effects model	F (1, 18) = 5.326, p = 0.0331
Fig. 3.8F	PVN CRH rearing start, by animal	baseline vs post	7 animals	Wilcoxon test	p = 0.9375
Fig. 3.8F	vHPC rearing start, by animal	baseline vs post	10 animals	Wilcoxon test	p = 0.0137
Fig. 3.9C	PVN CRH contraction in closed arm start, by motif	baseline vs post	110 instances in 8 animals	Mixed effects model	F (1, 14) = 0.3225, p = 0.5791
Fig. 3.9C	PVN CRH contraction in open arm start, by motif	baseline vs post	102 instances in 2 animals	Mixed effects model	not enough values
Fig. 3.9C	vHPC contraction in closed arm start, by motif	baseline vs post	207 instances in 13 animals	Mixed effects model	F (1, 24) = 6.021, 0.0218
Fig. 3.9C	vHPC contraction in open arm start, by motif	baseline vs post	116 instances in 4 animals	Mixed effects model	F (1, 6) = 0.5873, 0.4725
Fig. 3.9C	PVN CRH contraction in closed arm start, by animal	baseline vs post	8 animals	Wilcoxon test	p = 0.6406
Fig. 3.9C	PVN CRH contraction in open arm start, by animal	baseline vs post	2 animals	Wilcoxon test	not enough values
Fig. 3.9C	vHPC contraction in closed arm start, by animal	baseline vs post	13 animals	Wilcoxon test	p = 0.7354
Fig. 3.9C	vHPC contraction in open arm start, by animal	baseline vs post	4 animals	Wilcoxon test	p = 0.6250
Fig. 3.9C	PVN CRH contraction in closed arm start, by motif	baseline vs peak	110 instances in 8 animals	Mixed effects model	F (1, 14) = 23.18, p < 0.001
Fig. 3.9C	PVN CRH contraction in open arm start, by motif	baseline vs peak	102 instances in 2 animals	-	-
Fig. 3.9C	vHPC contraction in closed arm start, by motif	baseline vs peak	207 instances in 13 animals	Mixed effects model	F (1, 24) = 106.8, p < 0.001
Fig. 3.9C	vHPC contraction in open arm start, by motif	baseline vs peak	116 instances in 4 animals	Mixed effects model	F (1, 6) = 21.03, p = 0.0037
Fig. 3.9C	vHPC contraction in closed arm start, by motif	baseline vs trough	207 instances in 13 animals	Mixed effects model	F (1, 24) = 20.64, p < 0.001
Fig. 3.9C	vHPC contraction in open arm start, by motif	baseline vs trough	116 instances in 4 animals	Mixed effects model	F (1, 30) = 42.38, p < 0.001
Fig. 3.9C	PVN CRH contraction in closed arm start, by animal	baseline vs peak	8 animals	Wilcoxon test	p = 0.0110
Fig. 3.9C	PVN CRH contraction in open arm start, by animal	baseline vs peak	2 animals	Wilcoxon test	p = 0.0120
Fig. 3.9C	vHPC contraction in closed arm start, by animal	baseline vs peak	13 animals	Wilcoxon test	p < 0.001

Figure	Variable	Unit of Comparison	n	Test	Results
Fig. 3.9C	vHPC contraction in open arm start, by animal	baseline vs peak	4 animals	Wilcoxon test	$p = 0.012$
Fig. 3.9C	vHPC contraction in closed arm start, by animal	baseline vs trough	13 animals	Wilcoxon test	$p < 0.001$
Fig. 3.9C	vHPC contraction in open arm start, by animal	baseline vs trough	4 animals	Wilcoxon test	$p = 0.0867$
Fig. 3.9F	PVN CRH grooming start, by motif	baseline vs post	32 instances in 8 animals	Mixed effects model	$F(1, 46) = 1.283, p = 0.2633$
Fig. 3.9F	PVN CRH grooming start, by animal	baseline vs post	8 animals	Wilcoxon test	$p = 0.1484$
Fig. 3.9F	vHPC grooming start, by motif	baseline vs post	42 instances in 10 animals	Mixed effects model	$F(1, 66) = 1.459, p = 0.2314$
Fig. 3.9F	vHPC grooming start, by animal	baseline vs post	10 animals	Wilcoxon test	$p = 0.4316$

Discussion

This chapter described the moment-to-moment activity of ventral hippocampal (vHPC) and corticotropin-releasing-hormone cells of the hypothalamus (PVN^{CRH}) during stress- and anxiety-related tasks, with a particular focus on the foot shock assay, a test of inescapable stress, and the elevated plus maze, a widely recognized model for approach-avoidance conflict.

Our observations support earlier findings that vHPC neurons increase in activity when mice enter more aversive areas like the open arms of the elevated plus maze (Ciochi et al., 2015; Jimenez et al., 2018) and when they receive a foot shock (Jimenez et al., 2020). This increase in activity is consistent with the idea that vHPC is sensitive to environmental cues and potentially the animal's internal state as it navigates a threatening environment, and it may assist with the vHPC's role in contextual encoding.

vHPC activity was correlated with both exploratory and stress-related behaviors, which is likely important for its roles in anxiety and cognitive mapping. Increased activity during behaviors such as head dips and rearing may be important in assessing risk and

preparing for exploratory behavior. Though there is some evidence that pairs of neurons in vHPC can predict the extent of exploration into an exposed alley (Malagon-Vina et al., 2023), and that vHPC-prefrontal cortex projection neurons reflect approach to a transition between open and closed arms (Sánchez-Bellot et al., 2022), we did not observe specific changes in vHPC activity before mice moved from one zone of the elevated plus maze to another, in line with findings from single cell recordings of the vHPC (Jimenez et al., 2018).

The relatively muted response of PVN^{CRH} neurons to the elevated plus maze suggests that while these neurons are critical to the stress response in immediate threats like a shock, they may not be activated by stressors not posing an immediate or uncontrollable threat. This finding contrasts with other observations that PVN^{CRH} neurons respond in real time to other stressors such as shocks, restraint, and white noise (J. Kim et al., 2019; Yuan et al., 2019) and was surprising given the tendency of the HPA stress response to be triggered by stimuli as mild as handling or movement of a home cage (Spencer and Deak 2017). Instead, it seems that PVN^{CRH} neurons respond strongly to only a subset of threats.

Increased corticosteroid levels observed after elevated plus maze exposure in other studies may be more dependent on the initial transition from a safe environment to the maze or the handling associated with that transition than to any specific approach-avoidance behaviors in the elevated plus maze. In line with this explanation, picking up animals creates a sharp, transient increase in PVN^{CRH} activity (J. Kim et al., 2019), and placing mice into an open arm of an elevated plus maze without the ability to explore the maze causes an immediate increase in activity (Li et al., 2020). Recordings in the

current study began after a mouse was moved into the elevated plus maze, so the PVN^{CRH} neuron activity in our analysis did not account for initial responses to being transferred into the maze and focused on transitions initiated by the animal between different zones of the maze.

Previous work has shown that PVN^{CRH} neurons ramp in activity before fleeing a looming disc or running to escape a shock, and that ramping activity is larger before an escapable shock (Núria Daviu et al., 2020). These findings have led to a theory that PVN^{CRH} neurons may gate active escape or response behaviors in the face of threats (Nuria Daviu & Bains, 2021). In the current study, PVN^{CRH} briefly increased in activity when the mouse was exiting aversive open arms, in line with a potential permissive role for PVN^{CRH} neurons in escape behavior.

A permissive motor role for PVN^{CRH} activity might also account for the trend seen with freezing bouts: larger peaks in PVN^{CRH} activity preceded shorter bouts of freezing. Similarly, the release of corticosteroids is negatively correlated to amount of freezing in the immediate period after shocks (Marchand et al., 2007). While we might expect a greater peak to co-occur with greater freezing if there were a simple link between PVN^{CRH} activity and perceived aversiveness of an experience, our data instead supports a more nuanced role for PVN^{CRH} cells as preparation for future motion.

Given the nature of fiber photometry calcium recordings, there may be subpopulations of cells with different roles or sensitivities to features of the elevated plus maze which were not accessible in this study. Some evidence suggests that different subpopulations of PVN^{CRH} cells react in opposite directions to appetitive stimuli such as food consumption, though these identified subpopulations responded similarly

to aversive stimuli (S. Xu et al., 2020). Additionally, the assays implemented in the current study are only a small subset of the range of stressors that can activate the HPA axis, and presumably, PVN^{CRH} cells, so recording responses to other stimuli may add additional detail in describing how PVN^{CRH} activity is linked to behavior.

Together, these results inform our model of HPA axis regulation. vHPC and PVN^{CRH} cells are differentially activated by specific aspects of stressful experiences, suggesting that the vHPC influence on PVN^{CRH} cells may also be specific to particular contexts and modalities as well.

References for Chapter 3

- Ciocchi, S., J. Passecker, H. Malagon-Vina, N. Mikus, and T. Klausberger. 2015. "Brain Computation. Selective Information Routing by Ventral Hippocampal CA1 Projection Neurons." *Science* 348 (6234): 560–63.
- Cole, Anthony B., Kristen Montgomery, Tracy L. Bale, and Scott M. Thompson. 2022. "What the Hippocampus Tells the HPA Axis: Hippocampal Output Attenuates Acute Stress Responses via Disynaptic Inhibition of CRF+ PVN Neurons." *Neurobiology of Stress* 20 (September): 100473.
- Daviu, Nuria, and Jaideep S. Bains. 2021. "Should I Stay or Should I Go? CRHPVN Neurons Gate State Transitions in Stress-Related Behaviors." *Endocrinology* 162 (6). <https://doi.org/10.1210/endocr/bqab061>.
- Daviu, Núria, Tamás Füzesi, David G. Rosenegger, Neilen P. Rasiah, Toni-Lee Sterley, Govind Peringod, and Jaideep S. Bains. 2020. "Paraventricular Nucleus CRH Neurons Encode Stress Controllability and Regulate Defensive Behavior Selection." *Nature Neuroscience*, February. <https://doi.org/10.1038/s41593-020-0591-0>.
- Dos Santos Corrêa, Moisés, Barbara Dos Santos Vaz, Gabriel David Vieira Grisanti, Joselisa Péres Queiroz de Paiva, Paula Ayako Tiba, and Raquel Vecchio Fornari. 2019. "Relationship between Footshock Intensity, Post-Training Corticosterone Release and Contextual Fear Memory Specificity over Time." *Psychoneuroendocrinology* 110 (December): 104447.

- File, S. E., H. Zangrossi Jr, F. L. Sanders, and P. S. Mabbutt. 1994. "Raised Corticosterone in the Rat after Exposure to the Elevated Plus-Maze." *Psychopharmacology* 113 (3–4): 543–46.
- Füzesi, Tamás, Nuria Daviu, Jaclyn I. Wamsteeker Cusulin, Robert P. Bonin, and Jaideep S. Bains. 2016. "Hypothalamic CRH Neurons Orchestrate Complex Behaviours after Stress." *Nature Communications* 7 (June): 11937.
- Herman, James P., and Nancy K. Mueller. 2006. "Role of the Ventral Subiculum in Stress Integration." *Behavioural Brain Research* 174 (2): 215–24.
- Jimenez, Jessica C., Jack E. Berry, Sean C. Lim, Samantha K. Ong, Mazen A. Kheirbek, and Rene Hen. 2020. "Contextual Fear Memory Retrieval by Correlated Ensembles of Ventral CA1 Neurons." *Nature Communications* 11 (1): 3492.
- Jimenez, Jessica C., Katy Su, Alexander R. Goldberg, Victor M. Luna, Jeremy S. Biane, Gokhan Ordek, Pengcheng Zhou, et al. 2018. "Anxiety Cells in a Hippocampal-Hypothalamic Circuit." *Neuron* 97 (3): 670-683.e6.
- Kalueff, Allan V., Adam Michael Stewart, Cai Song, Kent C. Berridge, Ann M. Graybiel, and John C. Fentress. 2016. "Neurobiology of Rodent Self-Grooming and Its Value for Translational Neuroscience." *Nature Reviews. Neuroscience* 17 (1): 45–59.
- Kim, Jineun, Seongju Lee, Yi-Ya Fang, Anna Shin, Seahyung Park, Koichi Hashikawa, Shreelatha Bhat, et al. 2019. "Rapid, Biphasic CRF Neuronal Responses Encode Positive and Negative Valence." *Nature Neuroscience*, March.
<https://doi.org/10.1038/s41593-019-0342-2>.

- Lerner, Talia N., Carrie Shilyansky, Thomas J. Davidson, Kathryn E. Evans, Kevin T. Beier, Kelly A. Zalocusky, Ailey K. Crow, et al. 2015. "Intact-Brain Analyses Reveal Distinct Information Carried by SNc Dopamine Subcircuits." *Cell* 162 (3): 635–47.
- Li, Shi-Bin, Jeremy C. Borniger, Hiroshi Yamaguchi, Julien Hédou, Brice Gaudilliere, and Luis de Lecea. 2020. "Hypothalamic Circuitry Underlying Stress-Induced Insomnia and Peripheral Immunosuppression." *Science Advances* 6 (37). <https://doi.org/10.1126/sciadv.abc2590>.
- Malagon-Vina, Hugo, Stéphane Ciochi, and Thomas Klausberger. 2023. "Firing Patterns of Ventral Hippocampal Neurons Predict the Exploration of Anxiogenic Locations." *ELife* 12 (April). <https://doi.org/10.7554/eLife.83012>.
- Marchand, Alain R., Alexandra Barbelivien, Alexandre Seillier, Karine Herbeaux, Alain Sarrieau, and Monique Majchrzak. 2007. "Contribution of Corticosterone to Cued versus Contextual Fear in Rats." *Behavioural Brain Research* 183 (1): 101–10.
- Murphy, Kathleen Z., Eyobel Haile, Anna McTigue, Anne F. Pierce, and Zoe R. Donaldson. 2023. "PhAT: A Flexible Open-Source GUI-Driven Toolkit for Photometry Analysis." *BioRxiv : The Preprint Server for Biology*, March. <https://doi.org/10.1101/2023.03.14.532489>.
- Myers, Brent, Jessica M. McKlveen, and James P. Herman. 2012. "Neural Regulation of the Stress Response: The Many Faces of Feedback." *Cellular and Molecular Neurobiology*, February. <https://doi.org/10.1007/s10571-012-9801-y>.

- Pellow, S., P. Chopin, S. E. File, and M. Briley. 1985. "Validation of Open:Closed Arm Entries in an Elevated plus-Maze as a Measure of Anxiety in the Rat." *Journal of Neuroscience Methods* 14 (3): 149–67.
- Radley, Jason J., and Paul E. Sawchenko. 2011. "A Common Substrate for Prefrontal and Hippocampal Inhibition of the Neuroendocrine Stress Response." *The Journal of Neuroscience: The Official Journal of the Society for Neuroscience* 31 (26): 9683–95.
- Rodgers, R. J., J. Haller, A. Holmes, J. Halasz, T. J. Walton, and P. F. Brain. 1999. "Corticosterone Response to the Plus-Maze: High Correlation with Risk Assessment in Rats and Mice." *Physiology & Behavior* 68 (1–2): 47–53.
- Sánchez-Bellot, Candela, Rawan AlSubaie, Karyna Mishchanchuk, Ryan W. S. Wee, and Andrew F. MacAskill. 2022. "Two Opposing Hippocampus to Prefrontal Cortex Pathways for the Control of Approach and Avoidance Behaviour." *Nature Communications* 13 (1): 339.
- Segalin, Cristina, Jalani Williams, Tomomi Karigo, May Hui, Moriel Zelikowsky, Jennifer J. Sun, Pietro Perona, David J. Anderson, and Ann Kennedy. 2021. "The Mouse Action Recognition System (MARS) Software Pipeline for Automated Analysis of Social Behaviors in Mice." *ELife* 10 (November).
<https://doi.org/10.7554/eLife.63720>.
- Song, Cai, Kent C. Berridge, and Allan V. Kalueff. 2016. "'Stressing' Rodent Self-Grooming for Neuroscience Research." *Nature Reviews. Neuroscience*.
- Spencer, Robert L., and Terrence Deak. 2017. "A Users Guide to HPA Axis Research." *Physiology & Behavior* 178 (September): 43–65.

- Vom Berg-Maurer, Colette M., Chintan A. Trivedi, Johann H. Bollmann, Rodrigo J. De Marco, and Soojin Ryu. 2016. "The Severity of Acute Stress Is Represented by Increased Synchronous Activity and Recruitment of Hypothalamic CRH Neurons." *The Journal of Neuroscience: The Official Journal of the Society for Neuroscience* 36 (11): 3350–62.
- Walf, Alicia A., and Cheryl A. Frye. 2007. "The Use of the Elevated plus Maze as an Assay of Anxiety-Related Behavior in Rodents." *Nature Protocols* 2 (2): 322–28.
- Xu, Shengjin, Hui Yang, Vilas Menon, Andrew L. Lemire, Lihua Wang, Fredrick E. Henry, Srinivas C. Turaga, and Scott M. Sternson. 2020. "Behavioral State Coding by Molecularly Defined Paraventricular Hypothalamic Cell Type Ensembles." *Science* 370 (6514). <https://doi.org/10.1126/science.abb2494>.
- Yuan, Yuan, Wei Wu, Ming Chen, Fang Cai, Chengyu Fan, Wei Shen, Wenzhi Sun, and Ji Hu. 2019. "Reward Inhibits Paraventricular CRH Neurons to Relieve Stress." *Current Biology: CB* 0 (0). <https://doi.org/10.1016/j.cub.2019.02.048>.

Chapter 4: Ventral hippocampal modulation of the hypothalamic

CRH stress response

Introduction

Current models of the stress response highlight the importance of the hypothalamo-pituitary-adrenal (HPA) axis, which is gated by the corticotropin-releasing-hormone (CRH) cells in the paraventricular nucleus of the hypothalamus (PVN) (Spencer and Deak 2017). Many inputs converge onto the PVN^{CRH} cells to gate the HPA stress response, integrating information from other brain regions about the outside world and an animal's internal state (James P. Herman et al., 2016). One important input is the ventral hippocampus (vHPC).

Lesions of the hippocampus typically result in greater activation of the HPA stress response, as evidenced by larger increases in corticosteroids released into the blood and increased amounts of CRH RNA expressed in the PVN after a stressor (J. P. Herman et al., 1998; Mueller et al., 2004; Radley & Sawchenko, 2011) but see also (Tuvnes et al. 2003; Conforti and Feldman 1976). In line with this model, stimulation of the hippocampus in humans or animals under conditions of high HPA activation resulted in decreased CORT secretion (Dunn & Orr, 1984; Dupont et al., 1972; Mandell et al., 1963; Rubin et al., 1966). Anatomical and immunohistochemical evidence suggests that the vHPC achieves inhibition of PVN^{CRH} cells by sending excitatory outputs that pass through a GABAergic relay before reaching the PVN (Radley et al., 2009; Radley &

Sawchenko, 2011). Thus, the ventral hippocampus (vHPC) may be an important inhibitory modulator of the PVN.

Despite the evidence for vHPC's importance in modulating the HPA axis, no studies have directly examined how the inactivation of vHPC affects moment-to-moment PVN^{CRH} activity. Here, we recorded in PVN^{CRH} cells during different stressful experiences while chemogenetically inhibiting the excitatory cells of the vHPC. Previous studies have typically sampled stress hormones at long intervals of 15-30 minutes and are not sensitive to acute changes in the upstream brain regions. Our fiber photometry recording method allowed us to sample PVN^{CRH} activity on a second-to-second level. This chapter highlights the importance of vHPC in modulating acute responses to stress in the PVN^{CRH} cells.

Methods

Animals

Male and female Crh-IRES-Cre hemizygous mice were bred from pairs of homozygous Crh-IRES-Cre mice (*B6(Cg)-Crhtm1(cre)Zjh/J*, Jax #012704, *RRID:IMSR_JAX:012704*) and C57BL/6 mice (The Jackson Laboratory). Mice were housed under a 12 h light/dark cycle with ad libitum access to food and water. All experiments were conducted during the light cycle in accordance with the U.S. National Institutes of Health Guide for the Care and Use of Laboratory Animals and the institutional Animal Care and Use Committees at University of California, San Francisco.

Surgical Procedures

At 8-12 weeks old, mice were injected bilaterally with either rAAV5-CaMKIIa-mcherry (UNC Vector Core) or pAAV5-CaMKIIa-hM4D(Gi)-mCherry (Addgene) in the vHPC and unilaterally with Cre-dependent AAV1-syn-FLEX-jGCaMP7s-WPRE (Addgene) in the PVN at the following stereotaxic coordinates: *PVN* AP -0.6, ML -0.2, DV -4.9 (64 nL), DV -4.8 (32 nL), DV - 4.7(128 nL) from bregma; *vHPC* AP +/-3.20 ML +3.35, DV -3.85 (32 nL), DV -3.75 (96 nL), -3.65 (32 nL) from cortical surface. The fiber optic photometry cannula (\varnothing 400 μ m, Doric Lenses) was implanted over PVN (DV -4.60 from bregma) and secured with dental cement (C&B Metabond, Parkell).

During surgery, mice were anesthetized with 1.5% isoflurane and then head-fixed in a stereotaxic frame (David Kopf). Craniotomies were made with a round 0.5-mm drill bit (David Kopf), and a Nanoject II syringe (Drummond Scientific) was used with a pulled glass pipette to inject virus.

All mice were administered lidocaine, meloxicam, and buprenorphine during surgery and post-surgical care. Mice recovered for at least 5 weeks and were habituated to handling before experiments began. Experiments began after mice showed a clear photometry response in PVN when picked up by the tail.

Behavioral Experiments

On the day of each experiment, mice were weighed and then habituated outside the colony in a quiet room for 1-2 hours. Fiber photometry optical fibers were bleached for a minimum of 2 hours before each recording. Animals were injected i.p. with 0.5 mg/mL clozapine-N-oxide/0.5% DMSO in saline at a dose of 5 mg/kg 20 minutes before

the start of recordings. *Foot shock assay.* Animals underwent the shock paradigm in operant chambers (Med Associates) using FreezeFrame software system (Actimetrics) as follows: 3 shocks (2 sec each, 0.75 mA, 100 sec inter-shock interval) delivered through floor bars, with the first at 15 minutes. Each trial was 50 minutes long total, included pre and post shock periods. *Elevated plus maze.* Animals were first recorded in their homecage for 2-5 min. Animals were then transferred to the center of an elevated plus maze arena (150 lux) and remained in the arena while photometry recording took place for the duration of the experiment (10-15 min).

Animals were recorded in the elevated plus maze assay before foot shock to assess innate anxiety responses prior to any experience of shock.

Signal Processing, Behavioral Analysis, Quantification and Statistical Analysis, Verification of imaging sites and histology

Same as in Chapter 3

Results

To characterize the influence of vHPC over PVN^{CRH} cells during stressful experiences, we expressed GCaMP7s in the PVN and either an inhibitory DREADDs construct or a control fluorophore in the vHPC of mice (**Figure 4.1**). We recorded in both areas during the foot shock assay and the elevated plus maze assay, in parallel with our previous experiments in Chapter 3.

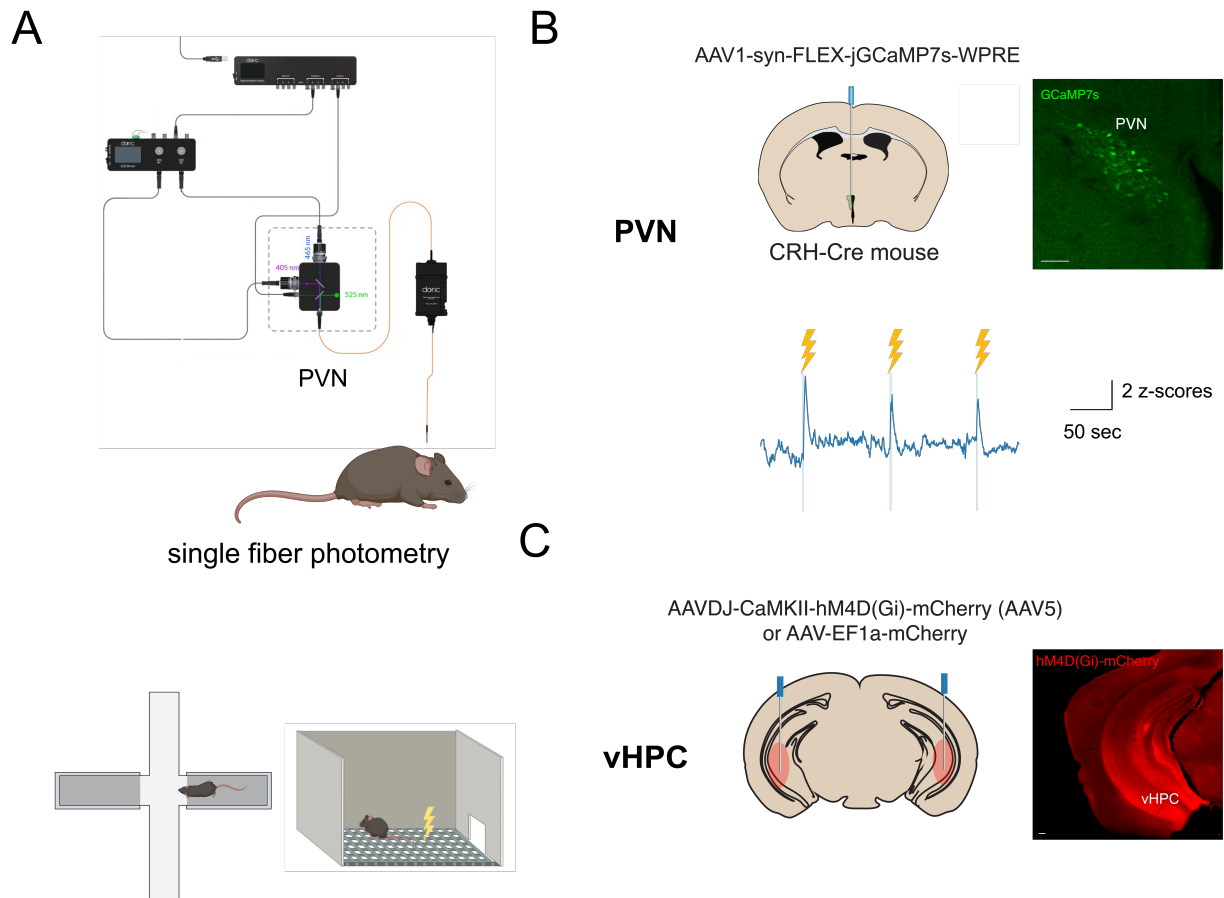


Figure 4.1. Recording bulk activity in PVN^{CRH} and DREADDs inhibition of vHPC during elevated plus maze and foot shock assay. (A) Diagram of PVN photometry recording and behavioral assays. (B) Viral strategy to record from CRH cells in the PVN. Viral expression of GCaMP indicator and example traces in response to a series of foot shocks. Blue bars indicate shocks. (C) Viral strategy and expression to inhibit excitatory cells in vHPC. Scale bars, 100 μ m.

In our experiments from Chapter 3, we observed that the PVN^{CRH} showed selective responses to more immediate stressors like a foot shock and during behaviors like freezing, while not responding strongly to exploration of the elevated plus maze assay. Given the purported role of vHPC in inhibiting the PVN^{CRH} cell activity, we anticipated that removing inhibitory vHPC inputs would unmask increases in PVN^{CRH}

activity. We predicted this effect would be most noticeable in contexts when vHPC activity is most prominent.

vHPC inhibition increases PVN^{CRH} neuron activity during freezing but does not affect PVN^{CRH} responses to shock

We first investigated whether inhibition of excitatory cells in the vHPC led to higher levels of activity in the PVN^{CRH} cells during a series of foot shocks.

We had observed earlier that both PVN^{CRH} and vHPC cells typically increase in activity during foot shocks, though vHPC cells stayed activated longer. With vHPC inhibition, PVN^{CRH} cell responses to the foot shock remained the same (**Figure 4.2A**).

However, the inhibition of vHPC caused a marked change in the activity of PVN^{CRH} cells around the start of a freezing bout (**Figure 4.2C**). When vHPC inhibition was present, PVN^{CRH} cells tended to show a greater, earlier rise in activity compared to that of control animals. A ramping response of activity prior to the start of freezing was also observed, reminiscent of the vHPC activity under normal conditions.

These results suggest that the prevailing model of vHPC inhibition over stress response circuitry like the PVN^{CRH} cells is not limited to slower effects on the scale of tens of minutes, as shown previously. In this case, vHPC exerts inhibitory control over PVN^{CRH} cells during specific behavioral epochs of a stressful experience, namely the initiation of the active coping behavior of freezing but does not noticeably change the responses to shocks.

Previous literature has found that PVN^{CRH} cells play a role in freezing. Mice that receive PVN^{CRH} stimulation show disruptions in typical freezing behavior

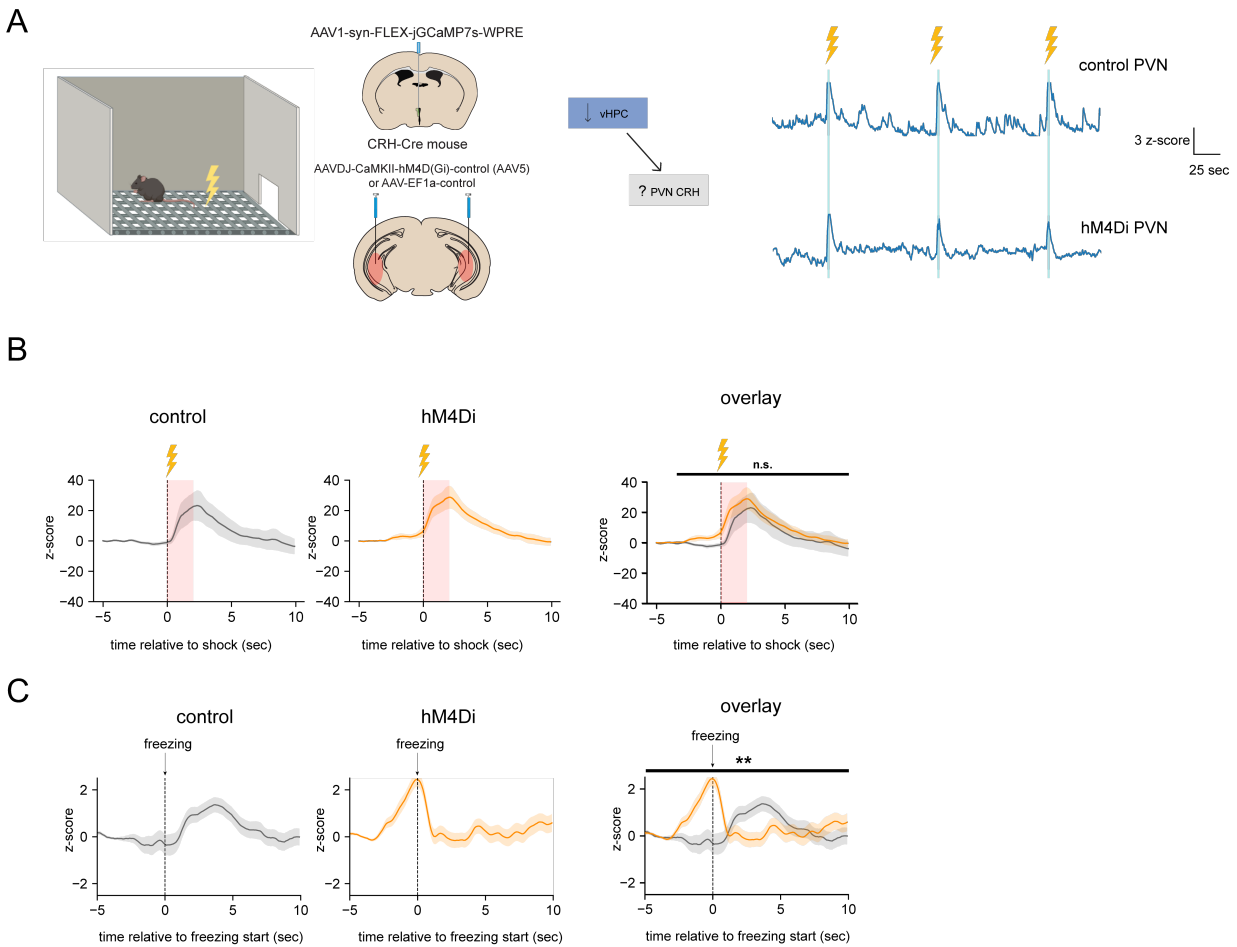


Figure 4.2. vHPC inhibition increases PVN^{CRH} neuron activity during the start of freezing but does not affect PVN^{CRH} responses to shock. (A) Diagram of viral strategy used to inhibit vHPC while recording PVN^{CRH} activity during a foot shock assay and example traces from PVN^{CRH} cells. (B) Calcium activity in PVN^{CRH} centered around the start of a 2 sec shock with and without vHPC inhibition. See Table 4 for statistical comparisons. (C) Same as (B) but aligned to the start of a freezing bout.

following foot shock (Füzési et al., 2016). Therefore, this change in activity might reflect the way typical vHPC inhibition sculpts freezing-related activity in PVN^{CRH} cells.

vHPC inhibition does not significantly alter anxiety-related exploration behavior in the elevated plus maze

We next characterized the effects of inhibiting ventral hippocampus on exploration of the elevated plus maze. Both control and experimental animals showed a preference for the closed arms of the maze, as expected (**Figure 4.3A**), but there was no difference in locomotion, latency to first entry, or speed (**Figure 4.3B, C, D**). Interestingly, we did not see effects on the anxiety-related exploration of the maze either, as both control and experimental animals showed similar levels of activity in the PVN^{CRH} cells in closed or open arms (**Figure 4.4B**). Additionally, animals did not show explore the open arms more as measured in time spent in the open arms (**Figure 4.4C**). Animals receiving inhibition of vHPC trended towards greater number of open arm entries, but the difference was not statistically significant (**Figure 4.4D**).

When the open/center area was further subdivided into open and center, we again did not see significant differences in PVN^{CRH} activity between control animals and animals receiving vHPC inhibition (**Figure 4.5**), though we noted that animals displayed less inter-individual variation in average activity in each of the zones of the maze.

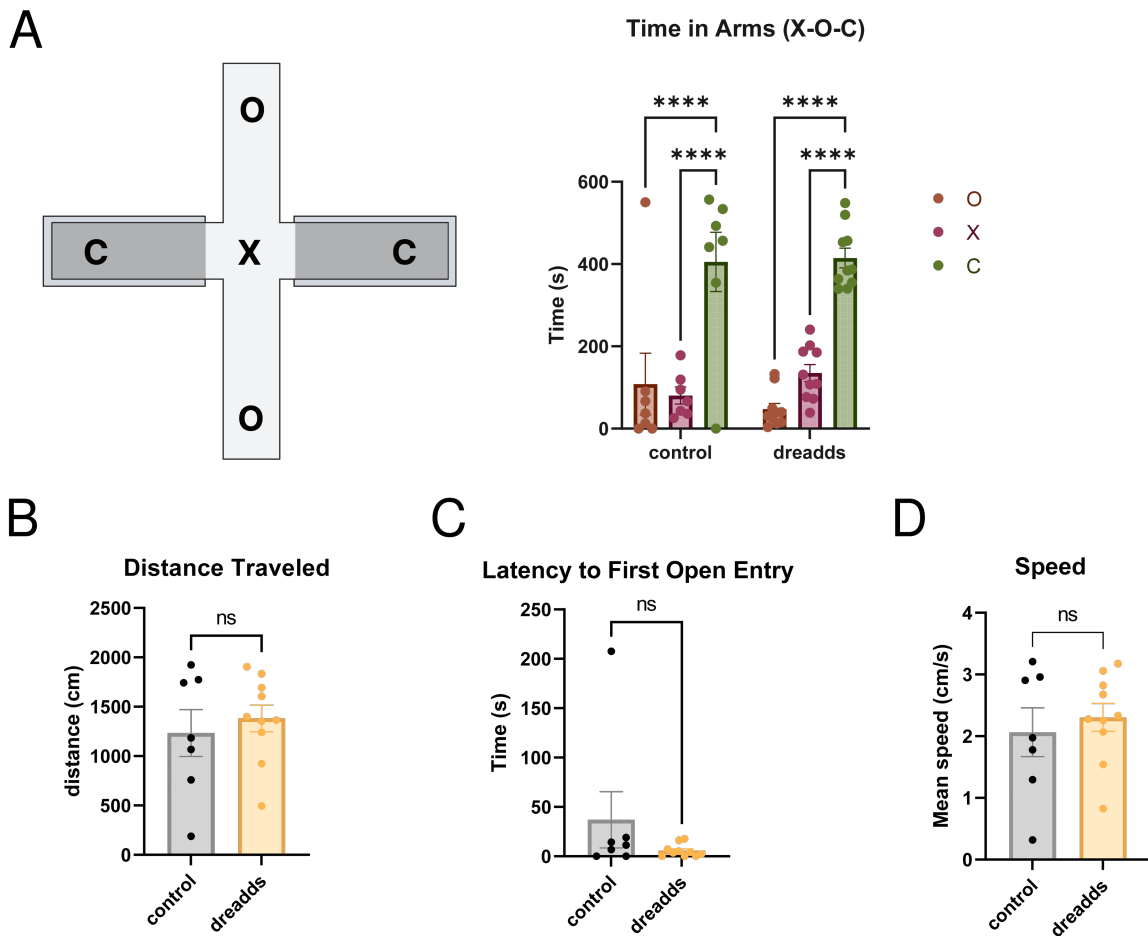


Figure 4.3. Inhibition of vHPC leads to similar motor and anxiety-related behavior in the elevated plus maze. (A) Time in arms during first 10 minutes of the elevated plus maze in control ($n = 7$ mice) vs. DREADDs ($n = 10$ mice). (Two-way ANOVA, arena compartment factor $F(2, 45) = 43.25, P < 0.0001$; experimental group factor $F(1, 45) = 0.001, P = 0.9749$, Sidak's multiple comparison test, control O vs X $p = 0.9567$; control O vs C, $p < 0.0001$; control X vs C, $p < 0.0001$; DREADDs O vs X, $p = 0.2456$; DREADDs O vs C, $p < 0.0001$, DREADDs X vs C, $p < 0.0001$ ($n = 10$ DREADDs mice, $n = 7$ control mice per compartment). This plot splits the open areas of the maze as described more commonly into the center and the connected arms. **(B)** Distance travelled in first 10 minutes of the elevated plus maze in control ($n = 7$) vs. DREADDs mice ($n = 10$ mice). (Unpaired t test, two tailed, $t(15) = 0.5770, p = 0.5725, 95\% \text{ CI} = -396.3 \text{ to } 690.6$). **(C)** Latency to first open arm entry in first 10 minutes of the elevated plus maze (not inclusive of center) in control ($n = 7$ mice) vs. DREADDs ($n = 10$ mice). (Unpaired t test, two-tailed, $t(15) = 1.324, p = 0.2054, 95\% \text{ CI} = -81.78 \text{ to } 19.12$) **(D)** Average speed in first 10 minutes of the elevated plus maze in control ($n = 7$ mice) vs. DREADDs ($n = 10$ mice). (Unpaired t test, two-tailed, $t(15) = 0.5671, p = 0.2891, 95\% \text{ CI} = -0.6629 \text{ to } 1.144$) Data are displayed as mean \pm SEM. C: closed arm, O: open arm, X: center.

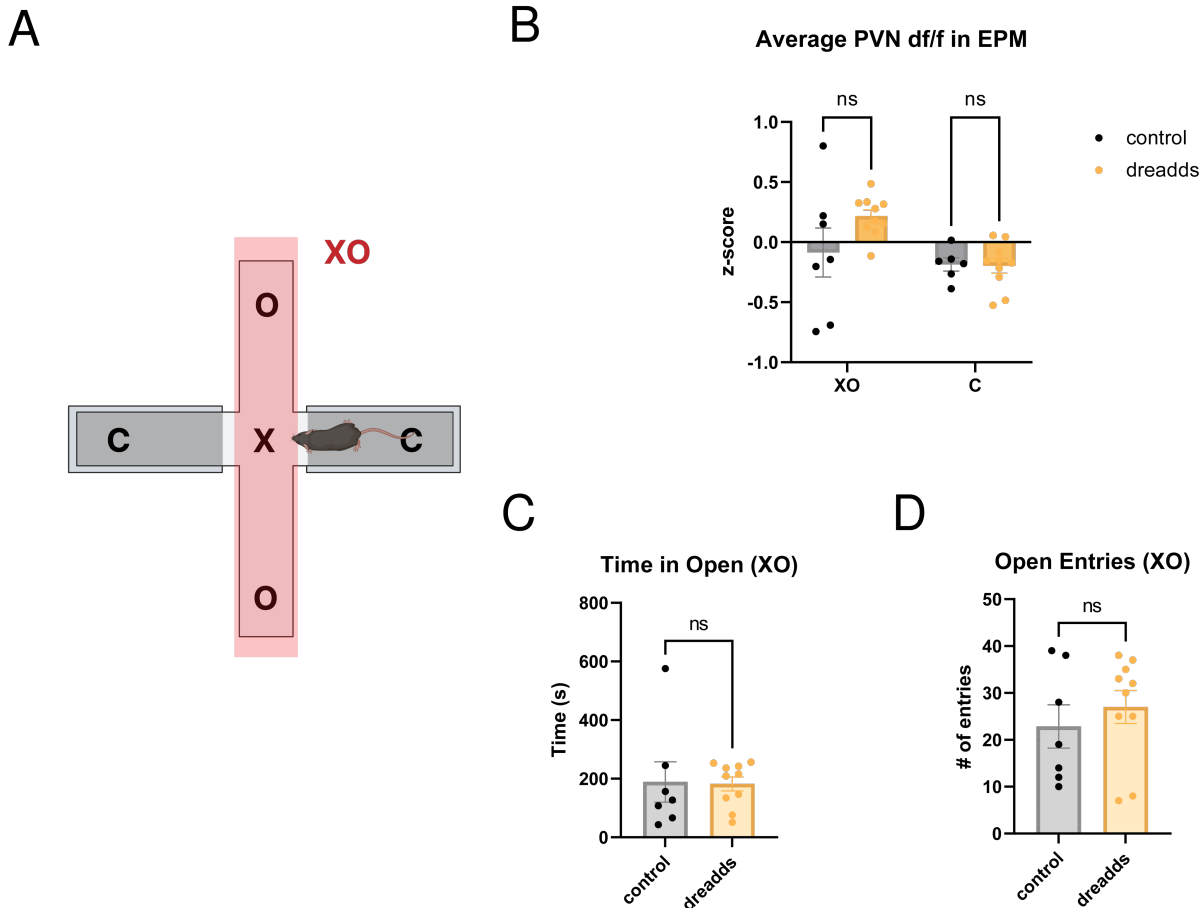


Figure 4.4. Inhibition of vHPC does not significantly affect anxiety-related behavior or overall PVN^{CRH} signal in the elevated plus maze. (A) Schematic of locations in the elevated plus maze, showing open arms (O), closed arms. **(B)** Average PVN df/f in first 10 minutes of the elevated plus maze by zone. (Two-way ANOVA, experimental group factor $F(1, 29) = 1.991, P=0.1689$; EPM zone factor $F(1, 29) = 6.176, P=0.0190$, Sidak's multiple comparison test, control XO ($n = 7$ mice) vs DREADDs XO ($n = 10$ mice) $p = 0.0821$; control C ($n = 6$ mice) vs DREADDs C ($n = 10$ mice), $p = 0.9960$. Data are displayed as mean \pm SEM. C: closed arm, XO: open arm, including center. (C), and the center zone (X). Here, the open zone is defined as a combination of the center as well as the exposed arms (XO). **(C)** Time in open zones in the first 10 minutes of the elevated plus maze in control ($n = 7$) vs. DREADDs mice ($n = 10$ mice). (Unpaired t test, two tailed, $t(15) = 0.1022, p = 0.9200$, 95% CI: -142.5 to 129.5). **(D)** Number of open zone entries in first 10 minutes of the elevated plus maze in control ($n = 7$ mice) vs. DREADDs ($n = 10$ mice). (Unpaired t test, two-tailed, $t(15) = 0.7250, p = 0.4796$, 95% CI = -8.037 to 16.32).

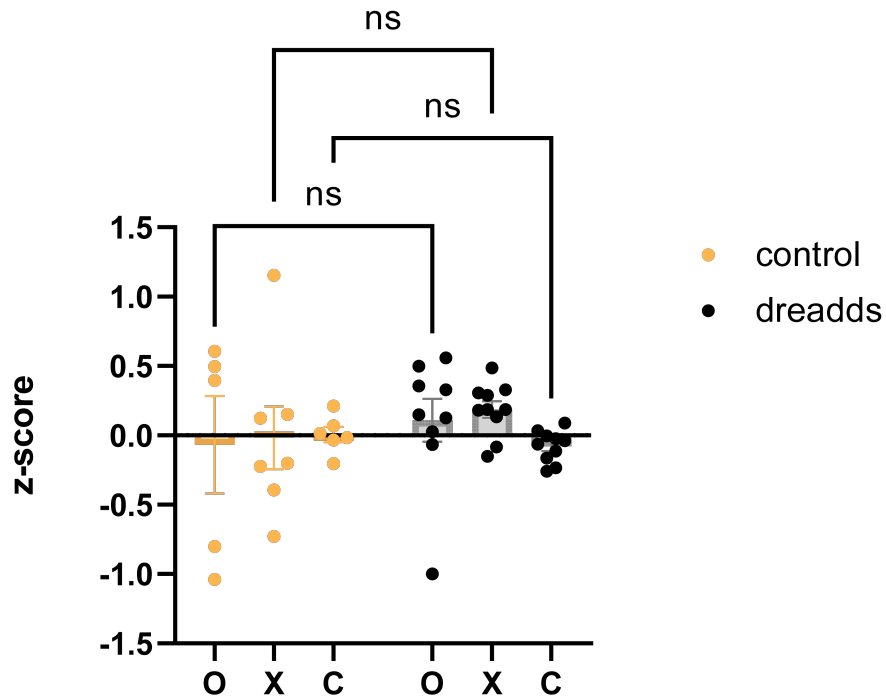


Figure 4.5. Inhibition of vHPC does not affect mean PVN^{CRH} activity in EPM compartments. Average z-scored df/f in each of the elevated plus maze compartments. (Two-way ANOVA, experimental group factor. This plot splits the open areas of the maze as described more commonly into the center and the connected arms. (Two-way ANOVA, experimental group factor $F(2, 41) = 0.3414$, $P = 0.7128$; Sidak's Multiple Comparisons Test, control O vs hM4Di DREADDs O ($n = 5$ control mice, 9 hM4Di DREADDs mice) $p = 0.8264$; center X vs hM4Di DREADDs X ($n = 7$ control mice, 10 hM4Di DREADDs mice) $p = 0.6839$; control C vs hM4Di DREADDs C ($n = 6$ control mice, 10 hM4Di DREADDs mice) $p = 0.9707$. Data are displayed as mean \pm SEM. C: closed arm, O: open arm, X: center.

Other studies have shown that silencing of excitatory cells in vHPC while a mouse is in the open arms can increase exploratory of open arms in the elevated plus maze (Jimenez et al., 2018), but the current study used a chemogenetic strategy inhibiting across the entire trial without specificity for zone. In addition, manipulation of only some projection pathways from vHPC can bias approach-avoidance behavior in similar tasks (Jimenez et al., 2018), so it is reasonable to not see behavioral effects of our less specific vHPC inhibition.

vHPC inhibition slightly increases the level of PVN^{CRH} activity during trajectories between zones in the elevated plus maze

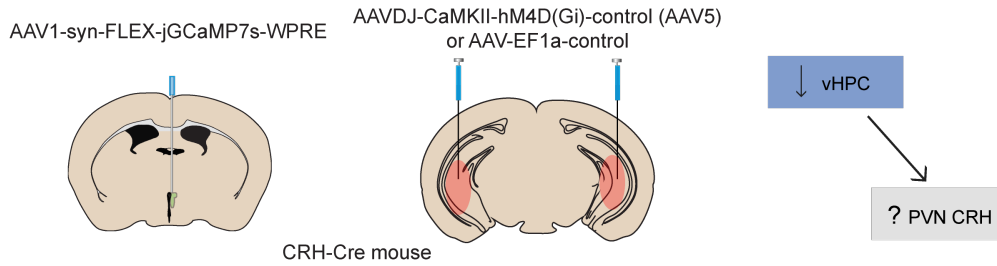
We next assessed the effects of vHPC inhibition on PVN^{CRH} activity while mice moved between zones in the elevated plus maze. We observed a modest unmasking of responses, where the PVN^{CRH} neurons showed a slightly greater response in transitions from open to closed arms and from closed to closed arms (**Figure 4.6**). It should be noted that this unmasking was evident when the average activity was normalized to the entire elevated plus maze trial, not when activity was normalized to the baseline period - 8 to -4 sec before a transition. We did not record enough open arm to open arm transitions to include in our analysis (3 transitions in 2 control animals, and 6 transitions in 3 hM4Di animals).

This slight elevation in activity is consistent with removing a vHPC inhibitory input that is normally present on PVN^{CRH} cells.

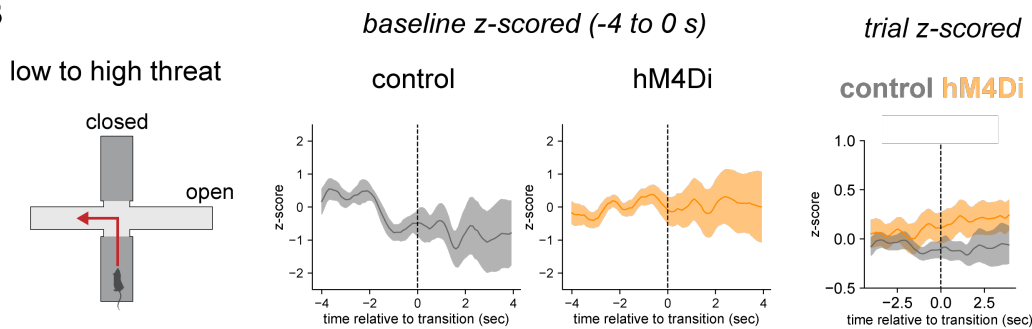
vHPC inhibition alters PVN^{CRH} responses to head dips and rearing in the elevated plus maze

Finally, we assessed the effects of vHPC inhibition on PVN^{CRH} activity during behaviors related to exploration and risk assessment (**Figure 4.7**). Here, we found that vHPC inhibition produced a marked increase in activity during protected and unprotected head dips. Rather than a constant activity, PVN^{CRH} activity now showed an increase.

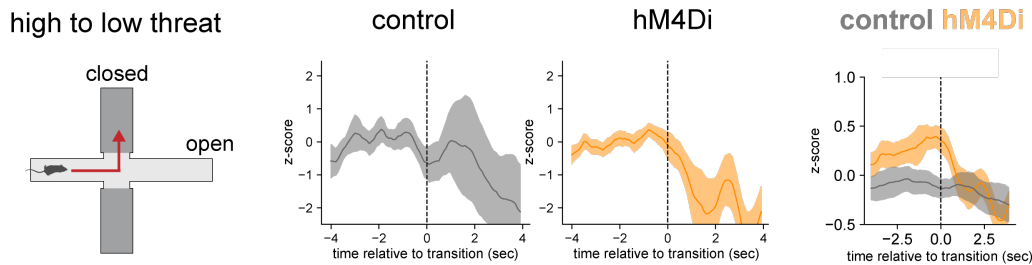
A



B



C



D

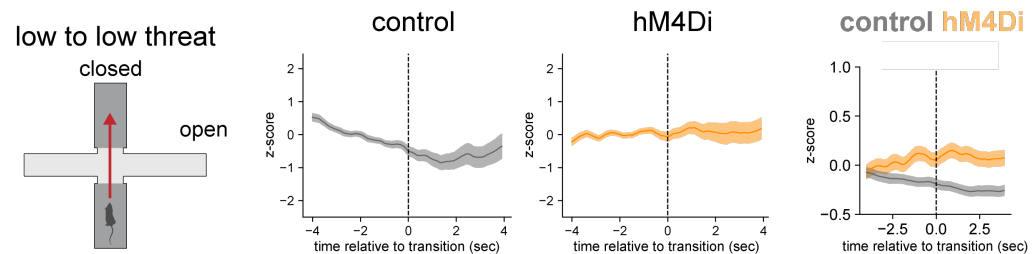


Figure 4.6. vHPC inhibition slightly increases PVNCRH activity during trajectories between threat levels in the elevated plus maze. (A) Diagram of viral strategy used to inhibit ventral hippocampal neurons while recording PVN^{CRH} activity. **(B)** When mice move from a closed arm to an open arm (increase in threat), vHPC inhibition causes a slight increase in PVN^{CRH} activity. n = 11 transitions in 4 control animals, n = 15 transitions in 5 hM4Di animals. (continued on the next page)

(Figure 4.6., continued from the previous page) **(C)** When mice move from an open arm to a closed arm, vHPC inhibition causes a slight increase in PVN^{CRH} activity. n = 7 transitions in 3 control animals, n = 19 transitions in 7 hM4Di animals. **(D)** When mice move from a closed arm to a closed arm, vHPC inhibition causes a slight increase in PVN^{CRH} activity. n = 103 transitions in 5 control animals. n = 125 transitions in 9 hM4Di animals. Data are represented as mean +/- SEM. Left and middle columns represent activity z-scored to the baseline period t = -4 s to t = 0 s. Right columns represent activity which is normalized to the entire elevated plus maze trial. Number of animals in each graph is determined by how many animals performed each trajectory.

On the other hand, rearing showed the opposite result, where vHPC inhibition caused significantly lower activity in PVN^{CRH} cells. Other behaviors did not show strong effects caused by vHPC inhibition.

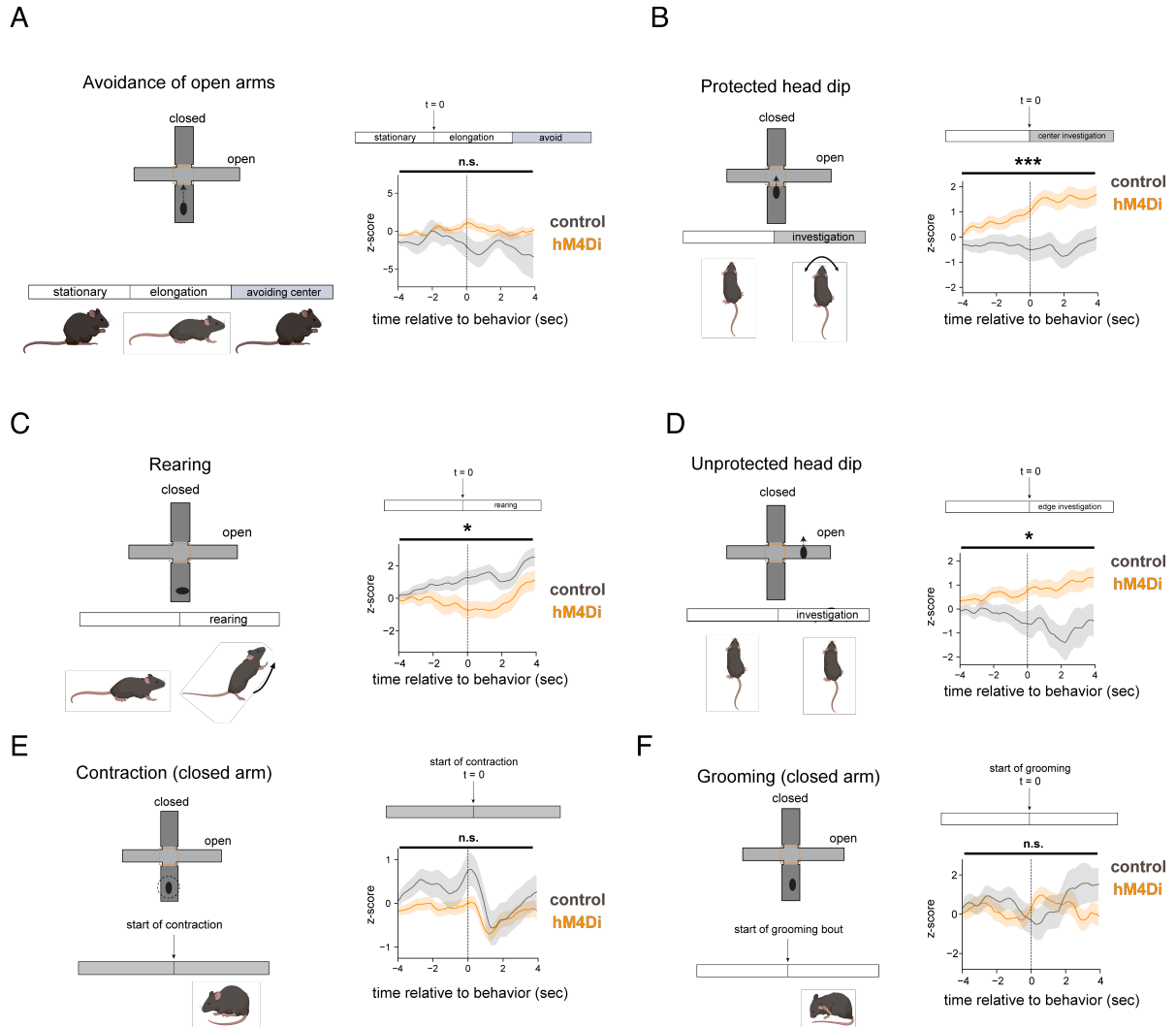


Figure 4.7. Inhibiting vHPC renders CRH neurons responsive to approach-related behavioral motifs. (A) Calcium activity in PVN^{CRH} and vHPC during avoid sequences, centered around the stationary-to-elongation transition. z-scores are normalized to the baseline value over the -8 to -4 sec preceding $t = 0$. **(B, C, D, E, F)** Calcium activity as in (A) but for protected head dip (B), rearing (C), unprotected head dips (D), contraction in the closed arm (E), and grooming (F) Data are displayed as mean \pm SEM. See Table 4 for statistics.

Table 4. Summary of statistical comparisons related to Figure 4.7.

Figure	Variable	Unit of Comparison	n	Test	Results
Fig. 4.5B	PVN CRH activity, shocks	control vs hM4Di factor	3 shocks each from 3 control animals and 4 hM4Di animals	Repeated measures ANOVA	F(1, 19) = 0.045, P = 0.51
Fig. 4.5C	PVN CRH activity, start of freezing	control vs hM4Di factor	28 freezing bouts from 3 control animals and 40 freezing bouts from 4 hM4Di animals	Repeated measures ANOVA	F (1, 620) = 8.589, P=0.0035
Fig. 4.7A	PVN CRH activity, start of elongation before avoidance (-4 to 4 sec window)	control vs hM4Di factor	4 instances from 3 control animals, 12 instances from 6 hM4Di animals	Repeated measures ANOVA	F (1, 14) = 3.691, P = 0.0753
Fig. 4.7B	PVN CRH activity, protected head dip (-4 to 4 sec window)	control vs hM4Di factor	72 instances from 5 control animals, 97 instances from 9 hM4Di animals	Repeated measures ANOVA	F (1, 166) = 13.29, P=0.0004
Fig. 4.7C	PVN CRH activity, rearing (-4 to 4 sec window)	control vs hM4Di factor	76 instances from 4 control animals, 49 instances from 8 hM4Di animals	Repeated measures ANOVA	F (1, 123) = 5.723, P=0.0183
Fig. 4.7D	PVN CRH activity, unprotected head dip (-4 to 4 sec window)	control vs hM4Di factor	58 instances from 5 control animals, 92 instances from 7 hM4Di animals	Repeated measures ANOVA	F (1, 148) = 6.373, P=0.0126
Fig. 4.7E	PVN CRH activity, contraction (-4 to 4 sec window)	control vs hM4Di factor	104 instances from 5 control animals, 226 instances from 9 hM4Di animals	Repeated measures ANOVA	F (1, 328) = 1.826, P=0.1775
Fig. 4.7F	PVN CRH activity, grooming (-4 to 4 sec window)	control vs hM4Di factor	29 instances from 5 control animals, 26 instances from 9 hM4Di animals	Repeated measures ANOVA	F (1, 53) = 0.2826, P=0.5972

Discussion

Our study provides new insights into the dynamic relationship between the ventral hippocampus (vHPC) and the PVN^{CRH} stress response, highlighting the nuanced role of the vHPC in modulating PVN^{CRH} neurons across different stressful experiences.

Previous studies pointed to a role for of vHPC in inhibiting the HPA stress response as measured in stress hormones downstream of PVN^{CRH} circuitry, highlighting a difference that appeared tens of minutes after the stressor. Our experiment was the first to expand this finding to the activity patterns observed during acute stress.

On the acute timescale, vHPC selectively inhibited PVN^{CRH} cells during certain behavioral timepoints. We observed that vHPC does not play a significant role in modulating PVN^{CRH} activity during foot shock but inhibits PVN^{CRH} activity during initiation of freezing. Since we showed in Chapter 3 that smaller peaks in PVN^{CRH} activity often occur before longer bouts of freezing, intact vHPC signals may serve to lengthen freezing bouts. This explanation is in line with the idea of post-shock freezing as a contextual fear response (Fanselow 1980) and vHPC as an important brain area in contextual fear memory (Jimenez et al., 2020; M. E. Wang et al., 2013).

In the elevated plus maze, vHPC seems to provide a small inhibitory tone during a mouse's movement from one compartment to another. According to our results, vHPC also appears to inhibit PVN^{CRH} activity during protected and unprotected head dips. Together, these patterns of activity suggest that the long-term effects of a vHPC inhibitory pathway over PVN^{CRH} cells are also visible on the short-term time scale.

Interestingly, the vHPC modulation during rearing behavior seemed to be excitatory, perhaps using a different relay pathway to reach the PVN^{CRH} cells. Some lesion experiments have suggested that under certain conditions, vHPC plays an excitatory role in the HPA axis (Conforti and Feldman 1976), so this could explain the apparent excitatory role of vHPC in this behavior. This effect might be carried by a feedforward excitatory relay rather than the most well-known GABAergic relay in the bed nucleus of the stria terminalis (BNST).

References for Chapter 4

- Abdallah, C. G., Wrocklage, K. M., Averill, C. L., Akiki, T., Schweinsburg, B., Roy, A., Martini, B., Southwick, S. M., Krystal, J. H., & Scott, J. C. (2017). Anterior hippocampal dysconnectivity in posttraumatic stress disorder: a dimensional and multimodal approach. *Translational Psychiatry*, 7(2), e1045.
<https://doi.org/10.1038/tp.2017.12>
- Addis, D. R., & Schacter, D. L. (2011). The hippocampus and imagining the future: where do we stand? *Frontiers in Human Neuroscience*, 5, 173.
<https://doi.org/10.3389/fnhum.2011.00173>
- Adhikari, A., Topiwala, M. A., & Gordon, J. A. (2010). Synchronized activity between the ventral hippocampus and the medial prefrontal cortex during anxiety. *Neuron*, 65(2), 257–269. <https://doi.org/10.1016/j.neuron.2009.12.002>
- Adhikari, A., Topiwala, M. A., & Gordon, J. A. (2011). Single units in the medial prefrontal cortex with anxiety-related firing patterns are preferentially influenced by ventral hippocampal activity. *Neuron*, 71(5), 898–910.
<https://doi.org/10.1016/j.neuron.2011.07.027>
- AlSubaie, R., Wee, R. W., Ritoux, A., Mishchanchuk, K., Passlack, J., Register, D., & MacAskill, A. F. (2021). Control of parallel hippocampal output pathways by amygdalar long-range inhibition. *eLife*, 10. <https://doi.org/10.7554/eLife.74758>
- Arszovszki, A., Borhegyi, Z., & Klausberger, T. (2014). Three axonal projection routes of individual pyramidal cells in the ventral CA1 hippocampus. *Frontiers in Neuroanatomy*, 8, 53. <https://doi.org/10.3389/fnana.2014.00053>

- Ayhan, F., Kulkarni, A., Berto, S., Sivaprakasam, K., Douglas, C., Lega, B. C., & Konopka, G. (2021). Resolving cellular and molecular diversity along the hippocampal anterior-to-posterior axis in humans. *Neuron*, *109*(13), 2091-2105.e6. <https://doi.org/10.1016/j.neuron.2021.05.003>
- Bagot, R. C., Parise, E. M., Peña, C. J., Zhang, H.-X., Maze, I., Chaudhury, D., Persaud, B., Cachope, R., Bolaños-Guzmán, C. A., Cheer, J. F., Deisseroth, K., Han, M.-H., & Nestler, E. J. (2015). Ventral hippocampal afferents to the nucleus accumbens regulate susceptibility to depression. *Nature Communications*, *6*, 7062. <https://doi.org/10.1038/ncomms8062>
- Barfield, E. T., & Gourley, S. L. (2019). Glucocorticoid-sensitive ventral hippocampal-orbitofrontal cortical connections support goal-directed action - Curt Richter Award Paper 2019. *Psychoneuroendocrinology*, *110*(104436), 104436. <https://doi.org/10.1016/j.psyneuen.2019.104436>
- Bespalov, A., & Steckler, T. (2021). Pharmacology of Anxiety or Pharmacology of Elevated Plus Maze? [Review of *Pharmacology of Anxiety or Pharmacology of Elevated Plus Maze?*]. *Biological Psychiatry*, *89*(12), e73. <https://doi.org/10.1016/j.biopsych.2020.11.026>
- Biane, J. S., Ladow, M. A., Stefanini, F., Boddu, S. P., Fan, A., Hassan, S., Dundar, N., Apodaca-Montano, D. L., Zhou, L. Z., Fayner, V., Woods, N. I., & Kheirbek, M. A. (2023). Neural dynamics underlying associative learning in the dorsal and ventral hippocampus. *Nature Neuroscience*, *26*(5), 798–809. <https://doi.org/10.1038/s41593-023-01296-6>

- Boldrini, M., Butt, T. H., Santiago, A. N., Tamir, H., Dwork, A. J., Rosoklija, G. B., Arango, V., Hen, R., & Mann, J. J. (2014). Benzodiazepines and the potential trophic effect of antidepressants on dentate gyrus cells in mood disorders. *The International Journal of Neuropsychopharmacology*, *17*(12), 1923–1933. <https://doi.org/10.1017/S1461145714000844>
- Chiang, M.-C., Huang, A. J. Y., Wintzer, M. E., Ohshima, T., & McHugh, T. J. (2018). A role for CA3 in social recognition memory. *Behavioural Brain Research*, *354*, 22–30. <https://doi.org/10.1016/j.bbr.2018.01.019>
- Ciocchi, S., Passecker, J., Malagon-Vina, H., Mikus, N., & Klausberger, T. (2015). Brain computation. Selective information routing by ventral hippocampal CA1 projection neurons. *Science*, *348*(6234), 560–563. <https://doi.org/10.1126/science.aaa3245>
- Cole, A. B., Montgomery, K., Bale, T. L., & Thompson, S. M. (2022). What the hippocampus tells the HPA axis: Hippocampal output attenuates acute stress responses via disynaptic inhibition of CRF+ PVN neurons. *Neurobiology of Stress*, *20*, 100473. <https://doi.org/10.1016/j.ynstr.2022.100473>
- Conforti, N., & Feldman, S. (1976). Effects of dorsal fornix section and hippocampectomy on adrenocortical responses to sensory stimulation in the rat. *Neuroendocrinology*, *22*(1), 1–7. <https://doi.org/10.1159/000122607>
- Cullinan, W. S. E., Herman, J. P., & Watson, S. J. (1993). Ventral subicular interaction with the hypothalamic paraventricular nucleus: evidence for a relay in the bed nucleus of the stria terminalis. *The Journal of Comparative Neurology*, *332*(1), 1–20. <https://doi.org/10.1002/cne.903320102>

- Daviu, Nuria, & Bains, J. S. (2021). Should I Stay or Should I Go? CRHPVN Neurons Gate State Transitions in Stress-Related Behaviors. *Endocrinology*, 162(6).
<https://doi.org/10.1210/endo/bqab061>
- Daviu, Núria, Füzesi, T., Rosenegger, D. G., Rasiah, N. P., Sterley, T.-L., Peringod, G., & Bains, J. S. (2020). Paraventricular nucleus CRH neurons encode stress controllability and regulate defensive behavior selection. *Nature Neuroscience*.
<https://doi.org/10.1038/s41593-020-0591-0>
- Dere, E., Dere, D., de Souza Silva, M. A., Huston, J. P., & Zlomuzica, A. (2018). Fellow travellers: Working memory and mental time travel in rodents. *Behavioural Brain Research*, 352, 2–7. <https://doi.org/10.1016/j.bbr.2017.03.026>
- Dos Santos Corrêa, M., Vaz, B. D. S., Grisanti, G. D. V., de Paiva, J. P. Q., Tiba, P. A., & Fornari, R. V. (2019). Relationship between footshock intensity, post-training corticosterone release and contextual fear memory specificity over time. *Psychoneuroendocrinology*, 110, 104447.
<https://doi.org/10.1016/j.psyneuen.2019.104447>
- Dunn, J. D., & Orr, S. E. (1984). Differential plasma corticosterone responses to hippocampal stimulation. *Experimental Brain Research. Experimentelle Hirnforschung. Experimentation Cerebrale*, 54(1), 1–6.
<https://doi.org/10.1007/BF00235813>
- Dupont, A., Bastarache, E., Endröczi, E., & Fortier, C. (1972). Effect of Hippocampal Stimulation on the Plasma Thyrotropin (THS) and Corticosterone Responses to Acute Cold Exposure in the Rat. *Canadian Journal of Physiology and Pharmacology*, 50(4), 364–367. <https://doi.org/10.1139/y72-054>

- Ennaceur, A. (2014). Tests of unconditioned anxiety - pitfalls and disappointments. *Physiology & Behavior*, 135, 55–71.
<https://doi.org/10.1016/j.physbeh.2014.05.032>
- Fanselow, M. S. (1980). Conditional and unconditional components of post-shock freezing. *The Pavlovian Journal of Biological Science : Official Journal of the Pavlovian*, 15(4), 177–182. <https://doi.org/10.1007/BF03001163>
- Fanselow, M. S., & Dong, H.-W. (2010). Are the dorsal and ventral hippocampus functionally distinct structures? *Neuron*, 65(1), 7–19.
<https://doi.org/10.1016/j.neuron.2009.11.031>
- File, S. E., Zangrossi, H., Jr, Sanders, F. L., & Mabbutt, P. S. (1994). Raised corticosterone in the rat after exposure to the elevated plus-maze. *Psychopharmacology*, 113(3–4), 543–546. <https://doi.org/10.1007/BF02245237>
- Füzesi, T., Daviu, N., Wamsteeker Cusulin, J. I., Bonin, R. P., & Bains, J. S. (2016). Hypothalamic CRH neurons orchestrate complex behaviours after stress. *Nature Communications*, 7, 11937. <https://doi.org/10.1038/ncomms11937>
- Gergues, M. M., Han, K. J., Choi, H. S., Brown, B., Clausing, K. J., Turner, V. S., Vainchtein, I. D., Molofsky, A. V., & Kheirbek, M. A. (2020). Circuit and molecular architecture of a ventral hippocampal network. *Nature Neuroscience*, 23(11), 1444–1452. <https://doi.org/10.1038/s41593-020-0705-8>
- Glangetas, C., Massi, L., Fois, G. R., Jalabert, M., Girard, D., Diana, M., Yonehara, K., Roska, B., Xu, C., Lüthi, A., Caille, S., & Georges, F. (2017). NMDA-receptor-dependent plasticity in the bed nucleus of the stria terminalis triggers long-term

anxiolysis. *Nature Communications*, 8, 14456.

<https://doi.org/10.1038/ncomms14456>

Godoy, L. D., Rossignoli, M. T., Delfino-Pereira, P., Garcia-Cairasco, N., & de Lima

Umeoka, E. H. (2018). A Comprehensive Overview on Stress Neurobiology:

Basic Concepts and Clinical Implications. *Frontiers in Behavioral Neuroscience*,

12, 127. <https://doi.org/10.3389/fnbeh.2018.00127>

Graham, J., D'Ambra, A. F., Jung, S. J., Teratani-Ota, Y., Vishwakarma, N., Venkatesh,

R., Parigi, A., Antzoulatos, E. G., Fioravante, D., & Wiltgen, B. J. (2021). High-

frequency stimulation of ventral CA1 neurons reduces amygdala activity and

inhibits fear. *Frontiers in Behavioral Neuroscience*, 15, 595049.

<https://doi.org/10.3389/fnbeh.2021.595049>

Herman, J. P., Dolgas, C. M., & Carlson, S. L. (1998). Ventral subiculum regulates

hypothalamo-pituitary-adrenocortical and behavioural responses to cognitive

stressors. *Neuroscience*, 86(2), 449–459. [https://doi.org/10.1016/s0306-](https://doi.org/10.1016/s0306-4522(98)00055-4)

[4522\(98\)00055-4](https://doi.org/10.1016/s0306-4522(98)00055-4)

Herman, James P., McKlveen, J. M., Ghosal, S., Kopp, B., Wulsin, A., Makinson, R.,

Scheimann, J., & Myers, B. (2016). Regulation of the Hypothalamic-Pituitary-

Adrenocortical Stress Response. *Comprehensive Physiology*, 6(2), 603–621.

<https://doi.org/10.1002/cphy.c150015>

Herman, James P., & Mueller, N. K. (2006). Role of the ventral subiculum in stress

integration. *Behavioural Brain Research*, 174(2), 215–224.

<https://doi.org/10.1016/j.bbr.2006.05.035>

- Hitti, F. L., & Siegelbaum, S. A. (2014). The hippocampal CA2 region is essential for social memory. *Nature*, *508*(7494), 88–92. <https://doi.org/10.1038/nature13028>
- Hu, J., Liu, J., Liu, Y., Wu, X., Zhuang, K., Chen, Q., Yang, W., Xie, P., Qiu, J., & Wei, D. (2021). Dysfunction of the anterior and intermediate hippocampal functional network in major depressive disorders across the adult lifespan. *Biological Psychology*, *165*(108192), 108192. <https://doi.org/10.1016/j.biopsycho.2021.108192>
- Jacobson, L., & Sapolsky, R. (1991). The role of the hippocampus in feedback regulation of the hypothalamic-pituitary-adrenocortical axis. *Endocrine Reviews*, *12*(2), 118–134. <https://doi.org/10.1210/edrv-12-2-118>
- Jimenez, J. C., Berry, J. E., Lim, S. C., Ong, S. K., Kheirbek, M. A., & Hen, R. (2020). Contextual fear memory retrieval by correlated ensembles of ventral CA1 neurons. *Nature Communications*, *11*(1), 3492. <https://doi.org/10.1038/s41467-020-17270-w>
- Jimenez, J. C., Su, K., Goldberg, A. R., Luna, V. M., Biane, J. S., Ordek, G., Zhou, P., Ong, S. K., Wright, M. A., Zweifel, L., Paninski, L., Hen, R., & Kheirbek, M. A. (2018). Anxiety Cells in a Hippocampal-Hypothalamic Circuit. *Neuron*, *97*(3), 670-683.e6. <https://doi.org/10.1016/j.neuron.2018.01.016>
- Kalueff, A. V., Stewart, A. M., Song, C., Berridge, K. C., Graybiel, A. M., & Fentress, J. C. (2016). Neurobiology of rodent self-grooming and its value for translational neuroscience. *Nature Reviews. Neuroscience*, *17*(1), 45–59. <https://doi.org/10.1038/nrn.2015.8>

- Kay, K., Chung, J. E., Sosa, M., Schor, J. S., Karlsson, M. P., Larkin, M. C., Liu, D. F., & Frank, L. M. (2020). Constant sub-second cycling between representations of possible futures in the hippocampus. *Cell*, *180*(3), 552-567.e25.
<https://doi.org/10.1016/j.cell.2020.01.014>
- Kheirbek, M. A., Drew, L. J., Burghardt, N. S., Costantini, D. O., Tannenholz, L., Ahmari, S. E., Zeng, H., Fenton, A. A., & Hen, R. (2013). Differential control of learning and anxiety along the dorsoventral axis of the dentate gyrus. *Neuron*, *77*(5), 955–968. <https://doi.org/10.1016/j.neuron.2012.12.038>
- Kim, J., Lee, S., Fang, Y.-Y., Shin, A., Park, S., Hashikawa, K., Bhat, S., Kim, D., Sohn, J.-W., Lin, D., & Suh, G. S. B. (2019). Rapid, biphasic CRF neuronal responses encode positive and negative valence. *Nature Neuroscience*.
<https://doi.org/10.1038/s41593-019-0342-2>
- Kim, J. S., Han, S. Y., & Iremonger, K. J. (2019). Stress experience and hormone feedback tune distinct components of hypothalamic CRH neuron activity. *Nature Communications*, *10*(1), 5696. <https://doi.org/10.1038/s41467-019-13639-8>
- Kim, W. B., & Cho, J.-H. (2017). Synaptic targeting of double-projecting ventral CA1 hippocampal neurons to the medial prefrontal cortex and basal amygdala. *The Journal of Neuroscience: The Official Journal of the Society for Neuroscience*, *37*(19), 4868–4882. <https://doi.org/10.1523/JNEUROSCI.3579-16.2017>
- Kinlein, S. A., Phillips, D. J., Keller, C. R., & Karatsoreos, I. N. (2019). Role of corticosterone in altered neurobehavioral responses to acute stress in a model of compromised hypothalamic-pituitary-adrenal axis function.

Psychoneuroendocrinology, 102, 248–255.

<https://doi.org/10.1016/j.psyneuen.2018.12.010>

Kirkby, L. A., Luongo, F. J., Lee, M. B., Nahum, M., Van Vleet, T. M., Rao, V. R., Dawes, H. E., Chang, E. F., & Sohal, V. S. (2018). An Amygdala-Hippocampus Subnetwork that Encodes Variation in Human Mood. *Cell*, 175(6), 1688-1700.e14. <https://doi.org/10.1016/j.cell.2018.10.005>

Kjaerby, C., Athilingam, J., Robinson, S. E., lafrati, J., & Sohal, V. S. (2016). Serotonin 1B receptors regulate prefrontal function by gating callosal and hippocampal inputs. *Cell Reports*, 17(11), 2882–2890. <https://doi.org/10.1016/j.celrep.2016.11.036>

Kjelstrup, K. G., Tuvnes, F. A., Steffenach, H.-A., Murison, R., Moser, E. I., & Moser, M.-B. (2002). Reduced fear expression after lesions of the ventral hippocampus. *Proceedings of the National Academy of Sciences of the United States of America*, 99(16), 10825–10830. <https://doi.org/10.1073/pnas.152112399>

Korte, S. M., & De Boer, S. F. (2003). A robust animal model of state anxiety: fear-potentiated behaviour in the elevated plus-maze. *European Journal of Pharmacology*, 463(1–3), 163–175. [https://doi.org/10.1016/s0014-2999\(03\)01279-2](https://doi.org/10.1016/s0014-2999(03)01279-2)

La-Vu, M., Tobias, B. C., Schuette, P. J., & Adhikari, A. (2020). To Approach or Avoid: An Introductory Overview of the Study of Anxiety Using Rodent Assays. *Frontiers in Behavioral Neuroscience*, 14, 145. <https://doi.org/10.3389/fnbeh.2020.00145>

Lazarov, A., Zhu, X., Suarez-Jimenez, B., Rutherford, B. R., & Neria, Y. (2017). Resting-state functional connectivity of anterior and posterior hippocampus in

- posttraumatic stress disorder. *Journal of Psychiatric Research*, 94, 15–22.
<https://doi.org/10.1016/j.jpsychires.2017.06.003>
- Lee, S.-H., Marchionni, I., Bezaire, M., Varga, C., Danielson, N., Lovett-Barron, M., Losonczy, A., & Soltesz, I. (2014). Parvalbumin-positive basket cells differentiate among hippocampal pyramidal cells. *Neuron*, 82(5), 1129–1144.
<https://doi.org/10.1016/j.neuron.2014.03.034>
- LeGates, T. A., Kivarta, M. D., Tooley, J. R., Francis, T. C., Lobo, M. K., Creed, M. C., & Thompson, S. M. (2018). Reward behaviour is regulated by the strength of hippocampus-nucleus accumbens synapses. *Nature*, 564(7735), 258–262.
<https://doi.org/10.1038/s41586-018-0740-8>
- Lerner, T. N., Shilyansky, C., Davidson, T. J., Evans, K. E., Beier, K. T., Zalocusky, K. A., Crow, A. K., Malenka, R. C., Luo, L., Tomer, R., & Deisseroth, K. (2015). Intact-Brain Analyses Reveal Distinct Information Carried by SNc Dopamine Subcircuits. *Cell*, 162(3), 635–647. <https://doi.org/10.1016/j.cell.2015.07.014>
- Li, S.-B., Borniger, J. C., Yamaguchi, H., Hédou, J., Gaudilliere, B., & de Lecea, L. (2020). Hypothalamic circuitry underlying stress-induced insomnia and peripheral immunosuppression. *Science Advances*, 6(37).
<https://doi.org/10.1126/sciadv.abc2590>
- Maguire, E. A., Gadian, D. G., Johnsrude, I. S., Good, C. D., Ashburner, J., Frackowiak, R. S., & Frith, C. D. (2000). Navigation-related structural change in the hippocampi of taxi drivers. *Proceedings of the National Academy of Sciences of the United States of America*, 97(8), 4398–4403.
<https://doi.org/10.1073/pnas.070039597>

- Malagon-Vina, H., Ciocchi, S., & Klausberger, T. (2023). Firing patterns of ventral hippocampal neurons predict the exploration of anxiogenic locations. *ELife*, 12. <https://doi.org/10.7554/eLife.83012>
- Mandell, A. J., Chapman, L. F., Rand, R. W., & Walter, R. D. (1963). Plasma Corticosteroids: Changes in Concentration after Stimulation of Hippocampus and Amygdala. *Science*, 139(3560), 1212. <https://doi.org/10.1126/science.139.3560.1212>
- Marchand, A. R., Barbelivien, A., Seillier, A., Herbeaux, K., Sarrieau, A., & Majchrzak, M. (2007). Contribution of corticosterone to cued versus contextual fear in rats. *Behavioural Brain Research*, 183(1), 101–110. <https://doi.org/10.1016/j.bbr.2007.05.034>
- McNaughton, B. L., Battaglia, F. P., Jensen, O., Moser, E. I., & Moser, M.-B. (2006). Path integration and the neural basis of the “cognitive map.” *Nature Reviews Neuroscience*, 7(8), 663–678. <https://doi.org/10.1038/nrn1932>
- Meira, T., Leroy, F., Buss, E. W., Oliva, A., Park, J., & Siegelbaum, S. A. (2018). A hippocampal circuit linking dorsal CA2 to ventral CA1 critical for social memory dynamics. *Nature Communications*, 9(1), 4163. <https://doi.org/10.1038/s41467-018-06501-w>
- Miloyan, B., Pachana, N. A., & Suddendorf, T. (2014). The future is here: a review of foresight systems in anxiety and depression. *Cognition & Emotion*, 28(5), 795–810. <https://doi.org/10.1080/02699931.2013.863179>
- Mitchell, C. S., Campbell, E. J., Fisher, S. D., Stanton, L. M., Burton, N. J., Pearl, A. J., McNally, G. P., Bains, J. S., Füzesi, T., Graham, B. A., Manning, E. E., & Dayas,

- C. V. (2023). Optogenetic recruitment of hypothalamic corticotrophin-releasing-hormone (CRH) neurons reduces motivational drive. In *bioRxiv* (p. 2023.02.03.527084). <https://doi.org/10.1101/2023.02.03.527084>
- Montagrin, A., Saiote, C., & Schiller, D. (2018). The social hippocampus. *Hippocampus*, 28(9), 672–679. <https://doi.org/10.1002/hipo.22797>
- Moustafa, A. A., Morris, A. N., & ElHaj, M. (2018). A review on future episodic thinking in mood and anxiety disorders. *Reviews in the Neurosciences*, 30(1), 85–94. <https://doi.org/10.1515/revneuro-2017-0055>
- Mueller, N. K., Dolgas, C. M., & Herman, J. P. (2004). Stressor-selective role of the ventral subiculum in regulation of neuroendocrine stress responses. *Endocrinology*, 145(8), 3763–3768. <https://doi.org/10.1210/en.2004-0097>
- Muir, J., Tse, Y. C., Iyer, E. S., Biris, J., Cvetkovska, V., Lopez, J., & Bagot, R. C. (2020). Ventral hippocampal afferents to nucleus accumbens encode both latent vulnerability and stress-induced susceptibility. *Biological Psychiatry*, 88(11), 843–854. <https://doi.org/10.1016/j.biopsych.2020.05.021>
- Murphy, K. Z., Haile, E., McTigue, A., Pierce, A. F., & Donaldson, Z. R. (2023). PhAT: A flexible open-source GUI-driven toolkit for photometry analysis. *BioRxiv : The Preprint Server for Biology*. <https://doi.org/10.1101/2023.03.14.532489>
- Myers, B., McKlveen, J. M., & Herman, J. P. (2012). Neural Regulation of the Stress Response: The Many Faces of Feedback. *Cellular and Molecular Neurobiology*. <https://doi.org/10.1007/s10571-012-9801-y>
- Naughton, M., Dinan, T. G., & Scott, L. V. (2014). Corticotropin-releasing hormone and the hypothalamic-pituitary-adrenal axis in psychiatric disease. *Handbook of*

Clinical Neurology, 124, 69–91. <https://doi.org/10.1016/B978-0-444-59602-4.00005-8>

Nyberg, N., Duvelle, É., Barry, C., & Spiers, H. J. (2022). Spatial goal coding in the hippocampal formation. *Neuron*, 110(3), 394–422.

<https://doi.org/10.1016/j.neuron.2021.12.012>

O’Doherty, D. C. M., Chitty, K. M., Saddiqui, S., Bennett, M. R., & Lagopoulos, J. (2015). A systematic review and meta-analysis of magnetic resonance imaging measurement of structural volumes in posttraumatic stress disorder. *Psychiatry Research*, 232(1), 1–33. <https://doi.org/10.1016/j.psychresns.2015.01.002>

O’Keefe, J., & Nadel, L. (1978). *The Hippocampus as a Cognitive Map*. Oxford University Press.

Okuyama, T., Kitamura, T., Roy, D. S., Itohara, S., & Tonegawa, S. (2016). Ventral CA1 neurons store social memory. *Science*, 353(6307), 1536–1541.

<https://doi.org/10.1126/science.aaf7003>

Oleksiak, C. R., Ramanathan, K. R., Miles, O. W., Perry, S. J., Maren, S., & Moscarello, J. M. (2021). Ventral hippocampus mediates the context-dependence of two-way signaled avoidance in male rats. *Neurobiology of Learning and Memory*, 183, 107458. <https://doi.org/10.1016/j.nlm.2021.107458>

Ono, D., Mukai, Y., Hung, C. J., Chowdhury, S., Sugiyama, T., & Yamanaka, A. (2020). The mammalian circadian pacemaker regulates wakefulness via CRF neurons in the paraventricular nucleus of the hypothalamus. *Science Advances*, 6(45).

<https://doi.org/10.1126/sciadv.abd0384>

- Padilla-Coreano, N., Bolkan, S. S., Pierce, G. M., Blackman, D. R., Hardin, W. D., Garcia-Garcia, A. L., Spellman, T. J., & Gordon, J. A. (2016). Direct Ventral Hippocampal-Prefrontal Input Is Required for Anxiety-Related Neural Activity and Behavior. *Neuron*, *89*(4), 857–866. <https://doi.org/10.1016/j.neuron.2016.01.011>
- Park, A. J., Harris, A. Z., Martyniuk, K. M., Chang, C.-Y., Abbas, A. I., Lowes, D. C., Kellendonk, C., Gogos, J. A., & Gordon, J. A. (2021). Reset of hippocampal-prefrontal circuitry facilitates learning. *Nature*, *591*(7851), 615–619. <https://doi.org/10.1038/s41586-021-03272-1>
- Pellow, S., Chopin, P., File, S. E., & Briley, M. (1985). Validation of open:closed arm entries in an elevated plus-maze as a measure of anxiety in the rat. *Journal of Neuroscience Methods*, *14*(3), 149–167. [https://doi.org/10.1016/0165-0270\(85\)90031-7](https://doi.org/10.1016/0165-0270(85)90031-7)
- Phillips, M. L., Robinson, H. A., & Pozzo-Miller, L. (2019). Ventral hippocampal projections to the medial prefrontal cortex regulate social memory. *ELife*, *8*. <https://doi.org/10.7554/eLife.44182>
- Pitman, R. K., Rasmusson, A. M., Koenen, K. C., Shin, L. M., Orr, S. P., Gilbertson, M. W., Milad, M. R., & Liberzon, I. (2012). Biological studies of post-traumatic stress disorder. *Nature Reviews. Neuroscience*, *13*(11), 769–787. <https://doi.org/10.1038/nrn3339>
- Poppenk, J., Evensmoen, H. R., Moscovitch, M., & Nadel, L. (2013). Long-axis specialization of the human hippocampus. *Trends in Cognitive Sciences*, *17*(5), 230–240. <https://doi.org/10.1016/j.tics.2013.03.005>

- Radley, J. J., Gosselink, K. L., & Sawchenko, P. E. (2009). A discrete GABAergic relay mediates medial prefrontal cortical inhibition of the neuroendocrine stress response. *The Journal of Neuroscience: The Official Journal of the Society for Neuroscience*, *29*(22), 7330–7340. <https://doi.org/10.1523/JNEUROSCI.5924-08.2009>
- Radley, J. J., & Sawchenko, P. E. (2011). A common substrate for prefrontal and hippocampal inhibition of the neuroendocrine stress response. *The Journal of Neuroscience: The Official Journal of the Society for Neuroscience*, *31*(26), 9683–9695. <https://doi.org/10.1523/JNEUROSCI.6040-10.2011>
- Radley, J. J., & Sawchenko, P. E. (2015). Evidence for involvement of a limbic paraventricular hypothalamic inhibitory network in hypothalamic-pituitary-adrenal axis adaptations to repeated stress. *The Journal of Comparative Neurology*, *523*(18), 2769–2787. <https://doi.org/10.1002/cne.23815>
- Rao, R. P., von Heimendahl, M., Bahr, V., & Brecht, M. (2019). Neuronal responses to conspecifics in the ventral CA1. *Cell Reports*, *27*(12), 3460-3472.e3. <https://doi.org/10.1016/j.celrep.2019.05.081>
- Reed, S. J., Lafferty, C. K., Mendoza, J. A., Yang, A. K., Davidson, T. J., Grosenick, L., Deisseroth, K., & Britt, J. P. (2018). Coordinated reductions in excitatory input to the nucleus accumbens underlie food consumption. *Neuron*, *99*(6), 1260-1273.e4. <https://doi.org/10.1016/j.neuron.2018.07.051>
- Rodgers, R. J., Haller, J., Holmes, A., Halasz, J., Walton, T. J., & Brain, P. F. (1999). Corticosterone response to the plus-maze: high correlation with risk assessment

- in rats and mice. *Physiology & Behavior*, 68(1–2), 47–53.
[https://doi.org/10.1016/s0031-9384\(99\)00140-7](https://doi.org/10.1016/s0031-9384(99)00140-7)
- Rosso, M., Wirz, R., Loretan, A. V., Sutter, N. A., Pereira da Cunha, C. T., Jaric, I., Würbel, H., & Voelkl, B. (2022). Reliability of common mouse behavioural tests of anxiety: A systematic review and meta-analysis on the effects of anxiolytics. *Neuroscience and Biobehavioral Reviews*, 143, 104928.
<https://doi.org/10.1016/j.neubiorev.2022.104928>
- Rubin, R. T., Mandell, A. J., & Crandall, P. H. (1966). Corticosteroid responses to limbic stimulation in man: localization of stimulus sites. *Science*, 153(3737), 767–768.
<https://www.ncbi.nlm.nih.gov/pubmed/5940897>
- Sahu, M. K., Dubey, R. K., Chandrakar, A., Kumar, M., & Kumar, M. (2022). A systematic review and meta-analysis of serum and plasma cortisol levels in depressed patients versus control. *Indian Journal of Psychiatry*, 64(5), 440–448.
https://doi.org/10.4103/indianjpsychiatry.indianjpsychiatry_561_21
- Sánchez-Bellot, C., AlSubaie, R., Mishchanchuk, K., Wee, R. W. S., & MacAskill, A. F. (2022). Two opposing hippocampus to prefrontal cortex pathways for the control of approach and avoidance behaviour. *Nature Communications*, 13(1), 339.
<https://doi.org/10.1038/s41467-022-27977-7>
- Sbisa, A. M., Madden, K., Toben, C., McFarlane, A. C., Dell, L., & Lawrence-Wood, E. (2023). Potential peripheral biomarkers associated with the emergence and presence of posttraumatic stress disorder symptomatology: A systematic review. *Psychoneuroendocrinology*, 147, 105954.
<https://doi.org/10.1016/j.psyneuen.2022.105954>

- Segalin, C., Williams, J., Karigo, T., Hui, M., Zelikowsky, M., Sun, J. J., Perona, P., Anderson, D. J., & Kennedy, A. (2021). The Mouse Action Recognition System (MARS) software pipeline for automated analysis of social behaviors in mice. *ELife*, *10*. <https://doi.org/10.7554/eLife.63720>
- Shpokayte, M., McKissick, O., Guan, X., Yuan, B., Rahsepar, B., Fernandez, F. R., Ruesch, E., Grella, S. L., White, J. A., Liu, X. S., & Ramirez, S. (2022). Hippocampal cells segregate positive and negative engrams. *Communications Biology*, *5*(1), 1009. <https://doi.org/10.1038/s42003-022-03906-8>
- Song, C., Berridge, K. C., & Kalueff, A. V. (2016). “Stressing” rodent self-grooming for neuroscience research [Review of “*Stressing*” rodent self-grooming for neuroscience research]. *Nature Reviews. Neuroscience*, *17*(9), 591. <https://doi.org/10.1038/nrn.2016.103>
- Sosa, M., & Giocomo, L. M. (2021). Navigating for reward. *Nature Reviews. Neuroscience*, *22*(8), 472–487. <https://doi.org/10.1038/s41583-021-00479-z>
- Sosa, M., Joo, H. R., & Frank, L. M. (2020). Dorsal and ventral hippocampal sharp-wave ripples activate distinct nucleus accumbens networks. *Neuron*, *105*(4), 725–741.e8. <https://doi.org/10.1016/j.neuron.2019.11.022>
- Spencer, R. L., & Deak, T. (2017). A users guide to HPA axis research. *Physiology & Behavior*, *178*, 43–65. <https://doi.org/10.1016/j.physbeh.2016.11.014>
- Strange, B. A., Witter, M. P., Lein, E. S., & Moser, E. I. (2014). Functional organization of the hippocampal longitudinal axis. *Nature Reviews. Neuroscience*, *15*(10), 655–669. <https://doi.org/10.1038/nrn3785>

- Suarez, A. N., Liu, C. M., Cortella, A. M., Noble, E. E., & Kanoski, S. E. (2020). Ghrelin and orexin interact to increase meal size through a descending hippocampus to hindbrain signaling pathway. *Biological Psychiatry*, *87*(11), 1001–1011. <https://doi.org/10.1016/j.biopsych.2019.10.012>
- Suarez-Jimenez, B., Albajes-Eizagirre, A., Lazarov, A., Zhu, X., Harrison, B. J., Radua, J., Neria, Y., & Fullana, M. A. (2020). Neural signatures of conditioning, extinction learning, and extinction recall in posttraumatic stress disorder: a meta-analysis of functional magnetic resonance imaging studies. *Psychological Medicine*, *50*(9), 1442–1451. <https://doi.org/10.1017/S0033291719001387>
- Tao, K., Chung, M., Watarai, A., Huang, Z., Wang, M.-Y., & Okuyama, T. (2022). Disrupted social memory ensembles in the ventral hippocampus underlie social amnesia in autism-associated Shank3 mutant mice. *Molecular Psychiatry*, *27*(4), 2095–2105. <https://doi.org/10.1038/s41380-021-01430-5>
- Tavares, R. M., Mendelsohn, A., Grossman, Y., Williams, C. H., Shapiro, M., Trope, Y., & Schiller, D. (2015). A map for social navigation in the human brain. *Neuron*, *87*(1), 231–243. <https://doi.org/10.1016/j.neuron.2015.06.011>
- Terranova, J. I., Yokose, J., Osanai, H., Marks, W. D., Yamamoto, J., Ogawa, S. K., & Kitamura, T. (2022). Hippocampal-amygdala memory circuits govern experience-dependent observational fear. *Neuron*, *110*(8), 1416-1431.e13. <https://doi.org/10.1016/j.neuron.2022.01.019>
- Trouche, S., Koren, V., Doig, N. M., Ellender, T. J., El-Gaby, M., Lopes-dos-Santos, V., Reeve, H. M., Perestenko, P. V., Garas, F. N., Magill, P. J., Sharott, A., & Dupret,

- D. (2019). A Hippocampus-Accumbens Tripartite Neuronal Motif Guides Appetitive Memory in Space. *Cell*, 0(0). <https://doi.org/10.1016/j.cell.2018.12.037>
- Tuvnes, F. A., Steffenach, H.-A., Murison, R., Moser, M.-B., & Moser, E. I. (2003). Selective hippocampal lesions do not increase adrenocortical activity. *The Journal of Neuroscience: The Official Journal of the Society for Neuroscience*, 23(10), 4345–4354. <https://www.ncbi.nlm.nih.gov/pubmed/12764123>
- Vogel, J. W., La Joie, R., Grothe, M. J., Diaz-Papkovich, A., Doyle, A., Vachon-Pressseau, E., Lepage, C., Vos de Wael, R., Thomas, R. A., Iturria-Medina, Y., Bernhardt, B., Rabinovici, G. D., & Evans, A. C. (2020). A molecular gradient along the longitudinal axis of the human hippocampus informs large-scale behavioral systems. *Nature Communications*, 11(1), 960. <https://doi.org/10.1038/s41467-020-14518-3>
- Vom Berg-Maurer, C. M., Trivedi, C. A., Bollmann, J. H., De Marco, R. J., & Ryu, S. (2016). The Severity of Acute Stress Is Represented by Increased Synchronous Activity and Recruitment of Hypothalamic CRH Neurons. *The Journal of Neuroscience: The Official Journal of the Society for Neuroscience*, 36(11), 3350–3362. <https://doi.org/10.1523/JNEUROSCI.3390-15.2016>
- Walf, A. A., & Frye, C. A. (2007). The use of the elevated plus maze as an assay of anxiety-related behavior in rodents. *Nature Protocols*, 2(2), 322–328. <https://doi.org/10.1038/nprot.2007.44>
- Wang, M. E., Fraize, N. P., Yin, L., Yuan, R. K., Petsagourakis, D., Wann, E. G., & Muzzio, I. A. (2013). Differential roles of the dorsal and ventral hippocampus in

- predator odor contextual fear conditioning. *Hippocampus*, 23(6), 451–466.
<https://doi.org/10.1002/hipo.22105>
- Wang, Q., Jin, J., & Maren, S. (2016). Renewal of extinguished fear activates ventral hippocampal neurons projecting to the prelimbic and infralimbic cortices in rats. *Neurobiology of Learning and Memory*, 134 Pt A, 38–43.
<https://doi.org/10.1016/j.nlm.2016.04.002>
- Watarai, A., Tao, K., Wang, M.-Y., & Okuyama, T. (2021). Distinct functions of ventral CA1 and dorsal CA2 in social memory. *Current Opinion in Neurobiology*, 68, 29–35. <https://doi.org/10.1016/j.conb.2020.12.008>
- Wee, R. W. S., & MacAskill, A. F. (2020). Biased connectivity of brain-wide inputs to ventral subiculum output neurons. *Cell Reports*, 30(11), 3644-3654.e6.
<https://doi.org/10.1016/j.celrep.2020.02.093>
- Wee, R. W. S., Mishchanchuk, K., AlSubaie, R., & MacAskill, A. F. (2021). Internal state dependent control of feeding behaviour via hippocampal ghrelin signalling. In *bioRxiv*. <https://doi.org/10.1101/2021.11.05.467326>
- Woods, N. I., Stefanini, F., Apodaca-Montano, D. L., Tan, I. M. C., Biane, J. S., & Kheirbek, M. A. (2020). The dentate gyrus classifies cortical representations of learned stimuli. *Neuron*, 107(1), 173-184.e6.
<https://doi.org/10.1016/j.neuron.2020.04.002>
- Xia, F., & Kheirbek, M. A. (2020). Circuit-Based Biomarkers for Mood and Anxiety Disorders. *Trends in Neurosciences*, 43(11), 902–915.
<https://doi.org/10.1016/j.tins.2020.08.004>

- Xu, C., Krabbe, S., Gründemann, J., Botta, P., Fadok, J. P., Osakada, F., Saur, D., Grewe, B. F., Schnitzer, M. J., Callaway, E. M., & Lüthi, A. (2016). Distinct Hippocampal Pathways Mediate Dissociable Roles of Context in Memory Retrieval. *Cell*, 167(4), 961-972.e16. <https://doi.org/10.1016/j.cell.2016.09.051>
- Xu, S., Yang, H., Menon, V., Lemire, A. L., Wang, L., Henry, F. E., Turaga, S. C., & Sternson, S. M. (2020). Behavioral state coding by molecularly defined paraventricular hypothalamic cell type ensembles. *Science*, 370(6514). <https://doi.org/10.1126/science.abb2494>
- Yang, A. K., Mendoza, J. A., Lafferty, C. K., Lacroix, F., & Britt, J. P. (2020). Hippocampal input to the nucleus accumbens shell enhances food palatability. *Biological Psychiatry*, 87(7), 597–608. <https://doi.org/10.1016/j.biopsych.2019.09.007>
- Yuan, Y., Wu, W., Chen, M., Cai, F., Fan, C., Shen, W., Sun, W., & Hu, J. (2019). Reward Inhibits Paraventricular CRH Neurons to Relieve Stress. *Current Biology: CB*, 0(0). <https://doi.org/10.1016/j.cub.2019.02.048>
- Zeidman, P., & Maguire, E. A. (2016). Anterior hippocampus: the anatomy of perception, imagination and episodic memory. *Nature Reviews. Neuroscience*, 17(3), 173–182. <https://doi.org/10.1038/nrn.2015.24>

Chapter 5: Conclusions

Stress responses, whether behavioral or physiological, are important for an animal's survival in the face of immediate or anticipated threat.

In this work, we aimed to address how the hippocampus and the hypothalamus coordinate to regulate neural and behavioral responses to a stressful stimulus on a moment-to-moment basis. We evaluated the activation of both regions during uncontrollable, immediate threat (foot shocks) and controllable, ambiguous threat (exploration of the elevated plus maze).

We established a distinction in neuronal responses between the vHPC and PVN^{CRH} cells. Both regions strongly increased in activity both to foot shocks themselves and the start of freezing after foot shocks, but only vHPC showed strong increases in activity when entering areas of higher potential threat in the elevated plus maze. These results show that vHPC is highly attuned to the aversive nature of an animal's surroundings, whereas PVN^{CRH} tends to be activated more by higher levels of potential threat, especially in preparation for active escape-related behaviors.

Our results indicated that vHPC neurons, compared to PVN^{CRH} neurons, are more dynamically responsive to immediate environmental stimuli in foot shock and elevated plus maze assays. We also found that vHPC and PVN^{CRH} neurons are not related in a simple one-to-one inhibitory relationship during stress. Increased vHPC activity did not always correspond to decreased PVN^{CRH} activity, likely due to the contributions of numerous other inputs onto PVN^{CRH} cells (James P. Herman et al., 2016).

Our study was also the first to assess PVN^{CRH} activity in freely moving animals during vHPC inhibition. From our results, we concluded that vHPC does modulate PVN^{CRH} cells, often during seconds when intact vHPC activity is responding most to an animal's surroundings. This modulation might serve to not only moderate the overall size of the downstream HPA stress response but also switch animals into a mode of absorbing information about their surroundings.

Our data are consistent with that vHPC plays its largest role in modulating PVN^{CRH} cells during behaviors which also recruit vHPC the most. Prior experiments suggested that hippocampal regulation of the HPA stress response could be specific to the modality of the stressor (J. P. Herman et al., 1998; Mueller et al., 2004), so the degree of selective inhibition observed in the current study could reflect a similar circuit mechanism of selective modulation.

This research has implications for understanding the limbic regions of the brain like the vHPC exert control over physiological and behavioral outputs of stress through the PVN^{CRH} cells and their outputs. We find that the specific modulation observed using neuroendocrine measures at longer timescales also applies to rapid changes in activity at the level of neural output.

In the long run, understanding the contributions of multiple brain areas to anxiety- and fear-related states can eventually assist us in better predicting the mechanisms that become dysregulated in psychiatric disease.

Publishing Agreement

It is the policy of the University to encourage open access and broad distribution of all theses, dissertations, and manuscripts. The Graduate Division will facilitate the distribution of UCSF theses, dissertations, and manuscripts to the UCSF Library for open access and distribution. UCSF will make such theses, dissertations, and manuscripts accessible to the public and will take reasonable steps to preserve these works in perpetuity.

I hereby grant the non-exclusive, perpetual right to The Regents of the University of California to reproduce, publicly display, distribute, preserve, and publish copies of my thesis, dissertation, or manuscript in any form or media, now existing or later derived, including access online for teaching, research, and public service purposes.

DocuSigned by:

Victoria Turner

00D82DE78B234CA...

Author Signature

12/4/2023

Date